

UNIVERSITY OF SOUTHAMPTON

**THE DESIGN OF A ROBOTIC HAND
WITH MULTIPLE ACTUATORS FOR
CHILDREN**

by

Thomas R. Redman

A thesis submitted in partial fulfillment for the
degree of Doctor of Philosophy

in the
Faculty of Physical Sciences and Engineering
School of Electronics and Computer Science

January 2016

UNIVERSITY OF SOUTHAMPTON

ABSTRACT

FACULTY OF PHYSICAL SCIENCES AND ENGINEERING
SCHOOL OF ELECTRONICS AND COMPUTER SCIENCE

Doctor of Philosophy

by Thomas R. Redman

This thesis details the development of a multi actuated hand designed for a five year old child. The thesis discusses the different methods of powering, controlling and manufacturing prosthetic devices; specifying the options chosen for this project.

Following a feasibility study into advanced paediatric prosthetics (Redman et al., 2011), this research has aimed at improving the state of the art. It presents a modular device that has a powered opposable thumb and four individually powered fingers. A study into curling finger designs has produced a novel curling design that combines a natural closure trajectory with a mechanical advantage that is higher than other curling fingers. The final research represents a significant step in improving the functionality of prosthetic hands for children. Curling fingers and a driven opposable thumb are both abilities that have not been presented in devices aimed at children. The hand compares favourably to all commercially available paediatric prosthetic hands and advanced adult devices.

The final point of this design that separates it from devices designed specifically for adults is that it can be easily scaled to produce versions for a range of age groups up to and including adults. This allows the research to start to address the issue of out-growing prosthesis. The device includes interchangeable modular parts that allow the hand to be “grown” with the child. These points are all aimed at increasing the acceptance of the child prosthesis. Acceptance of a device is the key to good prosthetic fitment. If the device is not fitted and then subsequently worn it renders any advancements inconsequential.

To allow regular replacement of parts the modules have been designed to be low cost enough to be considered disposable. To achieve this, an evaluation of the feasibility of using rapid prototyping as a construction material for prosthetic devices has been completed, which concludes that the right printed material is suitable for this application.

These features combine to deliver a device for children with a high level of dexterity that has only previously been seen on advanced adult devices. Thus, this thesis provided the basis for next generation rehabilitation devices for the next generation.

Contents

Academic Thesis: Declaration Of Authorship	xv
Acknowledgements	xvi
1 Introduction	1
2 Literature Review	5
2.1 Population Estimate	5
2.2 Anatomy and Biomechanics of the Human Hand	7
2.2.1 Types of Amputation	9
2.3 Users' Perspective	9
2.4 Prosthetic Hand Designs	11
2.4.1 Existing Prosthetic Hand Designs for Children	12
2.4.2 Existing Adult Prosthetic Hand Designs	15
2.4.3 Prosthetic Hand Research	18
2.5 Discussion	31
3 Technical Discussion	33
3.1 Normal Hand Measurements	33
3.2 Actuators used in Prosthetics	34
3.3 Actuation Mechanisms used in Prosthetics	38
3.4 Electromyography (EMG) Control	39
3.4.1 EMG Detection	40
3.4.2 EMG Control Schemes	42
3.5 Materials	43
3.6 Discussion	47
4 Research Approach	49
4.1 Requirements Specification	51
4.2 Rapid Prototyped Materials	53
4.3 Design Iterations	59
4.4 Final Modules	61
4.5 Discussion	61
5 Design and Analysis of Finger Mechanism	63
5.1 Rigid Fingers (VF1.0)	63
5.2 The Hybrid Finger	64
5.3 Finger Trajectory Analysis	64

5.3.1	Hybrid Finger (VFH1.0)	69
5.4	Input-Output Equations	72
6	Design of Metacarpophalangeal (MCP) Joint	77
6.1	MCP Version 1 (MCP V1.0)	77
6.2	MCP Version 2 (MCP V2.0)	78
6.2.1	MCP V2.1	78
6.2.2	MCP V2.2	80
6.2.3	MCP V2.3	80
6.2.4	MCP V2.4	82
6.3	MCP Version 3 (MCP V3.0)	84
6.3.1	MCP V3.1	84
6.4	MCP Version 4 (MCP V4.0)	86
6.4.1	MCP V4.1	87
6.4.2	MCP V4.2	87
6.4.2.1	Other Components:	88
6.5	Computer Aided Design (CAD) Analysis	90
7	Design and Analysis of Palm and Thumb Mechanism	95
7.1	Opposable Thumb MCP and Palm	95
7.1.1	TH V1.0	96
7.1.2	TH V2.0	96
7.1.3	TH V2.1	98
7.1.4	TH V3.0	100
7.1.5	TH V3.1	101
7.1.6	TH V5.1	102
7.1.7	TH V4.0	104
7.1.8	Palm V6.0	110
7.1.8.1	Palm V6.1	111
7.1.9	Proposed Device	111
7.2	Modelling	112
8	System Controller	115
8.1	PCB Design	118
8.1.1	Controller	118
8.1.2	Power supply	119
8.2	Controller Code Implementation	120
8.2.1	Slave Functionality	120
8.2.2	Master Functionality	123
8.2.3	Discussion	123
9	Conclusions	131
10	Future Work	141
10.1	Force & Slip Sensors	141
10.2	Testing	141
10.3	Children's Measurement Workshop	142
10.4	Additional Refinements	142

Glossary	144
A Fingertip positions with relation to normalised input angle	147
B Flowchart Symbols	151
C EMG TAR	153
References	163

List of Figures

1.1	System Block Diagram	2
2.1	Predicted Number of Upper Body Amputees by Age	7
2.2	Model of the Degrees of Freedom in the Human Hand	8
2.3	The Bones in the Human Hand	8
2.4	The Muscles and Tendons in the Human Hand	10
2.5	Types of upper limb amputations	11
2.6	Functional Prosthetic Devices	13
2.7	Prosthetic hands for children	14
2.8	Advanced Adult Prosthetic Hands; (a) Vincent hand by Vincent Systems, (b) iLimb hand by Touch Bionics, (c) iLimb Pulse by Touch Bionics, (d) Bebionic hand by RSL Steeper, (e) Bebionic hand v2 by RSL Steeper, and (f) Michelangelo hand by Otto Bock. All hands shown without cosmetic glove. Belter et al. (2013)	16
2.9	Grip types used in Activities of Daily Living. Taken from Assessors SHAP Protocol (SHAP Business Enterprise)	17
2.10	Otto Bock, System Electric Hand. (Otto Bock, b)	18
2.11	Tendon Driven Fingers	20
2.12	Schematic of a five link finger design	21
2.13	Diagram of the operating modes of the TBM hand's drive	26
3.1	Plot of ratio of a child's palm length to hand length and palm width to hand length against age	34
3.2	Plot of percentage different in child's hand to that of a sixteen year old	35
3.3	Diagram of a body powered prosthesis harness	36
3.4	Actuation Mechanisms	40
3.5	Example of a recording of an EMG of a healthy subject	41
3.6	Diagram showing the operation of SAMS	43
3.7	Diagram of the rapid prototyping PolyJet plastic manufacture process	45
4.1	Modular Diagram of the Device	50
4.2	Image showing the brittle failure of an SLA material due to ageing	55
4.3	Safety factor analysis of an impact on the axle of the MCP. Constructed with Objet High Temperature Material	57
4.4	Safety factor analysis of an impact on the front of the MCP. Constructed with Objet High Temperature Material	58
4.5	MCP Printed Using Fused Deposition Modelling Printer	59
5.1	CAD image of Finger V1.0	64

5.2	Diagram showing visualisation of rigid finger equations	65
5.3	Hybrid Finger Diagram	66
5.4	Hybrid Finger Diagram at point of maximin transmission	69
5.5	MatLab plot of the force transmission ratio and finger link trajectory . . .	70
5.6	CAD image of Hybrid Finger VH1.0	71
5.7	Trajectory of the tip of the first finger. Computed using Equations 5.22 and 5.23	74
5.8	Trajectory path of the first fingertip projected onto a closing human finger.	75
5.9	Overlaid image of a closing human finger against the trajectory of the hybrid finger.	76
6.1	CAD image of MCP V1.0	78
6.2	CAD image of MCP V2.1	80
6.3	CAD image for axle bearings	81
6.4	CAD image of MCP V2.3	82
6.5	CAD image of MCP V2.4	83
6.6	CAD image of MCP V3.1	84
6.7	CAD image of MCP V4.2	88
6.8	Safety factor analysis of an upwards impact on the axle of the MCP. Constructed with Objet FullCure720	92
6.9	Safety factor analysis of a downwards impact on the axle of the MCP. Constructed with Objet FullCure720	93
6.10	Safety factor analysis of an impact on the front of the MCP. Constructed with Objet FullCure720	94
7.1	CAD image of the palm TH v1.0	96
7.2	MCP-Palm Interface Specification v1.0	97
7.3	CAD image of the palm TH-V2.0	98
7.4	CAD image of the palm TH-V2.1	99
7.5	CAD image of the palm TH-V3.0	100
7.6	Diagram detailing 90° rotation of an elliptic object	101
7.7	CAD image of the palm TH-V3.1	101
7.8	Wire Thread Insert	103
7.9	CAD image of the tMCP TH V 5.1	103
7.10	CAD image of the tMCP TH V4.0	105
7.11	CAD image of the base and lid of the palm for TH V4.0. Viewed from the top.	107
7.12	CAD image of the base and lid of the palm for TH V4.0. Viewed from the underneath.	108
7.13	CAD image of Thumb T V4.0	109
7.14	Image of (T V4.0) test rig	109
7.15	MCP-Palm Interface Specification V2	110
8.1	Diagram of the Control System for the Hand	116
8.2	Flow diagram of the slave controller main loop	124
8.3	Flow diagram of the slave controller encoder counter routine	125
8.4	Flow diagram of the slave controller I2C processing protocol	126
8.5	Flow diagram of the slave controller force control routine	127

8.6	Flow diagram of the slave controller position control routine	128
8.7	Flow diagram of the slave controller PWM setup algorithm - Part 1 . . .	129
8.8	Flow diagram of the slave controller PWM setup algorithm - Part 2 . . .	130
9.1	Mass breakdown of the Finger and MCP	133
9.2	Mass breakdown of the Thumb	135
9.3	Mass breakdown of the Palm	135
9.4	Mass breakdown of the Hand	137
9.5	Images of Final Prosthetic Device.	139
C.1	Plot of two EMG signals taken from an adult males forearm against time	154
C.2	X-Y plot of three sets of finger data from two EMG channels on the forearm of an adult male.	155

List of Tables

2.1	Comparison of commercially available child myo-prostheses.	14
2.2	Comparison of commercially available advanced adult myo-prostheses. . .	15
3.1	Normal Measurements of a child's hand	34
3.2	Comparison of child hand sizes with a 16 year old's hand.	35
3.3	Normal Measurements of a 5 year old child's hand	36
3.4	Suggested Differential EMG Electrode Configuration	41
3.5	Materials Comparisons	46
4.1	Objet High Temperature Material (RGD525) Properties	56
4.2	Objet ABS-like Digital Material (RGD5160-DM) Properties	56
4.3	Table showing the iterations of metacarpophalangeal (MCP) joint	60
4.4	Table showing the iterations of finger designs	60
4.5	Table showing the iterations of the thumb metacarpophalangeal (tMCP) joint	60
4.6	Table showing the iterations of the Palm and Lid	61
4.7	Table showing the iterations of thumb designs	61
4.8	Table of the modules on final design	61
5.1	Inputs for hybrid finger analysis	68
5.2	Lengths for Lct on the hybrid finger	68
5.3	Predicted Output Forces	69
5.4	Dimensions of the hybrid fingertip	74
6.1	Objet FullCure720 Material Properties	90
8.1	Final Specification for Controller PCB	117
8.2	Required protection resistors	118
8.3	Available protection resistors	118
9.1	Cost of device components in low volumes	137
A.1	Table showing fingertip positions of the hybrid finger with relation to normalised input angle.	147
B.1	Flowchart Symbols	152

Academic Thesis: Declaration Of Authorship

I, Thomas Redman declare that this thesis and the work presented in it are my own and has been generated by me as the result of my own original research.

The Design of a Myoelectrically Controlled Hand with Multiple Actuators for Children

I confirm that:

1. This work was done wholly or mainly while in candidature for a research degree at this University;
2. Where any part of this thesis has previously been submitted for a degree or any other qualification at this University or any other institution, this has been clearly stated;
3. Where I have consulted the published work of others, this is always clearly attributed;
4. Where I have quoted from the work of others, the source is always given. With the exception of such quotations, this thesis is entirely my own work;
5. I have acknowledged all main sources of help;
6. Where the thesis is based on work done by myself jointly with others, I have made clear exactly what was done by others and what I have contributed myself;
7. Either none of this work has been published before submission, or parts of this work have been published as:

Redman, T., Sims, T., Chappell, P., Donovan-Hall, M., Cranny, A., Metcalf, C. and White, N. "The design of a myoelectrically controlled hand with multiple actuators for five-year old children", In: MEC '11 Raising the standard, 14 -19 August 2011, Fredericton, New Brunswick, Canada,. 83-86

Signed:

Date:

Acknowledgements

The author of this report would like to extend his thanks to his supervisor Paul Chappell and second supervisor Neil White for their guidance and advice during this research and the writing of this thesis.

I would also like to thank Paul Chappell, Dr Andy Cranny, Tara Sims, Dr Cheryl Metcalf and Dr Maggie Donovan-Hall for their work towards child prosthetic research at the University of Southampton. With, special thanks to Tara for her contribution towards our paper and subsequently the discussion on User Considerations (2.3). I also extend my gratitude to Mark Long and Ken Frampton and all the Zeplar Mechanical Workshop Staff for their guidance in the design and manufacture of the components for the hand. With their foresight many basic manufacturing issues that could have hindered the project were avoided.

I would like to recognise the work done by my undergraduate GDP team that started my interest in prosthetics that provided the feasibility that facilitated this PhD.

The author would also like to extend his gratitude to Gordon Paul for providing his time and access to his EMG amplifiers to gather the data for the initial EMG Tomography feasibility study as discussed in EMG Array Tomographic Reconstruction (Appendix C).

I dedicate my work to my family. Mum, Dad, GarGar, Georgina and Sophie, for their ongoing support and encouragement, without it I could not have completed my PhD. 153

Chapter 1

Introduction

The primary aim of this research is to improve the choice available to children with upper limb amputations. This choice is provided through the inclusion of modularity at all levels of the design. Also the aim is to allow individuals to specify and adjust their exact requirements to suit their specific needs.

There has been little attention paid to the design of small hands and the research was therefore focused on the design of a prosthetic hand for children aged five. This age group could therefore benefit the most from an improvement in the state of the art. The current commercially available hands designed for this age group do not fulfil the requirements. Older children aged ten or above are able to be fitted with the smallest adult devices. It was conjectured that the majority of children below five years would not have the cognitive ability to learn how to use an advanced prosthetic hand.

There have been greater advances in the design of prosthetic hands for adults compared to those for children. Although there have been developments to child prostheses, they have not been in line with those made to adult prostheses. It was decided that acceptance of the user should be a key consideration in the design of upper-body prosthetics. If the user does not use the prosthesis then any developments are rendered irrelevant. It is generally recognized that the younger a user is introduced to a myoelectrically controlled prosthesis, the greater their acceptance of the technology (Datta and Ibbotson (1998)); this encourages the fitment of functional and adaptable prosthetic limbs to young children.

To provide choice, hands designed specifically for the needs of children are required. Currently there are very few commercially available upper-limb prostheses specifically designed for children: the Otto Bock 2000 Electric Hand, Otto Bock (2011), and the RSL Steeper Scamp Myo Electric Hand, RSL Steeper are the most commonly fitted. Both of these hands have a single degree of freedom that are available in various sizes, and are driven by a single actuator that closes the first and second fingers onto the

thumb. Improvements in child prosthetics could be made with improved adaptability and an increased number of individually driven axes. To address this requirement, the development of prosthetics for children should be produced in conjunction with research into the acceptance and needs of children. This thesis describes the development of a prosthesis for young children designed with multi degrees of freedom and with high levels of modularity and functionality. The design process took into account considerations from both the user's perspective and from technical constraints.

A prosthetic device can be split into distinct section blocks (Figure 1.1). These blocks start with the detection of an Electromyographic (EMG) signal from the user. This is then conditioned and used as an input for the controller. One of several methodologies can be used to decide when and how much to actuate the device. The power created by the actuator is then transmitted through the finger mechanisms to grip objects.

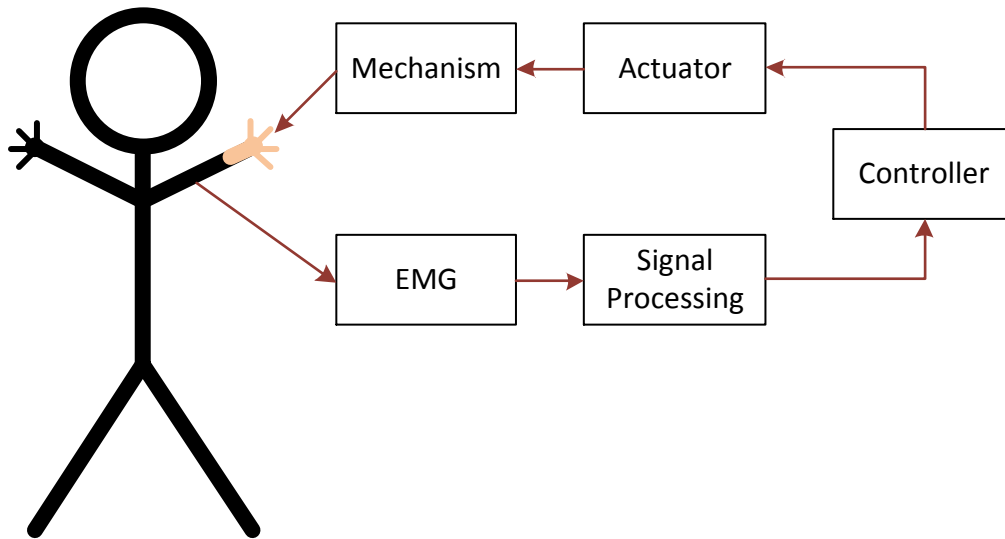


FIGURE 1.1: System Block Diagram

The novelties that are presented extend across the field of prosthetic hands for children. These novelties include:

- This is the first prosthetic hand for children, with multiple (six) actuators; designed specifically for children aged five years. Hands presented commercially and in research of this size typically have only a single degree of freedom, which means that the user is only able to form a single grip type. This research presents a prosthetic which is comparable in mass (221.2g) and size (63.0mm wide, 112.0mm long and 27.7mm deep) to commercially available children's prostheses however, it has six individual degrees of freedom.

- This research presents a device which is modular. This is the first prosthetic hand for children which is fully modular. This reduces the cost of the device, provides improvements in the servability and provides the ability to interchange components.
- The interchangeability of the hand, provided by the modular nature of the research has allowed for the development of a novel fitment strategy; in which a hand is considered "growable". As the wearer grows, individual components would be replaced with their larger variants to mean that the hand is always sized for the wearer. Currently a prosthetic for a child is fitted when it is too large and is then worn as the child grows until it becomes too small for them. This novel fitment strategy would aim to reduce prosthetic rejection, an important area of consideration in prosthetic design.
- Chapter 5 presents the design and modelling of a novel curling finger. This under-actuated hybrid design provides a humanoid fingertip trajectory, whilst minimising the mechanical disadvantages seen in other research. The design has a variable transmission ratio which is dependent on the input angle. This ranges from 2.5% at the edge of the operational envelope, and rises steeply to above 40% in the region where pinching is expected to occur. The high transmission ratio allows for actuation by motors suitable for prosthetic fitment. When fitted to this device, the fingers can apply between 2-8N of force from each fingertip, which is comparable to commercial devices for children.
- This prosthetic device for children is the first to offer a thumb with both driven closure and opposition that is suitable for fitment to a child. The fully actuated design facilitates the ability to form a range of humanoid grips. It is actuated by a motor mounted in the metacarpal of the thumb and another in the palm. This arrangement allows for a lightweight and compact prosthetic suitable for fitment to children.
- A novel modular controller for prosthetic applications is presented. The controller is a reconfigurable master-slave system that is based around the reuse of a single PCB module. This is the first control system for hand prosthetic applications that is completely modular, this therefore supports the reconfiguration of the device whilst aiding cost reduction.
- Finally this research has investigated the novel use of printed materials for powered prosthetic applications. Modelling of the components produced in Fused Deposition Manufactured (FDM) materials, showed that they would be able to withstand the force applied when the weight of an average 5 year old is applied to the device (186N). This material allows for the fast manufacture of customised components for the device whilst also representing low cost; all the plastic components for one hand can be manufactured for less than £200.

List of papers:

Redman, T., Sims, T., Chappell, P., Donovan-Hall, M., Cranny, A., Metcalf, C. and White, N. “The design of a myoelectrically controlled hand with multiple actuators for five-year old children”, In: MEC ’11 Raising the standard, 14 -19 August 2011, Fredericton, New Brunswick, Canada,. 83-86.

Storey, J., Redman, T., Wilson, P., and Bagnall, D. “Integrated Simulator and Hardware Platform for Dynamic Photovoltaic Array Optimization and Testing”, In: Journal of Nanoelectronics and Optoelectronics 10, no. 1 (2015): 104-113.

Chapter 2

Literature Review

A prosthesis is an extension of a human body, therefore, the literature review will focus on the amputee population. It will identify the demographic, what they want, what they have, and finally what needs to be developed for them. A study will be undertaken that aims to quantify the number of people living with upper body amputation that may require prosthetic fitment, and therefore potentially could benefit from this research. Secondly the human hand is examined to gain an understanding of the anatomy, mechanics, and abilities that a prosthetic device must attempt to replicate, as well as discussing the different types of upper body amputations. The users opinions of their devices are identified, before both existing and research based prosthetic hand designs are critiqued, to establish the areas where development is necessary.

2.1 Population Estimate

An estimate will be made of the number of five year old children requiring a prosthesis and hence the number of potential prosthetic devices that need to be manufactured each year to meet the demand.

As stated by Krebs et al. (1991) “Children with amputations are not miniature adults” and hence they require prosthetic devices that are customised to their needs. There have been very few studies estimating the number of people living with an amputation and even fewer that gauge the number that require prosthetic fitment. None have identified paediatric patients more specifically than under the age of 18 or 21 years. Ziegler-Graham et al. (2008) presents the first comprehensive estimates into the prevalence of limb loss in the US in over a decade. They estimate that there are 1.6 million people living in the US alone with limb loss (one in 190 people). Whilst, Ramirez-Garca et al. (2009) identifies that thirty percent of amputees suffer from an upper limb amputation and that ten percent of arm amputations are patients under 21. This suggests that it

can be estimated that there are 48,000¹ upper limb amputees, that are under 21 in the US.

A similar value can be found using data from Krebs et al. (1991). They found that “one tenth of one percent of the US population have a major limb reduction and that 13% of these individual are younger than 21 years of age”. As well as stating that one fifth (20%) of amputees suffer from a major limb reduction. This gives an estimation of 49,000² children living with upper body amputations in the US. (This uses 252 million as US population in 1991 (United States Census Bureau (2001))). These estimations correlate sufficiently that even with differences between the studies methodologies, definitions and groupings of types of amputations, a figure can be placed at 48,000 children (0-21yrs) with upper body amputations in the US.

$$\text{Amputees in Age Group} = 1600 + (69 * \text{Age}) \quad \text{While, } 0 < \text{Age} < 20 \quad (2.1)$$

Making the assumptions that the incidence of congenital cases is consistent year on year, and that the chance of acquired limb loss is linearly proportional to age, an expression for the number of children with upper body limb loss can be plotted, in Figure 2.1 and described as follows. Krebs et al. states that two thirds of all paediatric upper body limb deficiencies under the age of 21 are from congenital causes, suggesting that there are 32,000 children under 21 that have congenital deficiencies ($\approx 1600/\text{yr}$). Leaving 16,000 children with acquired upper body limb loss, this equates to 69 amputations per year per age group, giving Equation 2.1, which provides the estimation that there are approximately 1,945 children with upper body limb loss in the US aged five to six. Since the population of the US accounts for about 4.5% of the world (United States Census Bureau (2013)) it can be extrapolated that there are 42,800 amputees aged five worldwide or 8,650 living in the G8 + EU (Bracht (2010)) countries in 2010. The G8 countries consist of Canada, France, Germany, Italy, Japan, Russia, the UK and the United States of America. The number of these that could be fitted with a complete hand prosthesis could be as low as 13% as suggested by Krebs et al., however, due to the replacement cycle of child prosthetics this could be assumed to be the number of children fitted with a prosthesis each year. Assuming children require two prosthesis per year as stated by Doshi and LeBlanc (1998), an estimate for the number of prosthetic devices needed each year for five year old children is 500 in the US, 11,100 in the world and 2,260 in the G8 and EU countries.

¹ $(1.6 \times 10^6 * 30\% * 10\% = 48,000)$

² $(\frac{252 \times 10^6 * 0.1\% * 13\% * 30\%}{20\%} = 49,140)$

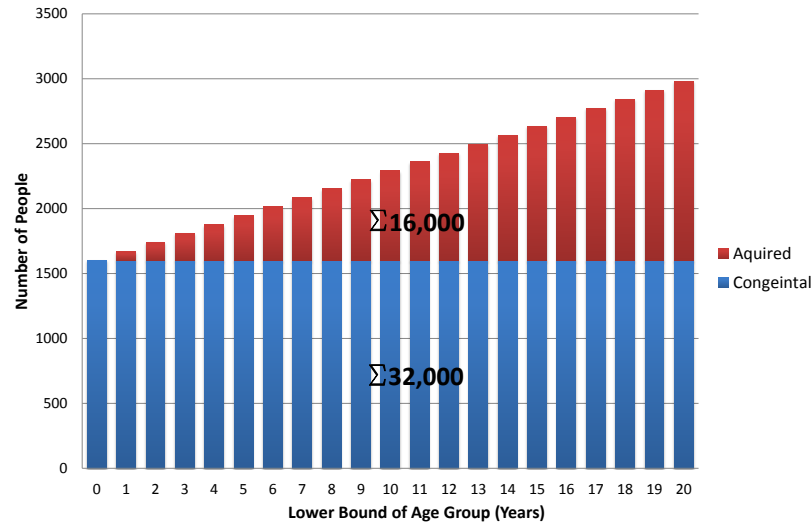


FIGURE 2.1: Predicted Number of Upper Body Amputees by Age

2.2 Anatomy and Biomechanics of the Human Hand

The human hand is a highly sophisticated tool. The tasks that we can undertake because of the opposable thumb has been credited as one of the reasons for the advance of the human race. There are many anatomical models for the human hand, with between 19 and 24 degrees of freedom (DOF) (Zecca et al. (2002)) dependant on the model. These models agree that each finger contains four DOF; three DOFs provide flexion and extension at each joint and another for abduction and adduction of the Metacarpophalangeal (MCP) joint. The thumb is attributed either four or five DOF; again three are for flexion and extension at each joint and one or two DOF for abduction and adduction. The abduction and adduction in the MCP joint is omitted in some models, due to the limited motion. The wrist flexes and extends the hand and can also abduct and adduct, which, provides a further two DOF. The hand can also be rotated by the radius and ulna in the forearm. A model showing the locations of the DOF in the hand and wrist is shown in Figure 2.2; this model can be used to demonstrate how different combinations of movements can be used to provide the different grip patterns of the hand.

The human hand has 27 bones, controlled with 33 separate muscles (Hu (1997)). It can be seen in Figure 2.3 that each finger consists of three bones; distal, intermediate and proximal phalanges. These bones are joined at two locations; the distal interphalangeal and the proximal interphalangeal joints, which provide the flexion that allows for finer finger control. Finally, the proximal phalange is connected to a metacarpal at the metacarpophalangeal joint, which provides the major flexion and abduction of the finger. The metacarpals of the fingers have limited freedom because their motion is loosely constrained to one another. The thumb has a similar structure but it does not have an intermediate phalange. Instead the metacarpal has a large range of movement allowing for the thumb to oppose the palm.

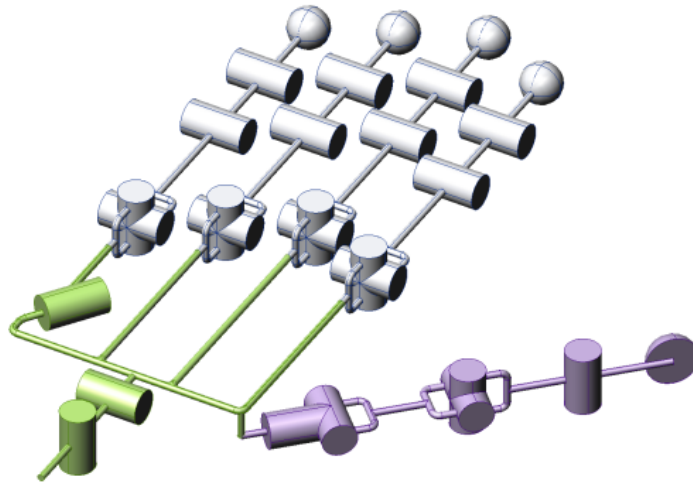


FIGURE 2.2: Model of the Degrees of Freedom in the Human Hand.
(Shadow Robot Company Ltd. (2011))

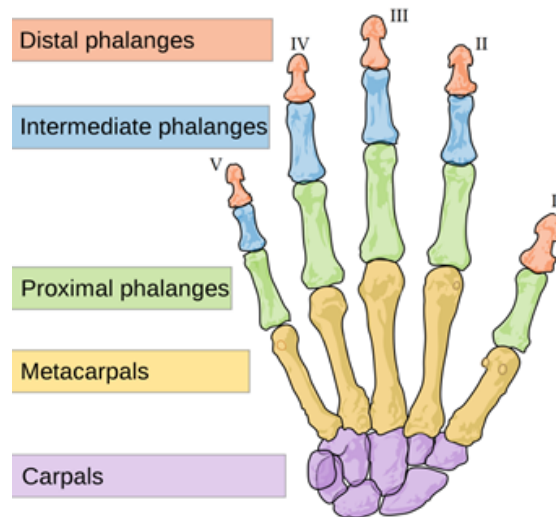


FIGURE 2.3: A diagram showing the bones in the human hand.
(<http://boneandspine.com/definitions/metacarpal/>)

The articulations that can be achieved in the different joints in the hand are as follows; interphalangeal articulations of the hand (the hinging between the finger bones), metacarpophalangeal articulations (where the fingers meet the palm), intercarpal articulations (where the palm meets the wrist) and trapeziometacarpal (TMC) (also known as the carpometacarpal (CMC)) articulations. This joint can achieve three different movements, flexion and extension in the plane of the palm, abduction and adduction in a plane at right angles to the palm (opposition), and circumduction (to move the thumb in a circular manner).

The hand is powered by muscles that are positioned both in the hand and in the forearm. These are connected to the fingers via tendons - bands of fibrous connective tissue with a high tensile strength. The muscles that provide the power and major movements for

the hand are located in the forearm. Those providing extension are on the top of the arm and those providing flexion are located on the bottom. Figure 2.4 identifies and shows the locations of the muscles and tendons that are responsible for the flexion and extension of the wrist and digits. These observations of the anatomy of a natural hand implies that, to make an artificial hand fittable to the widest group of patients, the actuators need to be mounted in the palm of the device.

2.2.1 Types of Amputation

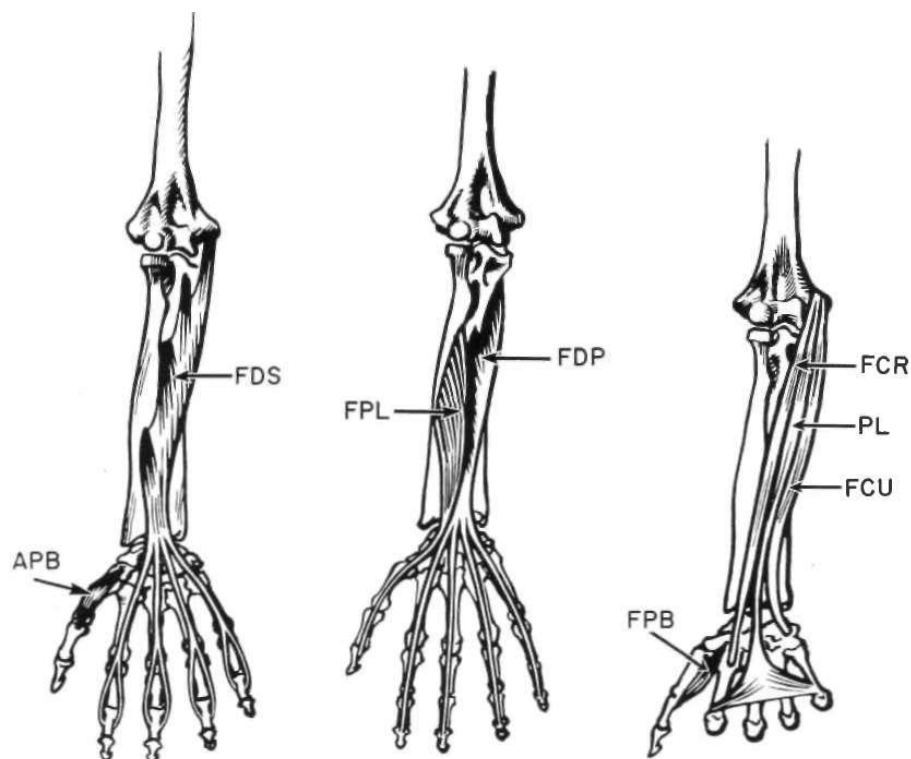
The level of, or location of, an amputation can have a dramatic effect on both the loss of function and the amount that can be recovered by the fitment of a prosthesis. Upper extremity amputations refer to hand and arm amputations, whereas a lower extremity amputation refers to leg amputations. The classification of an upper limb amputation can be grouped into one of seven categories; partial-hand amputations, wrist disarticulation (the separation of two bones at the joint), elbow disarticulation, transradial (below elbow amputations), transhumeral (above elbow amputations), shoulder disarticulation and forequarter (these can be seen in Figure 2.5). Generally the longer the remaining limb and the more joints that are kept intact, the easier it is to fit a prostheses for the amputee. This said, the only active prosthesis that can be fitted to patients with partial hand amputations is the i-LIMB, Touch Bionics (2011).

This research will be aimed at patients with amputations above wrist disarticulation. This allows for an entire hand to be designed whilst still providing a device that can be fitted to most amputees. As well as this, any partial hand amputation does not require an entire prosthetic hand, just powered fingers with a partial palm.

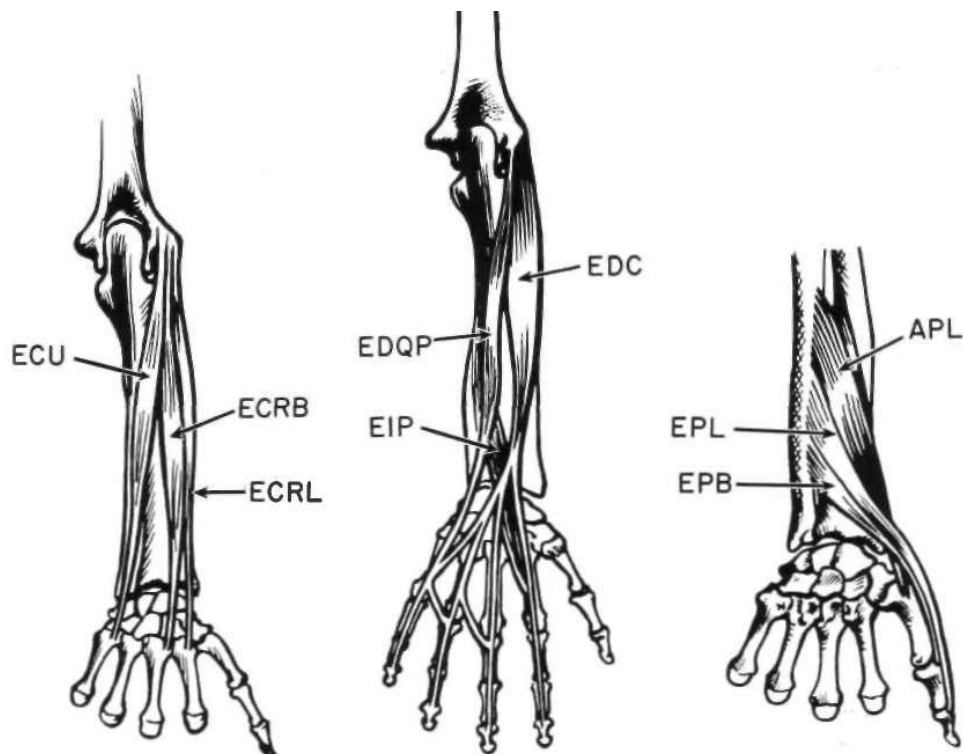
2.3 Users' Perspective

Rejection rates of upper limb prostheses amongst children have been reported to be as high as 50% (Shida-Tokeshi et al. (2005)); this indicates that upper limb prostheses currently being prescribed, are not meeting the needs of young people (Biddiss and Chau (2007)). Research into rejection of prostheses amongst adult users found dissatisfaction with the prosthesis to be linked to rejection (Donovan-Hall et al. (2002)), therefore highlighting the importance of considering the views of service users when developing new prosthetic devices. This is supported by Biddiss and Chau (2007) in their historical review of upper limb prosthetic use and abandonment, which concluded that “increased emphasis on participatory research and consumer satisfaction is needed”.

Biddiss et al. (2007) consulted prosthetic wearers of all ages in order to inform prosthetic design by identifying their key development priorities. These were reduced weight, lower cost, life-like appearance, improved comfort, enhanced wrist movement, better grip



(a) Flexors of wrist and digits



(b) Extensors of wrist and digits

FIGURE 2.4: A diagram showing the Tendons of in the human hand. See Glossary for extensions of muscles (Taylor and Schwarz (1955))

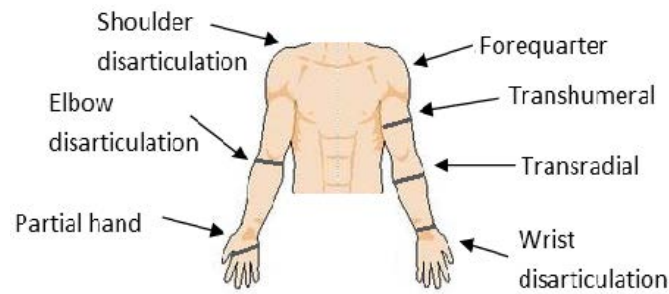


FIGURE 2.5: A diagram showing types of upper limb amputations. (Zaini et al. (2011))

control, and improved grip strength. The design priorities varied substantially across age groups, suggesting that upper limb prostheses designed from the users' perspectives would differ for children and adults. This supports the need for prosthetic hands for children to be designed alongside studies into user feedback. Before this user-led design, it is necessary to explore the technical feasibility of designing a hand of this size and mass.

Donovan-Hall at the University of Southampton carried out a study (Our Bodies Our Views (Unpublished)) using questionnaires and interviews to examine satisfaction with prostheses and reasons for prosthesis rejection in young people with upper limb loss, aged 5-18 years. Three factors were identified as important amongst the participants. They were the look of the prosthesis, the functional ability, and being involved in the selection of the prosthesis. Reasons identified for not wearing the prosthesis were as follows; it was uncomfortable (including being too hot and too heavy), it is only useful for specific tasks, the artificial appearance of the prosthesis (attracting unwanted attention), and wear and staining. This study also emphasises the importance of communicating with children when designing prosthetic devices.

It has been shown that children wearing an anthropomorphic prosthesis find it easier to gain acceptance from their peers; compared to those wearing a non-anthropomorphic prosthesis. This is clearly highlighted in a study (Fishman and Kay (1964)) where it was observed that children would chose to wear a less functional anthropomorphic hand over a functional hook whilst around peers. They would often revert to the more functional hook when in more socially relaxed environments.

2.4 Prosthetic Hand Designs

Upper limb prosthetic patients have a variety of expectations of their limbs, therefore require different prosthetic solutions. Because of this there are several different types of prosthetic limb, each type having different levels of functionality and appearance. The most basic, a cosmetic prosthesis is specifically designed to replicate the look of a human hand, usually with no functionality. These are typically produced on a patient

by patient basis where the importance lies heavily on either the subtlety or the visual effect of the prosthesis. The Alternative Limb Project (Barata, 2015) is an example of a modern cosmetic prosthesis manufacture, they produce highly customised and exotic prostheses. Their designs are individually customised for visual effects some have been fitted with feathers, gems and hidden compartments.

A functional prosthesis is a prosthesis that is designed to aid the wearer in performing tasks. They can be split into two categories; Static, and Driven. Static devices can be multi-purpose, such as hooks, however these tend to be task-specific tools intended to aid in every day activities, such cooking and eating (Figures 2.6(a) & 2.6(d)); as well as sporting aids (snooker rests (Figure 2.6(b))) and work tools (claw hammers (Figure 2.6(c))).

Driven prostheses, can be split again into either Body powered or Externally powered. Body powered prostheses are generally multi-purpose tools, that are driven through the use of tensioned cables across the wearers' shoulders. To operate the upper limb prostheses, the user tenses their back or stretches their arm forward. These end effectors can take the shape of claws, pliers, or can be anthropomorphic. Externally powered limbs are typically used in situations where the user wants to recover either dexterity or a powerful grip. During fitment they are customized to the users' needs by adapting the most suitable available prostheses; for this a wide range of devices are needed. This is reflected in the types of end-effectors that are available on the market; for example there are devices that are aimed at giving the user the maximum power and others dedicated to giving the greatest range of achievable grasps. Functional powered prostheses can be covered in a cosmesis to protect them and to give them a lifelike appearance. These limbs can be powered by many different actuation methods, from simple motor driven devices to hybrid dual actuated drives. The most common commercially available prosthesis, use basic actuation methods involving a single DOF drive. Touch Bionics, Otto Bock and Steeper have produced hands with multiple driven DOF and actuators, however, these have only been developed in adult sizes and are very expensive.

2.4.1 Existing Prosthetic Hand Designs for Children

A search has revealed that there are no historic research references to hands developed specifically for children. However, a paper by Childress published in 1985 looks at "Historical aspects of powered limb prostheses". He suggests that the first hydraulically powered limbs for children were fitted by Marquardt in 1965. The pioneering of the fitment of myoelectric hands to children was by Sorbye in the early 1970s, Sorbye (1977, 1980).

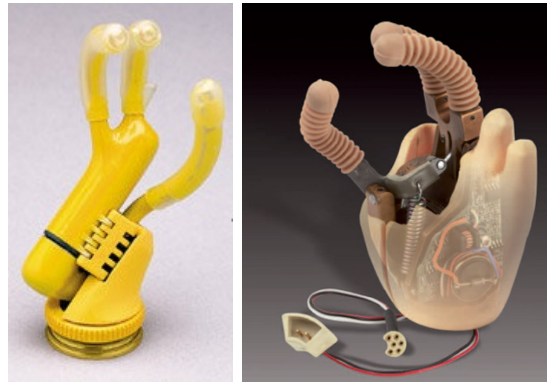
There are several commercially available myoelectric prosthetic hands that are specifically designed for children. These hands are all one axis devices driven by a single electric



FIGURE 2.6: Functional Prosthetic Devices. (RSL Steeper (2008))

motor; the method in which closure is actuated differs between manufacturers. The Otto Bock Electrohand 2000 Figure 2.7(a) uses a rotational closure of the thumb onto the forefinger. Whereas the RSL Steeper Scamp Figure 2.7(b) uses a pincer motion of the forefinger and thumb. Both of these designs have powered first and middle fingers with the option of a cosmesis to provide passive ring and little fingers. As discussed in the User Considerations (Section 2.3) these hands have several drawbacks that mean that they are not the ideal of prostheses. The first is that they are felt to be cumbersome and heavy, weighing up to 200g without a cosmesis. This means that they cause increased pressure on the socket, causing sores and skin irritation. The second drawback of hands for children is the usability. They are limited to one grip patterns. This, alongside their slow actuation speeds, greater than one second, means that they are not user friendly for young children who have ever changing needs and limited attention spans.

The specifications of the two commercially available child myo-prostheses are shown in Table 2.1. It is difficult to draw an exact comparison between the Otto Bock - Electrohand 2000 and the RSL Steeper - Scamp devices, as they use different methods to size the hands. Otto Bock sizing is gauged on a measurement around the knuckles, whereas RSL Steeper use the distance across the knuckle. The Electrohand 2000 comes in 5, 5.5, 6 and 6.5 inch sizes; these hand sizes are for ages 1.5-3, 3-6, 5-10 and 8-13



(a) 2000Hand, Otto Bock (2011) (b) ScampHand, RSL Steeper

FIGURE 2.7: Prosthetic hands for children

TABLE 2.1: Comparison of commercially available child myo-prostheses.

	Otto Bock Electrohand 2000	RSL Steeper Scamp
Age Range (Yrs)	1.5 - 13	0.5 - 6
Sizes	4	2
DOF	1	1
Type of actuation	Rotation of the fingers to thumb	Pinch of thumb to fingers
No. Grips	1	1
Mass (g)	86 - 130	143 - 200
Grip force (N)	8-35	-

years respectively. Whilst the Scamp comes in only 1.75 and 2 inch sizes for children aged 0.5-3 and 2-6 years. The closest comparison that can be drawn is that between the Otto Bock 5.5" and the RSL 2" hands as they are aimed at the same age range. Of these two hands, the Electrohand 2000 has the lowest mass although this may mean that the motor is smaller and the device has a lower grip force (this comparison cannot be made as the grip force of the scamp is not documented). As well as this, the masses are not specified whether these are with or without cosmesis or wrist joints. However, this is the only conclusion that can be drawn as there is no information released about closure speeds and open grip size.

These powered prosthetic hands are controlled via electromyography, using either one or two differential contacts placed on surviving muscle tissue. Most single DOF devices, including paediatric prostheses use a range of similar control methodologies, these are: Digital, Proportional and Voluntary state. Digital control methods use the input signal to select either of the two states, open or closed. Proportional control uses the size of the input EMG signal to determine either the closure speed or force of the hands actuation. Finally, voluntary methods choose a predetermined state that the hand will default into when there is no signal. When a signal is present, the hand will close/open using either a digital or proportional response. Although there are more advanced and

modern control schemes, these tend not to be applicable to child prosthetics due to the single DOF offered by these hands. A review into prosthetic control methodologies is completed in the Technical Discussion in Chapter 3.

2.4.2 Existing Adult Prosthetic Hand Designs

There are far more designs, for both single degree of freedom hands and multifunctional hands, for adult prostheses than the child equivalents. This is due, in part, to the US Armed Forces providing funding for prosthetic research to serve the needs of their military personnel returning from conflicts (Kuniholm (2009)). Development is also less restricted in adult hands due to having more space and also the mass can be higher compared to a hand designed for children. Therefore, a greater variety of components and design solutions can be used in an adult hand.

There are various advances that have been made in adult prosthetic designs that have not been transferred to the smaller sizes needed for children. They can be categorized as; an increased number of actuators, individual finger actuation, composite polymer materials and improved dexterity.

Examples of adult hands are the System Electric Greifer DMC VariPlus by Otto Bock (a), which is a non-anthropomorphic design that can achieve grip forces of up to 160N. It is used for tasks that require a large gripping force or in manual handling. The Touch Bionics i-LIMB (Touch Bionics (2011)) hand has individual motors mounted into the fingers. This design means that it is the only device that allows for adaptation of the palm making it available for fitment to patients that have suffered partial amputations of the hand. Finally the RSL Steeper bebionic v2 hand, uses individually powered fingers to achieve fourteen everyday grip patterns. With this ability, users are able to complete many more everyday tasks whilst wearing the prosthetic. All of these advances improve the usability of the prosthetic and reduce the periods in which wearing the prosthetic offers no advantage to the user, therefore lowering the likelihood of rejection.

TABLE 2.2: Comparison of commercially available advanced adult myo-prostheses.

	Ottobock System Electric	Touch Bionics I-Limb Ultra Revolution	RSL Steeper BeBionic v3	Ottobock Michelangelo
Motors	1	5	5	4
No. Grips	1	13	14	7
Weight (g)	460	460-465	488-520	400
Grip force (N)	100	136N	75	100
Speed (mm/s)	300	-	260	325
Opening time (s)	0.33	1.20	0.90	0.37
Opposable thumb	N	Y	Y	Y
Powered opposition	N	N	N	Y

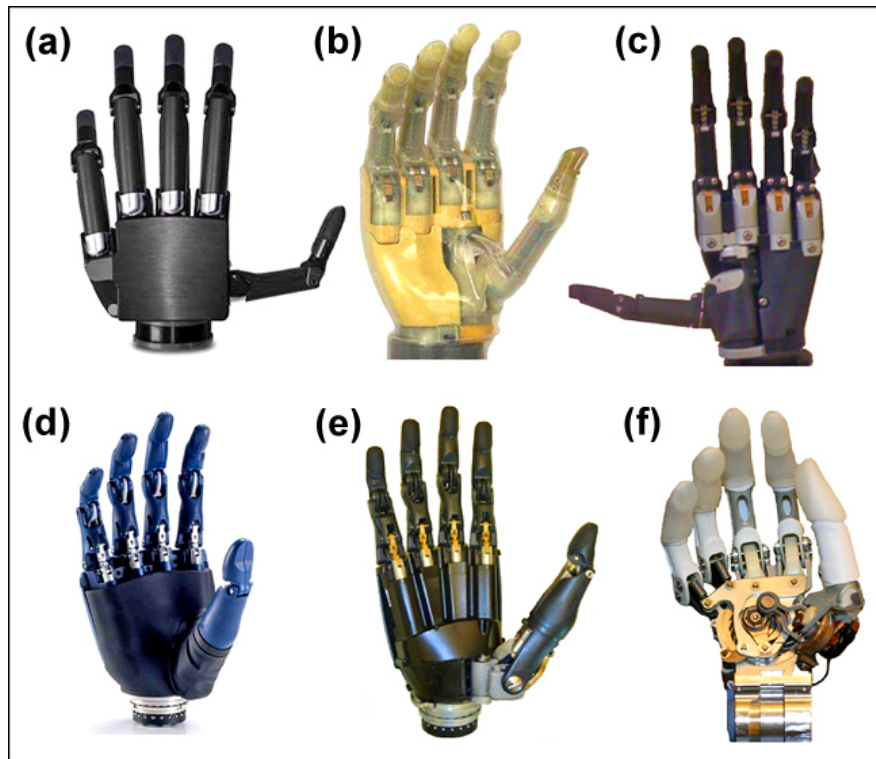


FIGURE 2.8: Advanced Adult Prosthetic Hands; (a) Vincent hand by Vincent Systems, (b) iLimb hand by Touch Bionics, (c) iLimb Pulse by Touch Bionics, (d) Bebionic hand by RSL Steeper, (e) Bebionic hand v2 by RSL Steeper, and (f) Michelangelo hand by Otto Bock. All hands shown without cosmetic glove. Belter et al. (2013)

Figure 2.8 shows the most advanced adult prosthesis that are commercially available. These have varying features, actuation speeds and closure forces, however all feature at least separate finger and thumb actuation. This provides the ability to form multiple different grip types; with individually actuating fingers the Bebionic v3 and iLimb revolution hands are able to form fourteen and twenty four separate grips respectively. These grips range from the traditional cylindrical grip to a modern computer mouse grip. Commercially available hands demonstrate clearly the link between individual finger actuation and possible grip variety. The Michelangelo hand which actuates all fingers together is only able to form seven grips compared to two of the other hands presented that have thirteen and fourteen grips.

Achievable Prosthetic Grip Patterns

As discussed the human hand is a highly adapted end effector that is able to form considerable numbers of grip patterns and digit combinations. The Southampton Hand Assessment Procedure (SHAP) (SHAP Business Enterprise) is a process for assessing the functional level of a hand, by assigning a normalised score of functionality. This test process identifies six different grip types used in Activities of Daily Living (ADL). These grips can be seen in Figure 2.9 and comprise; Tip, Lateral, Tripod, Spherical,

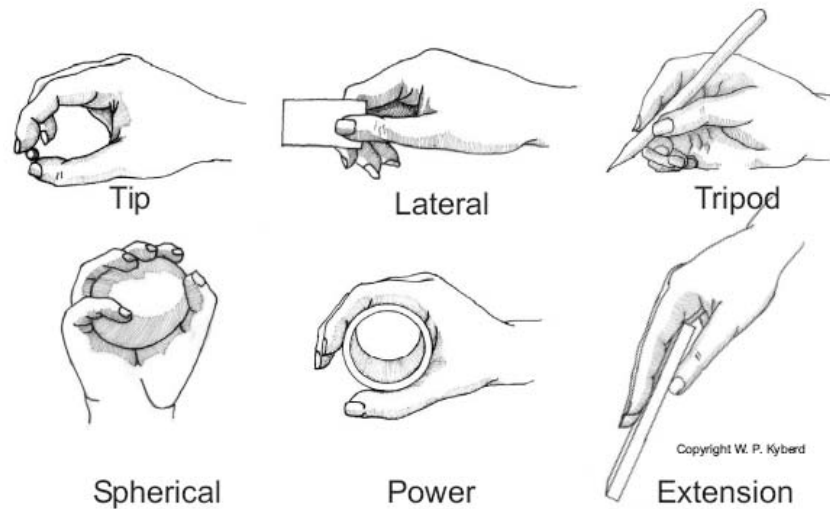


FIGURE 2.9: Grip types used in Activities of Daily Living. Taken from Assessors SHAP Protocol (SHAP Business Enterprise)

Power and Extension. Prosthetic hands do not yet have this functionality. Each of the advanced prosthetic devices that have been discussed offer slightly differing grips patterns, although these can all be grouped into categories; Precision grips, Power grips, Advanced (Additional) grips and Gestures. Precision grips tend to only utilise a single finger and thumb to achieve fine tasks where the user requires greater control. Power grips are designed for transference of force and therefore combine all the digits in a robust manner for example carrying a case or opening a door. Most advanced prosthetics are able to form basic gestures such as a flat palm or point. Finally, the advanced grips are more complex than the other grip types discussed, they tend to involve a two stage hold and then interact process that allows the user to do tasks such as manoeuvre a computer mouse or spray a trigger operated bottle. The iLimb Revolution also allows for the programming of user defined grips. The major limitation to the grips that can be formed is the control mechanism behind them. To ensure usability a device must be programmed to utilise only a few of these grips at any one time.

The uptake of the most advanced devices has been limited due to the cost and required training. One of the most regularly fitted hands is the System Electric hand by OttoBock (Otto Bock, b), Shown in Figure 2.10. It only has one powered DOF however, due to the ease of use, robustness and the competitive price, many patients favour them. It has been identified that there is not this level of choice available to patients requiring a prosthetic hand for children. This is because of two main reasons, the first is that the funding for recent research has been directed at military service personal and therefore adult devices. As well as this due to the size constrains the devices designed for children are much more restrictive on implementable solutions. Therefore there has been less impetus into the development of this field.



FIGURE 2.10: Otto Bock, System Electric Hand. (Otto Bock, b)

2.4.3 Prosthetic Hand Research

Recent published research on prosthetic hands is limited to a few specific areas. This is almost exclusively aimed at adult devices with multiple underactuated curling fingers (when an object has more degrees of freedom than actuators), therefore research advances in both adult and child will be discussed in this section. This research is predominantly based around devices that are either actuated by a DC-motor or a body harness however, others are powered by compressed gas, servos and hybrid tendon-spring drives. The confidentiality of commercial technology associated with companies has restricted the publication of some of the new ideas and developments. Sinha (2011) presents a very low cost solution which has two DOF that drive the fingers and the thumb closed. It uses a standard tendon and spring actuation method to produce a multi jointed finger, with the motors used to wind the tendon shorter. This design does not add anything significant to the field, however it stands to show that there is very little work being published in this field.

Research into prosthetic hands can be split into two categories, the first comprises body powered prostheses grouped alongside active prostheses with externally mounted actuation (actuators mounted outside of the hand typically in the forearm). Whilst, the second comprises designs for active prostheses with internally mounted actuators. These categories have been chosen because the externally mounted and body powered devices have to use a power transmission system, which normally actuates using a push/pull action. This is typically achieved with cable drive and therefore means they are technically interchangeable. However, the powered devices in this category can only be fitted to people with a higher level of amputation, as they require space to accommodate the

fitment of the drive system. This means that the prosthesis will have a smaller target market and therefore has less commercial viability.

Research into Prosthetic Finger Designs -

There are two main categories of finger design that are presented in both the research and existing commercially available prostheses, these are a fixed (solid) finger and flexing finger designs. Solid fingers are presented in Redman et al. (2011); Tang et al. (2011) as well as the Ottobock System Electric Hand (Otto Bock, b). This finger design provides efficient force and speed characteristics however the fingertip trajectory is unnatural and this can be a source of rejection.

There are different mechanisms presented for flexing fingers (tendon driven, gear driven and link driven). Although the analysis methodology and data published for each varies, conclusions can be drawn on the efficiency and practicality of each method. Tendon driven fingers are usually presented in research where a body harnesses is used as the power source. The basic actuation of this type of curling finger uses three hinged joints with the tendon attached at the tip of the finger; as the tendon is shortened or pulled the links rotate inwards. There are several methods of implementing this design: Doshi and LeBlanc (1998); LeBlanc et al. (1997) presents multiple iterations of their design starting from simple plastic tube phalanges to custom shaped nylon phalanges (Figure 2.11) with a shaped tendon guide. Massa et al. (2002) improves on the principals of this design by adding pulleys at each of the joints to reduce tendon friction. Neither of these authors present conclusive analysis or testing of the force transmission characteristics.

Bundhoo and Park (2005) presents a finger design that has multiple tendon driven DOF. This finger has independent MCP extension and adduction as well as coupled closure of the DIP and PIP joints. The design uses Smart Metal Alloy (SMA) tendons to provide the actuation; these are typically limited by their rate of actuation or the total contraction. Although it is mentioned in the conclusions, the paper avoids a discussion about the range of contraction of SMAs. This could however be overcome as they could be interchanged with rigid tendons and another actuation method. Doshi and LeBlanc (1998) experimentally analyse the force characteristics against the Ottobock System Electric Hand. However the test conditions are not consistent (the Ottobock hand gloved and the research hand un-gloved). This means that the conclusions are likely to be flawed. Bundhoo and Park (2005) calculate the torque around the finger joints that would be required to form a stable grip, showing that these forces could be achieved with SMA technology. Although, traditional motor gearbox actuators would be unlikely to provide the necessary torque within the other requirements of these prosthetic hands (speed and size). Due to the lack of a discussion into the force transfer ratios, it can only be assumed that other finger designs fail to overcome the large mechanical disadvantages presented by the use of a tendon mechanism.

The final tendon design worthy of mention is from Yang et al. (2004) who uses unguided springs as the structure for the fingers. The spring would provide a robust solution that would withstand a high level of accidental damage. However, this design does not present a solution to prevent sideways and twisting motion of the fingers during gripping.

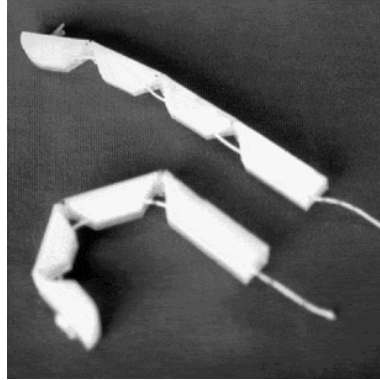


FIGURE 2.11: Tendon Driven Fingers. (Doshi and LeBlanc (1998))

Han and Huang (1998) present a design that uses multiple gears along the finger to provide actuation at each joint. The trajectory of the finger curling is not discussed. However the research states that the gear ratio is one to one. Therefore this provides proportionally flexing joints, although this could be altered with a different gear ratio. The drawback of this system is that for the gears to be robust they are typically made of metals. When multiple gears are used the mass of a gearbox becomes prohibitive. This is reflected in the conclusion where they state that the hand is “not light enough”.

Guo et al. (1993) presents a conceptual design for the linked curling finger, which has since been developed by several groups (Asyali et al., 2011; Dechev et al., 2001; Fukaya et al., 2000; Kyberd and Chappell, 1994; Light and Chappell, 2000), with Tang et al. (2011) reimplementing the Fukaya et al. design. The fingers vary in their precise operation and flexing mechanism design, although all are based around the curling nature of the six bar linkage six-bar linkage. Light and Chappell uses a system of five linkages (seen in Figure 2.12) to form a curling trajectory. The design is flexible as it can be adapted to be driven by both linear or rotational inputs. (Asyali et al., 2011; Kyberd and Chappell, 1994; Light and Chappell, 2000) have implemented rotational designs, whilst, the others are designed for a linear input. Linked fingers are a significant development in producing human like movements. All of these designs provide viable solutions to the action of the fingers however, the linkage causes a large mechanical disadvantage, Dechev et al. (2001) reports a mechanical transmission ratio of less than 10:1, that leads to lower gripping forces. The current state of the art in motor design fails to compensate for this disadvantage without a large increase in the mass, which is unreasonable in prosthetic design. The second reported issue with these designs is that, if the finger makes contact with an object on its lower links (those nearer the MCP Joint, labelled knuckle block) the top of the finger does not curl around the object, thus an incomplete grasp could be formed.

There have been several papers that have mathematically modelled the finger actuation paths, namely Allen-Prince and Walton (2011); Guo et al. (1993), however, each design has different mechanical transmission characteristics and a different mathematical model. No paper exists that directly models these finger designs against each other, though it appears that a direct trade-off exists between the finger curl characteristics and the mechanical disadvantage across the finger.

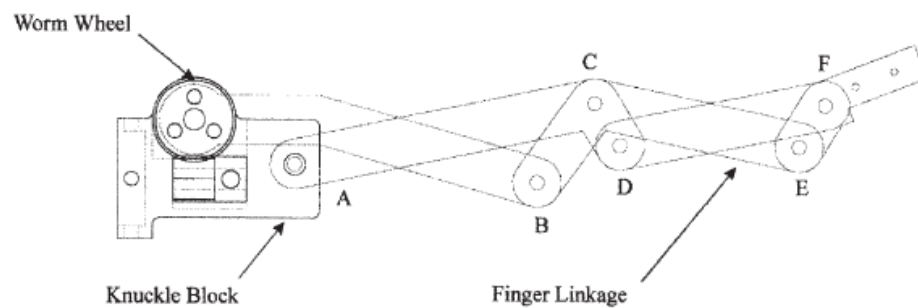


FIGURE 2.12: Schematic of a five link finger design used to provide a curling action. The six joint locations are shown as A-F. (Light and Chappell, 2000)

Several different solutions for prosthetic finger designs have been presented although, there are only a few that are viable for prosthetic fitment. The six-bar linked fingers and the tendon driven designs present a good curling action but have a high level of mechanical disadvantage. This discounts them as viable designs in small hands, as the actuators needed to give sufficient tip forces, are prohibitively large or heavy. It is suggested by Doshi and LeBlanc (1998) that the DIP joint could be fixed, without significant loss of finger curling action. This arrangement would retain a natural curling action but would not suffer from so much mechanical disadvantage as the more complicated designs. A linkage design that is not as complicated as in the five and six bar linkage design would accomplish this.

Research into Thumb Designs -

It is accepted that the ability of the human hand is highly dependent on the opposable thumb. Bell (1833) stated that “the length, strength, free lateral motion, and perfect mobility of the thumb, depends the power of the human hand”. This is supported by the opinion of Colditz (1995) “it is clinical consensus that the loss of thumb function causes a minimum of 50% of the hand’s subsequent disability”. Light et al. stresses the significance of a functional opposable thumb, as the single most important development in a device’s ability to return a patient’s dexterity.

The abilities of the thumb designs presented vary dramatically, from those similar to that of the Ottobock system electric hand by Galiano et al. (2007), to anthropomorphic robotic hands with four thumb motors by Yamano and Maeno (2005). Asyali et al. (2011); Sinha (2011) discuss systems with individually actuated thumb closure, that have

no opposition. These designs allow the contact point of the first finger and thumb to be varied during a pinching action. Without thumb opposition the number of grip patterns that the devices can achieve is limited. This gives rise to the conclusion that without opposition, thumb closure advancement alone adds very little to the functionality of the device whilst increasing weight and complexity.

There are two examples of an opposable thumb in child hand research (Dechev et al., 2001; Hu, 1997), both of these designs poses a thumb that is manually opposable with closure coupled to the fingers. Hu (1997) presents a device with one DC motor aimed at children aged six. The closure of the thumb is driven simultaneously with the fingers through a gear linkage. Thumb opposition is an un-powered axis that can be manually positioned into one of three pre-set positions when the hand is completely opened. The design uses a helical gear mechanism to transmit power to the thumb when rotated, by altering the contact position of the gears. A pin is automatically engaged during closure to lock the thumb in position. The second of these paediatric hands (Dechev et al., 2001) is a tendon driven device that uses friction to maintain the thumb's opposition once it is manually manoeuvred into the desired opposition, whilst, the coupled tendon drive is used to actuate the closure.

Both of these solutions present methods for providing an opposable thumb. That said they both have drawbacks, the hand by Hu (1997), is heavy due to the large number of gears required. As well as that there are potential problems with the automatic locking mechanism. Firstly the thumb can only be positioned into one of three locations, limiting the number of feasible grip patterns. The second is that the hand must be fully opened to alter the opposition of the thumb. These issues would limit the operational efficiency of the device, and therefore could reduce user satisfaction. Whereas, the Dechev et al. tendon mechanism is a viable solution for transmitting power across an opposable thumb however, tendon drives are typically slow to actuate, a problem reported in the research carried out by Dechev et al..

The Southampton Hand (Kyberd and Chappell, 1994; Light and Chappell, 2000) and NTU-Hand 3 (Han and Huang, 1998) present adult devices with a powered thumb opposition and closure, using geared linkages driven individually by two DC motors. In both situations, during opposition the entire thumb closure mechanism is rotated, including the motor and axle supports. This means that the opposition module must be capable of transmitting all force subjected to the thumb including the masses of the closure drive system. As well as this, the drive system for opposition must be capable of moving and braking the mass of the closure drive system. These constraints add to the design complexity, however as long as they are addressed they do not prevent this as a solution. The drawback of these two solutions is that the positioning of the thumb's closure mechanism, means that the motors protrude in a non-anthropomorphic manner into the wrist region, causing a region where items could become inadvertently trapped, between motor and wrist.

Massa et al. (2002) presents a variant to this design, comprising a mixed DC-motor and tendon drive system. The tendon drive translates the thumb closure actuation to the palm therefore reducing the complexity and mass of the thumb. Opposition is powered through a DC-motor gear system which is also mounted on the palm. This device presents a solution to the issues raised with the other adult thumb designs (Han and Huang, 1998; Kyberd and Chappell, 1994; Light and Chappell, 2000). However this design relies upon tendon linkages and, as previously discussed, these can be slow and suffer from poor force transmission.

In summary, there are two possibilities to power the closure of a thumb; it can either be coupled to the actuation of the fingers or driven separately. When compared with current commercial child prosthesis the devices presented in the research provide advancements in the design of the thumb. Although when contrasted with current adult devices, the research is found lacking. Several designs for both adult and paediatric prosthetic thumbs have been discussed. These designs have differing abilities and functionalities. Most rely upon an amount of manual operation, that means that their operational efficiency is limited. Whilst the designs that aim to provide both driven thumb closure and actuation, advance the field, each design has drawbacks that outweigh the advancements.

From observation of the grip types in Section 2.4.2 it can be suggested that flexion in the thumb is not required in most gripping tasks. It is only required for dexterous tasks such as writing. Since the current control methodologies employed for prosthetics do not allow for this level of dexterity, it could be possible to sacrifice the flexing to allow for greater transmission forces.

This leads to the conclusion that the advantages of having a flexing thumb on an prosthetic hand are limited to the ability to form a lateral grip and to vary the contact point of the finger and thumb. Neither of these necessitate a large closure force, and could be achieved with a smaller actuator. By using a smaller motor for the closure of the thumb, the designs presented in the research for the Southampton Hand and the NTU-Hand 3, could be implemented without incurring the issues caused by inertia of this actuator.

Prosthetic Research for Children -

As previously stated there has been very little recent published work on upper body prosthesis for children. Of this research, there is no documentation of fitment or clinical trials. Dechev et al. (2001); Galiano et al. (2007); Hu (1997) present electronically powered prosthesis that can be controlled with an EMG input. LeBlanc et al. (1997) and (Doshi and LeBlanc, 1998) present a bodily powered design that is aimed at reducing the cost of a prostheses for children. It is a cable actuated approach with four active fingers and a passive thumb, designed to be actuated via a body powered harness, that could be driven by an externally mounted motor. This research does not discuss a specific age group instead it hints that it is designed to be scalable. While the approach widens the impact of the research however without discussion of the scaling methodology,

the minimum hand size cannot be ascertained. This is the first paediatric prosthesis to have four driven fingers but this does limit the force applied at each of the fingertips as the input force is split between each finger. Also the passive thumb could impair the functionality of the hand as manual manipulation would limit the operation speed and could prevent some grips from being stable.

There are growing numbers of devices that are produced by non-professional people; these devices are built around open source designs that are customised and manufactured using 3D printing devices. e-NABLE (2014) provides the files and instructions to build a range of tendon driven devices, that rely on the flexion of the wrist to actuate the fingers. The design has been aimed at scalability and ease of manufacturing, all components are readily available and low cost. These devices are not dissimilar to other tendon systems, however, they demonstrate that the correct design can utilise current rapid prototype technology to produce a range of similar devices that are able to increase choice to pediatric patients. Another design by e-NABLE (2014), the Limbitless Arm it is a myoelectric prosthesis, that is designed to be fitted to patients with high transradial amputations. It is an example of a tendon driven device that is driven by an actuator (servo motor) that is mounted inside the forearm.

The research presented by Dechev et al. (2001); Galiano et al. (2007); Hu (1997) shows three devices with varying DOF that are all actuated by a single DC motor. The most simple is the hand by Galiano et al. (2007), a prosthesis designed for a specific four year old paediatric patient. The hand has very similar design to that of the successful OttoBock - System Electric Hand for adults and a similar operation to the RSL Scamp hand. The device has a mass of 185g, approximately sixty percent bigger than commercial equivalents. Apart from re-proving that the existing basic System Electric Hand design can be miniaturised, the report contains no significant advances to the field. As well as this, designing a product specifically for one user can be detrimental to its wider application for other users.

Two other paediatric devices by Dechev et al. (2001); Hu (1997) both have four fingers and a thumb that have coupled closure, as well as manual thumb opposition. These hands are aimed at similar age groups (children aged six and over and children aged between seven and eleven respectively), this target age is slightly older than the target for this research and this allows for greater mass and size constraints. The hand developed by Hu has one DC motor in the palm that provides the actuation through a gear linkage, to simultaneously close the fingers and thumb. As discussed the opposition of the Hu thumb is un-powered, it can be manually positioned into one of three pre-set positions when the hand is completely opened. The report states that the hand came out slightly worse but comparable when tested in practical situations to the Otto Bock system Electric Hand. Although this research presents a novel thumb, it is heavier than existing prosthetic designs and does not provide greater functionality to the user. The final drawback is that the motion of all of the fingers is coupled, so that the motor will stall

when contact is made with a single finger, rather than all the fingers contributing to a grip. This could mean that not all fingers make contact to an object and therefore it could struggle to maintain a stable grip on certain object shapes.

In summary, there have been few examples of research into prosthetic devices for paediatric patients. While the publications discussed cover a range of areas, none present a fully realisable design that could be transitioned into fitted devices. The exception to this statement is the hands that have been developed by non-professional people using rapid prototyping technology. These devices are designed with manufacturability and customisation in mind, demonstrating the possibilities of this technique for low cost and customised devices. But, as they are designed for children with high transradial amputations, they would only be suitable for a low percentage of users.

Research in Force Balancing Mechanisms -

Devices that drive multiple fingers with a single actuator can suffer from unstable grips; because when an object causes a finger to stall, all of the coupled fingers stall as well. This can lead to situations where a larger object is held in a pinch grip as the other fingers have not become engaged. It is only really necessary in tendon devices and systems with coupled finger actuation, as this can be completed electronically in hands with multiple finger actuators. There are two methodologies for counteracting an unstable grip, as discussed next:

Fukaya et al. (2000) presents a solution for a cable driven device, that has been designed to be fitted to a humanoid robot for human/robotic interaction research. It is a pivoted linkage that provides an adaptive grasp for realistic finger movement. The approach to adaptive grasp used by this project is an arrangement of five load leveller mechanisms arranged in a tree formation so that all the fingers are attached to separate end points. This design allows the fingers to move independently and means that force will only be applied to an object once all have made contact; therefore reducing the likelihood of an object being pushed out of the grasp. However, this is a complicated design, since there are fourteen moving parts between the input tendon and the fingers. In its present form, is not strong enough to be used for prosthetic applications because of its construction from low strength materials for weight reduction. Additionally because force is only applied once all the fingers have made contact, if any of the thirty nine links or connections in the hand fail, then the mechanism will fail.

Designs using hybrid tendon-spring drives have been demonstrated (Dechev et al., 2001; Massa et al., 2002). These force balancers, where some compliance has been added to the mechanism, use a compression spring on each of the tendons to create an adaptive grasp that allows the hand to apply differing pressures by each finger to an object. Figure 2.13 shows how the power is transmitted across the spring allowing for different forces to be transmitted across the device. These systems have three operating modes;

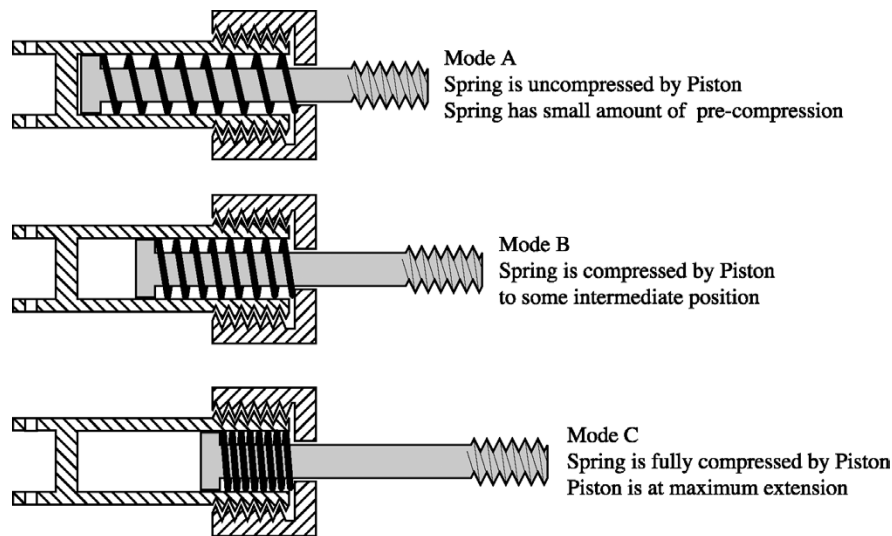


FIGURE 2.13: Diagram of the operating modes of the TBM hand's drive.
(Dechev et al., 2001)

Mode A the finger has not applied pressure, Mode C the linkage is at maximum extension (equivalently rigid), it applies the full force of the actuator and in Mode B the transmission force is variable between no transmission and full compression of the spring (Mode C). These systems enable the hand to use a single larger motor to drive several fingers that are apparently independent. The operating mechanisms of the systems are the same (Dechev et al., 2001; Massa et al., 2002) but the implementations differ. The Dechev et al. design uses individual force balancers for each finger, whereas the Massa et al. research has a single force balancer with individual spring connections. There are drawbacks to this approach. Dechev et al. (2001) conclude that the design provides greater functionality, however at the cost of actuation speed and fingertip force. This is because the springs add a mechanical disadvantage that must be overcome.

Due to the drawbacks, currently there are no designs for a force balancing mechanism that are practical for fitments to a prosthetic device.

Research into Prosthetic Modularity -

Modularity in a design can be both an advantage and disadvantage. The term module is defined as "a set of standardized components for a design" Oxford Dictionaries (2010). Modules of components can serve two functions. Either, standardized components are used together to construct a more sophisticated component, or the modules can be substituted with each other to alter the characteristics and function of a bigger component. Examples of this can be found on modern cars where some parts are used across several different models or different modules are used on the same model of car to create different specifications. Both of these methodologies could be applied to prosthetics, as well as the modularity allowing for reconfigurability during manufacture or by the user, post fitment.

Modular products often have a lower repair time than those without modularity. This is because broken modules can be very easily replaced by low skilled workers and be repaired once the product is functioning again. Modules can be redesigned individually without adapting the entire product. This means that new and updated products can be produced quickly and efficiently at a low cost. A study into the design practices of Nippondenso using panel meters as a case study (Whitney, 1993) highlights how homogeneous design and modularity can be used to achieve a large number of variants from a limited number of distinct modules. The case study shows how a product with six modules each with up to four variants, totalling 17 components, can be used to build 288 individual product configurations. This meant that Nippondenso could offer lots of design variants whilst managing device cost.

There are however inherent disadvantages of using modular systems. The first of these is the initial cost of design and production. The major cause of this is the need for standardization. The interfaces of the modules need to be accurately specified and designed to allow correct assembly. An everyday example of this is bank cards. They are all exactly 0.76 mm thick (International Organization for Standardization (2003)). The dimensions of the cards need to be accurately specified including the position of the contacts for them to work in card readers across the world. These interfaces also contain more parts than the non-modular equivalents. These extra components can add mass and cost to the design, making it heavier. The final problem that can be encountered specifically when the same module has been integrated into several products is module failure. If the module becomes susceptible to failure this will compromise the reliability of the entire range of products, not just one.

Modularity has been a factor in several design philosophies for artificial hands (Han and Huang, 1998; Kyberd and Chappell, 1994; Kyberd et al., 2001; Light and Chappell, 2000), as well as a steady movement towards a more modular-type commercially available prosthesis (BeBionic, iLimb and Michelangelo hands). Kyberd and Chappell have implemented the same knuckle block and finger design for all four fingers. Therefore reducing the total number of different components in the design. Han and Huang have utilised this same design methodology, as well as presenting multiple designs for the individual modules. This allows the device to be adapted depending on the desired cost and functionality. This research has highlighted how choice can be greatly improved; by designing an alternative for three of the modules the research had developed eight different versions of their device. This level of choice could help to improve user satisfaction and therefore alleviate the issue of device rejection.

Modularity is increasingly used in prosthetics to improve manufacture and servicing. However only Han and Huang has attempted to use modularity to increase the choice provided to the wearer. Nippondenso has already shown this to be an effective method for increasing choice, by integrating this into paediatric prosthetics many of the issues highlighted in Section 2.3 by Donovan-Hall et al. could be improved, therefore reducing

rejection. In this project each major component will be a module. They will be designed so that each could be redesigned and replaced quickly and easily by either a prosthetist or by the user.

Low Cost Prosthetics Research -

As well as choice, cost is an important factor in paediatric prosthetic design; as discussed previously, children require the regular replacement of their prostheses to match their growth. When establishing a replacement cycle, a cost benefit analysis must be considered. Therefore, one approach to reducing the latency between replacements is to reduce the cost of a prosthesis. To this end Doshi and LeBlanc (1998); LeBlanc et al. (1997) have taken the opinion that the devices should be low cost enough to be considered disposable. Their approach centres around repeated modules and low cost materials. Although the body powered design that are developed only have a basic functionality, the reported final cost of approximately \$50 justifies this approach. To achieve this cost they have utilised additive manufacturing techniques with light weight foam to create the structure of the devices. Additive manufacture is typically a process that is used to aid the design of prosthetics. Asyali et al. (2011); Bahari et al. (2011); Tang et al. (2011) all use rapid prototyping to proof of concept their designs. Others have been exploring the possibility of additive materials as a final material for the entire product; the e-NABLE hand (e-NABLE, 2014) design costs approximately \$350, the mechanical chassis of the device is entirely printed, only the cables and a few screws are needed to produce a fully tendon driven device. e-NABLE <http://enablingthefuture.org/> Anecdotal evidence from hobbyists demonstrates that the materials are strong enough to produce functional devices as well as proof of concept systems.

Research into Finger Mounted Sensors -

Kargov et al. (2007) highlights how the lack of feedback is detrimental to the usability and function of advanced prosthetics. This statement was affirmed during personal communications with both prosthetists and prosthetic wearers, who demonstrated that the lack of feedback to the user or controller caused many grasping operations to fail.

Pylatiuk et al. (2006) presents the first self contained vibro-tactile device that uses a customised force sensitive resistor (FSR) to detect and communicate force. The research fits the device to a hand and shows a correlation between force feedback and reduced grip force. Asyali et al. (2011); Bahari et al. (2011); Kargov et al. (2007) all use FSRs as fingertip mounted sensors to provide sensory feedback to the hand or the user. Asyali et al.; Kargov et al.; Pylatiuk et al. use sensors mounted on the fingertips to provide vibro-sensory feedback to the user. This allows the wearer to adjust the grip strength as necessary to maintain a stable grip. Asyali et al. only discusses the implementation of the sensors on their device, whereas Kargov et al.; Pylatiuk et al. states the implementation as well as the advantages of the sensory feedback. They have shown that user force feedback reduces the applied grip force by half whilst, improving control without visual feedback. Pylatiuk et al. also demonstrates that vibro-sensory feedback fitted to either

the patients skin or to the prosthetic device can provide a reduction in the required gripping force of up to 76%. This research also comments positively on the acceptance of this technology by the users.

Bahari et al. has used sensors in a closed loop system to maintain a stable grip. The research includes a characterization of the sensors but does not discuss the benefit of the practical application suggesting that these tests were not completed at the time of print. At the University of Southampton, there has been significant research into the possibility of adding force (Cotton et al. (2005)), slip (Lowe et al. (2010)) and texture sensors (Muridan et al. (2010)) to upper limb prosthetic devices. This research has shown that it is possible to add sensors to the fingers of prosthetic devices that provide clear and accurate tactile data. Yet this research has not had rigorous testing on fully functioning devices, and therefore awaits to be implemented on commercial devices.

In summary, this research demonstrates that vibro-tactile feedback to the user improves grip force and ability of prosthetic devices. Whilst identifying that the feedback also improves acceptance. Although functional this research has all failed to show commercial implementation or to be incorporated into existing technology. Thus, these advances have failed to reduce prosthetic rejection as has been eluded in the presented research. A gap in the field is evident, which has been identified by funding organisations. The EPSRC has just awarded a large collaborative grant to Nazarpour et al. (2015) to investigate the next generation sensory feedback for assistive devices.

Humanoid Hands for Robotics -

Research into robotic hands has provided few designs that provide advancement to prosthetic design. Most robotic devices are not suitable for prosthetic fitment. This is typically because of three factors; mass, size and power consumption. Yamano and Maeno (2005) have designed an advanced robotic anthropomorphic hand, actuated with a combination of motors and elastic elements that drive a pulley design. It has four actuators in each finger, one driving each of the three joints and another providing adduction. The thumb also has four actuators that drive the closure of all the joints and provide opposition. This is lighter than most existing robotic hands, however it still has a mass of 853g and is much too heavy to be used as a prosthetic design. The design is specific to robotic research and it has not been designed to be robust enough to withstand the operating environments that prosthetic hands need work in. However, it is a design that exemplifies sixteen independently driven DOF, including an opposable thumb, that is able to form greater than 16 grip patterns.

Research into non-anthropomorphic designs usually have shapes similar to pincer style robotic actuators. Some of these designs have been shown to be able to replicate humanoid grip patterns Ulrich et al. (1989). Most of these designs are centred around gripper development and these are usually too heavy to be considered for prosthetic use.

Typing -

The last hand of note is the design that is presented by Thayer and Priya (2011) called the Typing DART Hand. As suggested by the name this design is specifically designed to give the wearer the ability to type. It is primarily designed as a robotic research device but the task that is being attempted is more complicated than it may be perceived. It may be assumed by people that have not attempted to type with a prosthetic that it is a trivial task. However, it requires a multitude of controlled movements of the fingers and wrist, including abduction and adduction of the fingers. As well as a method for supporting the hand without mashing the keyboard is required; as supporting the limb quickly becomes tiresome. The final solution is a tendon driven design with nineteen servo motors mounted in the forearm. This is a novel design for the fingers. It is actuated by three pairs of tendons each controlled by its own servo motor, two control the closure and the other controls the abduction and adduction. The design has a solid proximal phalange with a universal joint at the MCP to allow for the two DOF. This is then connected to the distal phalange via a four bar linkage which makes up the intermediate phalange. This design allows for a good curling motion and with a high number of individually controlled axes of motion. The wrist then has another three directly coupled servo motors that provide abduction/adduction, flexion/extension and rotation. It is assumed, due to lack of documentation that there are four motors that control each joint of the thumb individually. The final design of the hand and forearm is a flexible and can form many grip positions. It has a similar range of motions, mass and size to that of a human male hand, although the grasp speed and fingertip force are markedly lower. Thayer and Priya presents an advanced robotic device that with some development could be fitted as a prosthetic device with a high level of functionality. However, the wearer would have to have an elbow dis-articulation or above. Two of these hands, placed in the right positions can support their weight on a firm surface whilst, typing using any of the keys on the QWERTY section of the typewriter keyboard, without the need to move the arm section of the device.

Thayer and Priya (2011)

Pneumatically Actuated Prosthetic Research -

The Fluidic hand presented by Kargov et al. (2007) and Gaiser et al. (2009) and featured in Baggott (2008) is the only example of a hydraulic hand that is completely self-contained. The hand aimed at adult fitment has active joints in all of the MCP joints and in the PIP joints of the first and second fingers, and there are two joints at the base of the thumb that allow for closure and opposition. This gives eight separate DOF that are all individually controlled by miniaturised valves that redirect power from a miniature hydraulic pump placed inside the palm. The hydraulic actuation causes a smooth and more natural motion of the fingers than other designs. A basic vibro-tactile (Vibrational feedback) system is used to transmit feedback to the user. It operates using a commercially available Force Sensing Resistors (FSR) to detect contact, and uses an

analogue circuit to directly drive the vibrational motor. This is a very simple yet effective method to transmit feedback to the user. This hand has a mass of 353g without a cosmesis, has a 110N maximum grip force and an operating noise of <45dB(A) at one meter (approximately equivalent to a radio in the background). These characteristics are better than the market leading Ottobock System Electrohands. With the smooth actuation provided by the hydraulics, and the favourable comparison with commercially-available hands, this design could suggest that the new state of the art may be hydraulic. The one drawback is that all of the drive components are custom-built miniature devices, leading to two conclusions; the design would be prohibitively expensive and, at present, could not be miniaturised further, therefore, it is not a viable solution for child prostheses.

2.5 Discussion

In this literature review it has been shown that an estimated 250 five year old children could benefit from an advanced prosthetic upper limb device in the US; and 1,100 in the G8 and EU countries.

From the literature search it has been found that commercially available myoelectric prosthetic hands for children offer significantly less functionality than the adult equivalents. Hands for children that are available provide a single degree of closure whilst, the viable devices that are presented in the research literature offer limited additional functionality. Donovan-Hall et al. (2012) as well as others have highlighted how this lack of functionality is a primary precursor to high rates of rejection. Indicating that a route to minimise rejection of pediatric prosthesis is the development of advanced devices.

Research into both adult and child prostheses have been identified, posing the clear gap in the progress between the two disciplines. Dechev et al. (2001) has presented the most complete research into an advanced prosthetic hands designed for children. It contains several novel advancements in child prosthetics. However its fitment viability is limited by a relative high mass and a low actuation speed. Dechev et al. as well as others (Guo et al.; Light and Chappell) have solutions for an under-actuated curling finger design, which curls at both the PIP and DIP joints, although when presented alongside transmission characteristics these devices transmit limited forces.

Doshi and LeBlanc suggest in their conclusion that a solid DIP joint could help provide a better solution for a curling finger design, it would increase force transmission without dramatically detracting from the realism of the finger movement and the effectiveness of the grip function. Integrating this proposition into the design for a linked curling finger could provide a curling finger with a lower mechanical disadvantage and a realistic curling action.

A design concept can be gleamed from all the advanced adult hands. To minimise cost and increase potential market a modern device contain a high level of modularity to allow a varied market with a range of possible end applications. Areas such as cost, modularity and force sensing have also been identified as disciplines where advancements have been made, and where further development is necessary. However it is clear that the primary focus of future research should be to develop a child's hand that is viable for commercial fitment that encourages lower rates of rejection. This device should aim to have multiple DOF, including a thumb that is capable of closure and opposition, to match the devices becoming available for adult fitment.

The design philosophy of this research is to increase children's acceptance of their prostheses. This aim will be fulfilled through the development of a highly functional humanoid prosthetic hand, able to form most common grips, with an anthropomorphic finger closure trajectory and a thumb that has both driven opposition and closure. Cost and mass are major stated obstacles to rejection, whilst the literature drives the reasoning that a prosthetic hand must be adapted to the user and fitted to suit the needs of every day tasks. This design philosophy aims to reduce the rate of rejection by providing increased functionality to the user

The research that has already been completed at the University of Southampton (Redman et al., 2011) shows that this goal is feasible but posses varied technical challenges and performance trade-offs.

Chapter 3

Technical Discussion

To realise the stated design philosophy there are a constraints that must be considered and different technical solutions that could be employed. This chapter will firstly discuss the physical constraints of designing devices for a children's demographic. Then the viability of the different technical options will be identified and discussed. It will start with a investigation into possible actuation methods followed by drive mechanisms and typical control methodologies. in order to facilitate research into a prosthetic hand .

The available solutions for each aspect are identified and discussed, endorsing the research route that best supports the design intent.

3.1 Normal Hand Measurements

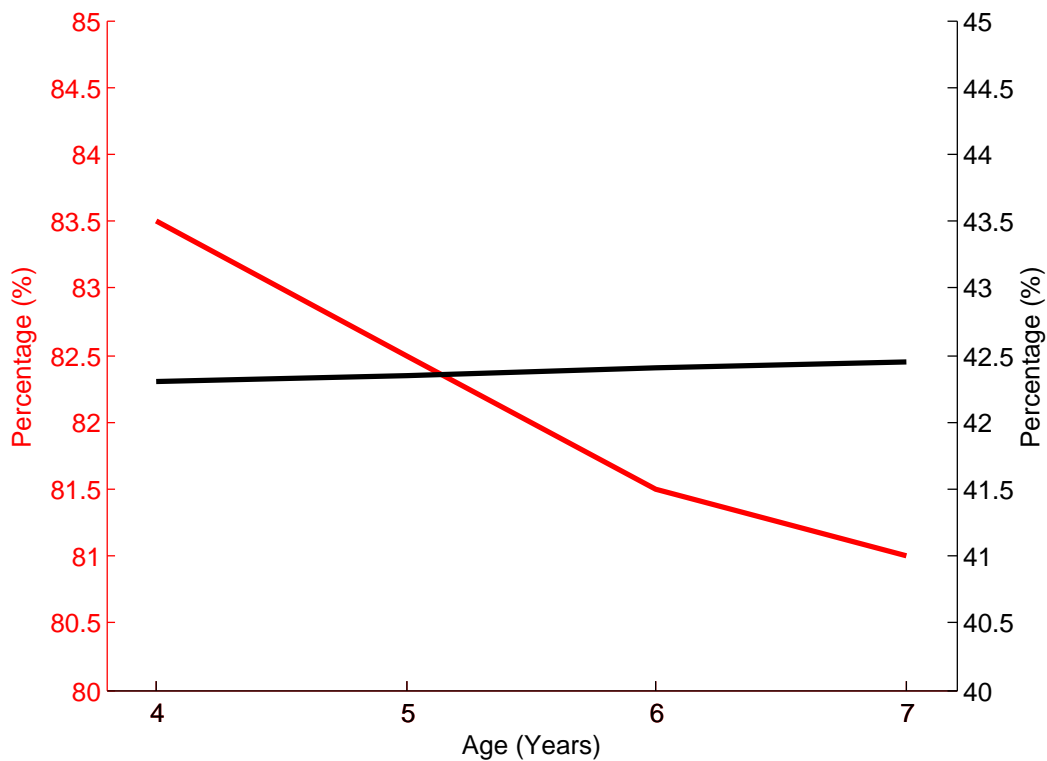
A child's hand is smaller than that of an adults. Because of this when designing prostheses for children there are issues introduced due to the tighter size and mass requirements. Table 3.1 shows the normal measurements of a child's hand taken from Hall (1989). It can be seen that that size of the hand increases as the child ages. However irrespective of age, the proportions of the hand are virtually unchanged as the child matures. These are averaged values, however for the research described in the thesis it will be assumed that these sizes are accurate representations for the specific age groups. Another assumption is that at 16 years a persons hand is the size of an adults (decided by comparison of adult hand sizes).

Table 3.2 shows the comparison of normal measurements of a child's hand compared to that of an adults. It can be seen that at each age the ratios between the measurements are relativity constant, this allows for an average to be taken for each age compared to that of a 16 year old. Another observation is that the average for each age increases by approximately 3% each year. This suggests that the hand grows proportionally and therefore a five year old's hand is approximately two thirds smaller than that of the

TABLE 3.1: Normal Measurement of a child's hand aged 4, 5, 6 & 7 years compared to that of a 16 year old's hand. (Table adapted from Hall (1989).)

	4 yrs	5 yrs	6 yrs	7 yrs	16 yrs
Hand length, mm	120.0	125.0	130.0	137.5	187.0
Middle finger length, mm	50.0	52.5	55.0	57.5	80.0
Palm length, mm	68.0	72.0	75.0	78.5	107.0
Palm width, mm	54.0	57.0	59.5	62.0	82.5
Ratio of palm width to hand length, %	83.5	82.5	81.5	81.0	80.0
Ratio of palm length to hand length,%	42.30	42.35	42.40	42.45	42.75

FIGURE 3.1: Plot of ratio of a child's palm length to hand length (Black), % and palm width to hand length (Red), % against age



average 16 year old. When data for a child of five years was missing the average of these values was used to scale any available adult data.

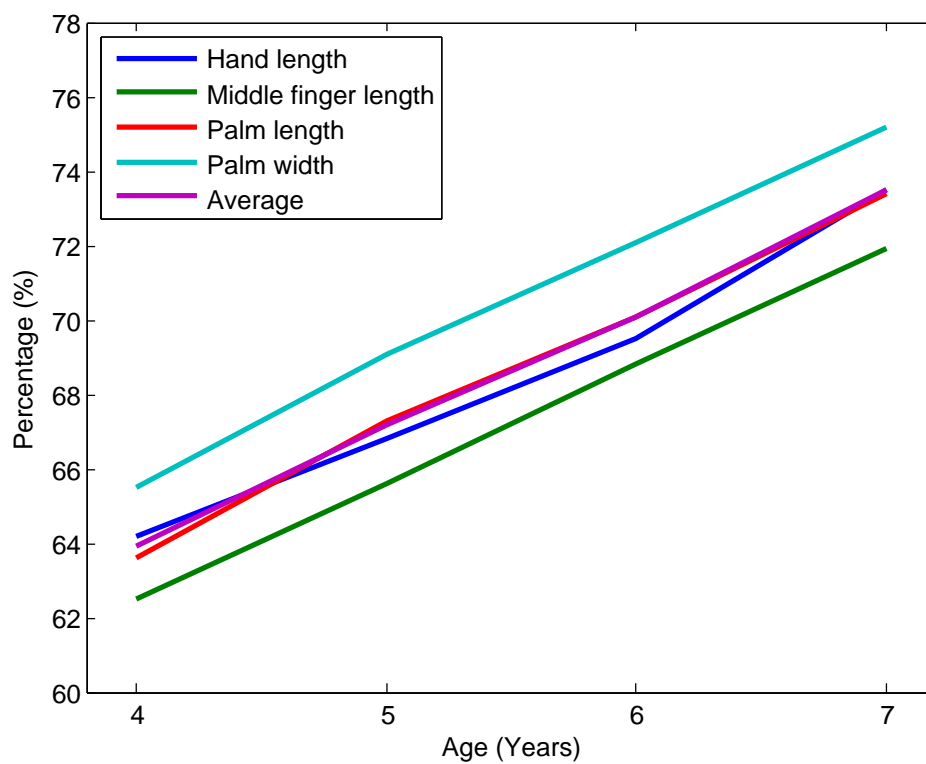
3.2 Actuators used in Prosthetics

There are several established methods of actuating prosthetic hands. These methods are body power, electric motors, shape memory alloy and compressed air. Each of these have their own advantages and disadvantages.

TABLE 3.2: Comparison of 4, 5, 6 & 7 year old child hand sizes with a 16 year old's hand. (16 Year old assumed to be adult)

	4 yrs, %	5 yrs, %	6 yrs, %	7 yrs, %
Hand length	64.2	66.8	69.5	73.5
Middle finger length	62.5	65.6	68.8	71.9
Palm length	63.6	67.3	70.1	73.4
Palm width	65.5	69.1	72.1	75.2
Average	63.9	67.2	70.1	73.5

FIGURE 3.2: Plot of percentage different in child's hand to that of a sixteen year old



Body Power: Uses specific movements of the wearer to actuate the prosthesis. Power is transferred from a joint to the limb with the use of a harness and cables. Usually this system is actuated with the tensing of the shoulders and back. An example of this can be seen in Figure 3.3. This is a good method for providing sensory feedback to the user. It provides an effective grip, however, the positions in which the limb can effect a secure grip are limited (Carey et al. (2009)) and at certain times, altering the limb position can cause it to drop the object in its grasp. The disadvantage of this type of drive system is that the opposing force is provided by an elasticated module. This force is always present and therefore must be overcome to produce actuation. Thus, the total force that can be applied by the prosthesis

TABLE 3.3: Normal Measurement of a 5 year old child's hand.

Hand length, mm	125.0
Middle finger length, mm	52.5
Palm length, mm	72.0
Palm width, mm	57.0
Ratio of palm width to hand length, %	82.5
Ratio of palm length to middle finger length, %	42.35

is the user input force minus the elastic force of the prosthetic. Kuniholm (2009) states that this design has changed little since it was patented in 1912, by D.W. Dorrance, Hosmer Dorrance Corp. (2012)

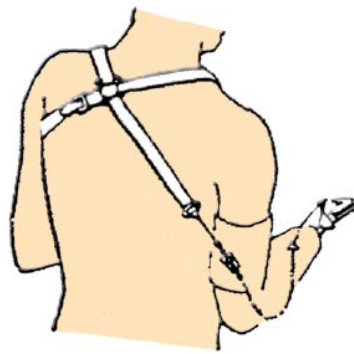


FIGURE 3.3: Diagram of a body powered prosthesis harness on a wearer.
(<http://www.waramps.ca/nac/life/stages.html>)

Electric Motors: Direct Current (DC) electric motors are used in most prescribed externally powered prostheses. This is because they offer several advantages without the varied drawbacks that other actuators possess. DC motors offer high power and speed, whilst providing reliable controllability. However, they still have disadvantages caused by the need for batteries, which are limited in power and increase the mass of the design. There are two common types of DC motor brushed and brushless motors. In principal the operation of both is the same, a field produced by the electrical current causes rotation. However, these methods differ. A brushed motor uses a mechanical link called a commutator to alternate the field and cause rotation. In contrast, a brushless motor uses electronic circuitry to cause this alternating field. There are many advantages and disadvantages of both. The key points are that the brushed motor is low cost and easy to control however the commutator causes friction on the rotor, limiting the speed and lifetime of the motor. Whereas the brushless motor is more expensive as control circuitry is required to switch the currents and track the position of the rotor. The benefit of these type of motors is the high speeds and high reliability. Servo Motors used in radio controlled (RC) models are another form of DC motor that has an inbuilt position feedback. This means that they are controlled by a signal that indicates

the desired position. They are often used in RC applications ahead of other actuators due to the low cost and ease of operation. However they usually have low output torque and only have a range of approximately 180°.

Shape Memory Alloy (SMA): Shape memory alloys are metals that react to changes in temperature, with a change in their shape; they are typically longitudinally contracting and radially expanding. Depending on the material, actuation can be caused by either temperature or the application of current. An application of current is technically secondary actuation, since the process causes internal heating due to resistance, thus causing actuation.

In prosthetic design SMA actuators could be implemented in two different methodologies. The first would be using the actuator to drive a tendon based system resembling the human body, where the actuator would be used to pull the tendon which would in-turn drive the actuation. The other application methodology would be to build parts of the exoskeleton from SMA, as the device is actuated this would cause the physical shape of that component to change and actuate the hand.

There are advantages due to the simplistic nature of shape memory alloy actuators, however, they are usually slow to respond and take time to return to their original shape. The return speed can be increased with the use of a spring. This however, introduces a force that needs to be overcome, reducing the total applied force and causing an additional delay in the response time of the system. Another drawback of this system is that it can be affected by changes in the ambient temperature. This could cause inadvertent actuation during activities such as cooking or transferring between hot and cold environments. The lifetime of this system is proportional to actuation distance. This means that the more actuation that is achieved, the lower the total number of cycles (the less time it will last); this reduces the reliability of the product. An example of a device that uses this type of actuation is the hand presented by Bundhoo and Park (2005), although the research concluded that more research was required into bundles of SMA, to provide sufficient actuation forces.

For these reasons the current state of the art of SMA technology is unlikely to be able to provide sufficient actuation and reliability for use in prosthetic applications.

Compressed Air: These designs are normally lighter than the equivalent electrically driven alternatives. This is because the power is produced by compressors which are usually mounted externally. This means that the compressed air needs to be piped to the hand from a unit worn on a belt. The draw back of this technology is that these tubes are vulnerable to damage and snagging, as well as users finding this extra equipment irritating and cumbersome to carry. This system is still useful, due to the high forces and actuation speeds that are produced. The use of compressed gasses can lead to excessive acoustic noise.

Of the actuation solutions that have been discussed the DC motor is the most viable solution to provide multiple actuators on a prosthetic device. Bodily power would not be able to provide multiple actuation, Shape Memory Alloys would not be able to provide the speed and range of actuation, whilst, pneumatics would likely require an external compressor which was felt to be non optimum. From this point onwards, the research will focus on a prosthetic hand that is an externally powered prostheses, powered with a DC electric motor.

3.3 Actuation Mechanisms used in Prosthetics

In prosthetics the actuator cannot directly power the movement of the finger, however there are several methods of transferring the power from the actuator to the fingers. Some of these methods are more practical than others, each having their own advantages and disadvantages.

Capstan & Bowstring: This mechanism uses a cord wound around a pulley to transfer rotational to linear motion and, in certain circumstances, the linear to rotational motion. The cord used is usually a wound metal or plastic cord because they are able to transmit high forces without stretching. This device is able to transmit power around corners and into different planes with the use of pulleys or rotation around the bow string. This allows for them to be used in situations where the contact angles or transmission routes are variable. However the cord is susceptible to wear and therefore to breaking. Another problem that can occur is the cord slipping, this causes a loss in the total power transmitted and would cause the system to lose its exact position. Since this system can be driven in both directions to sustain a grip the actuator must be used to apply a constant pressure or an external locking mechanism must be used. These systems can be used to actuate tendon driven systems such as the one shown in Figure 3.4(a). The cable is used to draw the tip of the finger towards the knuckle, causing closure.

Lead Screws: A lead screw is a rotary to linear gear system. They work on the principle that, a nut that cannot rotate that is on a rotating thread will be driven along the thread. These are regularly used in workshop machinery, such as lathes, to control the position of the cutting tools. Lead screws allow for high precision control however are affected by increasing frictional losses as the transmitted forces increase. The method used to negate this is ball screws. This device works on the same principle, however it uses ball bearings to transmit the load between the nut and the screw. These designs are more complicated than a simple lead screw because they require the ball bearings to be recycled around the nut; See Figure 3.4(b). This means that the ball screw is significantly heavier than the lead screw.

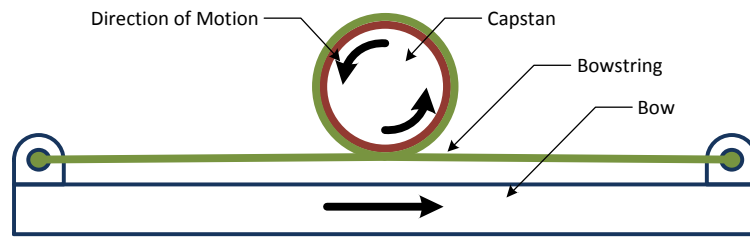
For these reasons the lead screw and ball screws are not regularly used in prosthetics. An advantage of this is that it can only be driven from the screw the nut cannot transmit rotational power to the screw. This means that it has an inbuilt self locking.

Direct Gearbox: This system uses a motor gearbox with the drive output positioned on the axis of rotation. This system is used on many conventional child prosthetic devices because it provides a basic yet efficient actuation. The other reason for the use of direct gearboxes is that they are relatively low cost and therefore they can be constructed to give high reliability. If the gearing ratio is large enough then the system can only be driven from one direction, this creates an auto locking situation. However these are often heavy.

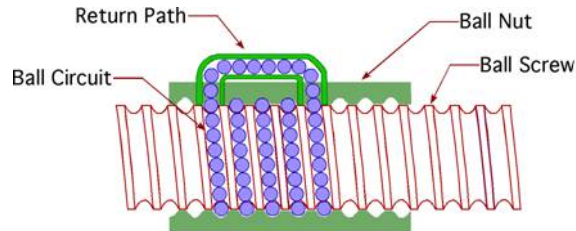
Worm-Wheel: A worm wheel is a rotary to rotary gear chain with a high reduction ratio, that translates the motion through 90° . This is achieved through the use of a threaded rod (called the worm) and a traditionally shaped gear (called the wheel). As the worm is rotated, the wheel is driven around by the thread; each full rotation of the worm drives the wheel by a single thread. This means a worm wheel has a much higher reduction ratio than a conventional gear system, within the same space. The worm can either be hollow designed to turn on an axle, or be incorporated onto the shaft. There are specialized worm wheel combinations that have concave sections that increase the number of teeth meshing. These specialized gears can therefore transmit greater forces than conventional worm-wheels. An advantage of worm wheels is that they typically can only be driven by the worm. This means that they provide self locking. The disadvantage is that they are heavy due to the volume of the worm. Due to the translation of the motion they are unsuitable for some gearbox applications.

3.4 Electromyography (EMG) Control

Electromyography (EMG) control is the use of the electrical signals produced by the muscles to act as the input to the controller. It was first used to control a prosthesis by Reiter in 1948 (Zecca et al., 2002). These inputs can be used in several different methods. The most simple and common method used is digital sensing to select an open and closed state. There is advanced research into the characterization of different EMG signals. This would allow the user to select the desired states with the actuation of specific muscles. This has not yet been achieved due to the stochastic nature of the EMG signal; for a particular muscle no two signals are identical (Micera et al., 1999).



(a) Capstan and Bowstring mechanism.



(b) Ball Screw & Nut Showing Ball Return Path and Circuit. (<http://www.daerospace.com/MechanicalSystems/PowerScrewsDesc.php>)



(c) Worm Wheel. (HPC Gears Ltd (2011))

FIGURE 3.4: Actuation Mechanisms

3.4.1 EMG Detection

EMG is the method used to detect the electrical signals produced during skeletal muscle contractions. These signals can be interpreted and used to control the actions of prosthetic limbs. The electrical potentials in the body are caused by groups of muscle cells as they are activated. These groups are called Motor Units; they are the smallest group of muscle fibres that can be individually triggered within each muscle. The size varies significantly depending on the function of the specific muscle and the level of control required. The muscles in the hamstring have large motor units whereas the motor units in the eye are very small.

There are two main methods of detecting the signal. The first is using intramuscular electrodes this method uses a wire or a needle to detect the signal from inside the muscle. This method detects the clearest and most isolatable signal. This method is most commonly used in the assessment and classification of muscular control. It is not

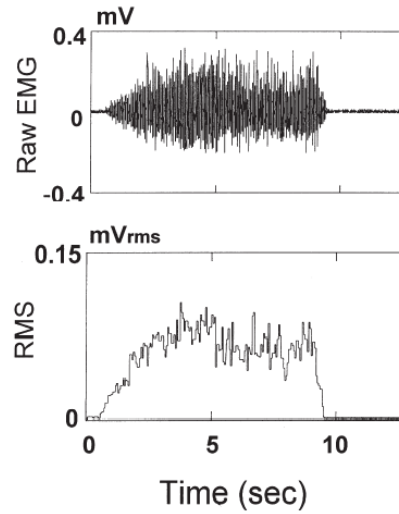


FIGURE 3.5: Example of a recording of an EMG of a healthy subject. (A) The raw EMG signal; (B) The signal extracted by a comb filter applied to the EMG signal of (A); (C) The RMS of signal (B). (Adapted from Frigo et al. (2000))

often that this method is used in prosthetics as the wire or needle becomes irritating if left inside the muscle for long periods of time. Another method of detection using surface mounted electrodes that are often dry and do not require conducting gel. This method is most commonly used in prosthetics, and uses flat metal electrodes placed on top of the skin to detect the signals. Although this technique provides a lower level of signal than intramuscular detection it causes significantly less irritation and is completely non-invasive. Non-invasive techniques reduce the need for specialized user training and effectively removes all chances of infection.

For prosthetics the EMG signal that is detected is a local differential signal, which is typically detected using three electrodes a positive, a negative and a ground electrode. This system provides a robust system with a high common mode rejection. Luca (1997) states that when using differential electrodes the shape and area of the electrode surfaces and the separation between the electrodes surfaces are non trivial. This is because they affect the amplitude and the frequency content of the signal that is detected. They therefore suggest an electrode with the characteristics shown in Table 3.4.

TABLE 3.4: Suggested Differential EMG Electrode Configuration (Luca (1997))

- Bandwidth of 20 - 500 Hz with a roll-off at least 12 dB/octave
- Common mode rejection ratio >80 dB
- Noise <2 μ V RMS (20 - 400 Hz)
- Input impedance >100 mega Ohms
- Align the detection surface oriented perpendicularly to the length of the muscle fibres

EMG detection and control gives a useful and flexible control that most users are able to adapt to using. The more basic control structures are more easy to adapt to and therefore can actually prove the most implementable. Traditional single or double EMG

control works successfully but has not advanced commercially in line with developments in hand prosthetics. If better detection systems were commercialised then these hands could have individual control for each finger and therefore, an infinite number of grasp patterns

3.4.2 EMG Control Schemes

The EMG input can be utilised to drive one of a few control methodologies. The precise implementation of each system varies from patient to patient and hand to hand as the abilities and requirements of the patient vary. The current state of the art for the control schemes ranges from a simple digital control to complex virtual menu systems controlled from dual inputs. These are described next.

Digital Schemes are the most basic system for controlling prostheses. They work by selecting either an open or closed state depending on the input. Typically the device will actuate with an input signal and then automatically return to a prehensile state when the signal is removed. These systems are regularly used in child prosthetics since there is no requirement to have a more complex system. The advancement of this methodology is an analogue system; they have the same functionality as the digital version except, that the closure speed or force is proportional to the EMG signal.

Double EMG electrode systems allow for control systems with multiple grip patterns. These schemes use virtual menus and input combinations to select the different grips, and then actuate the device. This allows controllers to be developed that use level based menus to select their grips. This simple yet effective method of controlling hands with training can allow users to quickly achieve multiple grips. These can be cyclical processes or traditional hierarchical menus. An example of the cyclical menu systems is the Southampton Adaptive Manipulation Scheme (SAMS) (Light et al., 2002) this method uses two EMG inputs and tactile sensors on the prosthesis.

It can be seen in Figure 3.6 that the hand has five states. In the position state the hand takes a prehensile posture and begins to close. The fingers stop when they make contact with an object. The hold position makes use of the tactile sensors to maintain a stable grip. From this the object can either be squeezed or released. After releasing the cycle begins again. This is a similar methodology to those used by the commercial systems.

A new development in the control of adult prosthetic devices is the “grip chips” developed by Touch Bionics. These devices are bluetooth enabled disks, that are programmed by the user to activate specific grip modes. To initiate the grip, the user simply swipes the hand past the chip, then actuates the open and closure as normal. The intention is for these chips to be placed on or near objects that require specific grips. This development dramatically reduces the complexity in changing the configuration of the hand and increasing the usability.

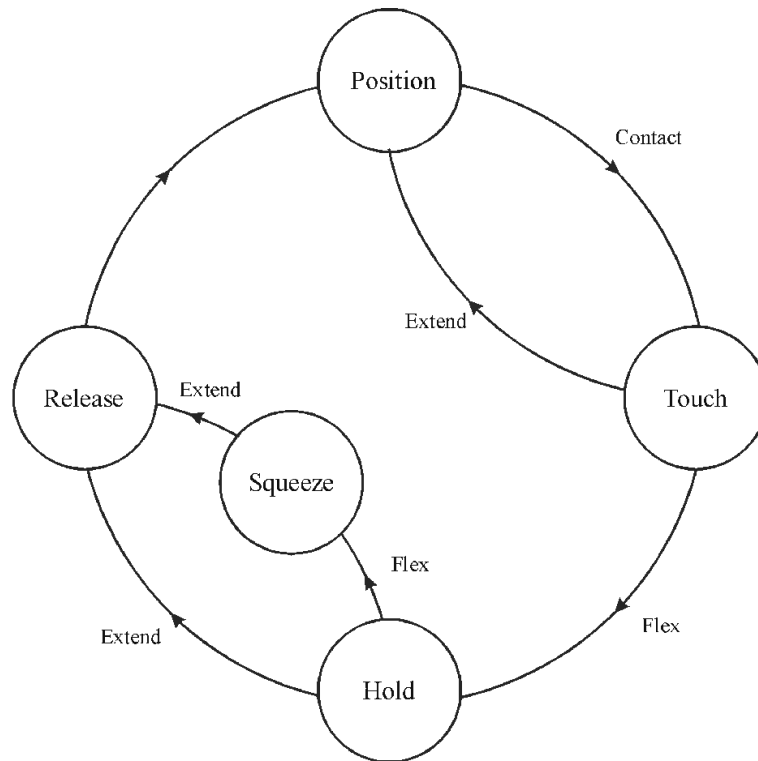


FIGURE 3.6: Diagram showing the operation of SAMS. (Light et al., 2002)

Multiple methodologies have been discussed that provide differing levels of control to the patient. All are driven by EMG control and no one system is a fit for all patients. For this reason it is felt that a device should be adaptable. Although the control methodology is an important factor when choosing a prosthetic device, current microcontrollers provide the ability to alter the control methodology. To allow for a development unrestricted by control method, the device presented in this thesis will not be designed for a specific control methodology. Instead it will provide both a digital communication input that can communicate with a microcontroller and an analogue input for interfacing with current EMG sensors. This will allow the prosthetic device to interface with both current and future control methodologies.

3.5 Materials

The choice of material in any design is fundamental. It has the obvious implications on the strength properties of the design. However, it also affects which machining methods can be used, therefore affecting the form and cost of the design. In prosthetics the two main materials that are used are metals and plastics. There is another material, Rapid Prototyped Plastic that is popular in product development. This material is starting to be used for products, as the materials developed for it become more durable.

Metals: Metals are the strongest of the materials discussed in this project. They have a higher density, and components tend to have a high mass which is a disadvantage. Metals and plastics can be manufactured using many processes such as milling and drilling. These processes are all well established construction techniques that can be accurately controlled giving high finishing tolerances. The main reason for the use of metals in prosthetics is the high forces that can be transmitted and the impact forces that it can withstand. The drawback of this material is the cost of both the material and the manufacture; complex components made in small volumes can become prohibitively expensive. This is due to the multiple machining processes that are required to form the required shape.

Engineering Plastics: Plastics are inexpensive materials that have many different characteristics. Those defined as engineering plastics are lightweight materials that have good strength properties; they are often rigid but can withstand a reasonable stress before failure. Plastics typically have a high resistance to corrosion from acids and other corrosive substances, therefore making them a good product to use where waterproofing or protection from harsh environmental factors is needed. Usually plastics are susceptible to deformation at temperatures above two hundred degrees centigrade. Depending on the exact material, they will either melt or degrade, meaning that they are unsuitable for high temperature applications. As with metals plastic products made in small volumes can become expensive. This can be more than hundreds of times greater than the material costs.

Rapid prototyped PolyJet Plastic: This material is produced using a 3D printer that builds up two dimensional layers of plastic to form a product. There are other techniques that can be used to rapid prototype plastics however the Objet PolyJet process is described here as it is the process that is available at the university. The manufacture process can be seen in Figure 3.7. It uses a UV light to cure layers of liquid polymer printed on top of each other. This process is repeated to create a 3D product from layers of 2D layers. The shape of some products requires a support material to be used to build a feature during construction. This material is easily washed away after construction to reveal the component. Unlike other processes this uses an additive construction method; using a mixture of plastic materials to create a digital material. This means that, depending on the design, there can be significantly less material lost during construction.

This material has several advantages that the other materials cannot achieve due to the additive nature. The first is that fully constructed functional products can be produced without the need for assembly since two components can be constructed together, pre-assembled with a clearance that allows for movement. The second significant advantage with this form of construction is that the materials are digital. This means that the mixture of the two plastics can be altered as a layer is printed to vary the mechanical properties. An example of this is that two different

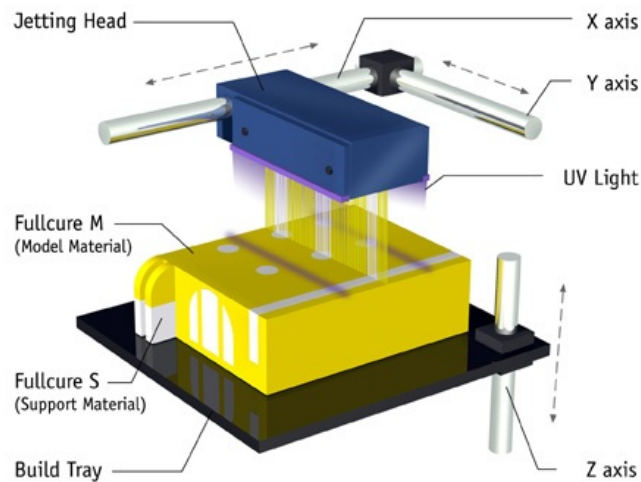


FIGURE 3.7: Diagram of the rapid prototyping PolyJet plastic manufacture process. (Objet Geometries Ltd. (2011))

materials, one elastic and one stiff, can be used in differing combinations to produce materials with varying elastic properties. This advantage can be extended since the ratio of a digital material can be altered during the printing process to create a product with different properties distributed throughout the component. This can be used to manufacture many advantageous profiles such as hinges and soft grips. A property that is unavoidable with these materials is that they have a low melting point. This is because they must be melted to allow manipulation during printing. The significant drawback of this type of material is that there is a lack of complete material specifications published by the manufacturers. In some circumstances they could fail due to unforeseen fatigue due to ageing, wear or chemical attack. The other drawback of this material is that due to the layered nature of the product it will possibly not have isotropic characteristics; this is similar to composite materials such as carbon fibre. These characteristics are not specified in the data sheets for the products. If this characteristic was present then, unlike carbon fibre, the directionality of the strengths (therefore the weaknesses) cannot be realigned. The whole product must have the same directionality which could create weak points in the design. The final drawback of this material is that due to a support material having to be used during the construction the product cannot be made to strict tolerances.

This method has several advantages over traditional construction techniques. The first advantage is the speed of construction, for a project with multiple small and complex components, this significantly decreases time to complete the manufacturing process. The second advantage of this process is that it has a low cost compared to other techniques. This is because of the increased speed of the process and that it is almost entirely computer controlled. It has been found that this process can be up to ten times cheaper than traditional techniques.

Fused Deposition Plastics: This is a method used to facilitate rapid prototyping (termed fused deposition modelling (FDM)), where an extruded plastic filament is melted and then deposited into layers by a robotic stage, much like the Objet machines. Depending on the printer this method is able to produce parts made from multiple materials; ABS, HIPS (High Impact Polystyrene), PLA (Polylactic Acid), PVA (Polyvinyl Alcohol). The resolution of these machines is limited by the extrusion nozzle and the height resolution of the print head. The minimum wall thickness of a component is determined by the extrusion size, and is typically between 0.3mm and 0.5mm, and This nozzle has a positional resolution of 10 micron in the X, Y axes and can resolve layers down to 20 microns. The materials produced by this process have similar properties as those printed by the Objet devices, including the isotropic nature developed by the layering process. The advantage of this process over the Objet system is cost; the print material is about one twentieth of the price and the printers can be purchased for as little as £500. This comes at a trade off as these printers do not have the print resolution that the Object device has they do not have a digital material capability that allows the Objet systems to vary the material properties during printing.

An example of a FDM system is the ROBOX C Enterprise UK LTD. (2015) printer. It is available for less than £800 from multiple on-line retailers. It has an extrusion size of 0.3mm and a resolution of 7,7,20 microns in the X, Y and Z axes respectively. The material for this device cost approximately £30 for a reel containing 600g of material.

TABLE 3.5: Materials Comparisons

	Aluminium	Stainless Steel 316	Titanium	Nylon 6,6	Object ABS like	ROBOX ABS
Material Mass, g/cm ³	2.70	7.99	4.51	1.14	1.2	1.0
Youngs Modulus, GPa	70	193	116	2	2.6	2.25
Tensile Strength, MPa	90	515	520	90	55	44
Melting point, °C	660	2500	1668	255	58	88
Isotropic	N	N	N	N	Y	Y
Cost per tonne, £	2,220	4,450	17,000	2,000	990,000	50,000
Cost per m ³ , £	6,000	34,600	76,500	2,300	1,200,000	50,000

A direct comparison of the most suitable materials for prosthetic development are shown in Table 3.5. Care must be taken comparing the cost per tonne and cost per m³. Care should also be taken when comparing the materials for additive manufacturing (rapid prototyping) and subtractive manufacturing (traditional manufacturing methods) because manufacturing with subtractive process incurs additional costs due to the machining and the material that is removed.

3.6 Discussion

The physical dimensions of the average child's hand against age has been presented; therefore defining the critical size of the research device. It was shown that the average five year old child has an average hand that is 125.0mm long and 57.0mm wide. This has an average middle finger length of 52.5mm and a palm length of 72.0mm.

This chapter has evaluated the different technical solutions that are available to this research. Outlining the advantages and drawbacks of each option. It was decided that the research will rely upon actuation via DC motors combined with an option of possible actuation mechanisms. DC motors were chosen as the most suitable option because, it offers the best solution for providing multiple actuators into a light weight and adaptable device. It is also the methodology used in all current commercially available actuated hand prostheses.

It was highlighted that the device could be manufactured from a variety of materials. Traditional metals and engineering plastics were discussed alongside FDM plastics. Each material has advantages in their physical properties, metals have high strength but a high mass whilst, engineering plastics have a low mass and low strength. FDM materials have the benefit of a low cost and adaptable manufacturing method as a trade-off against the material strength. This research will investigate the feasibility of using FDM materials as a manufacturing material for prosthetic applications. With this methodology low cost components could be manufactured while allowing for individual customisation during manufacture.

To allow for a development unrestricted by control method, the device presented in this thesis will not be designed for a specific control methodology. Instead it will provide both a digital communication input that can communicate with a microcontroller and an analogue input for interfacing with current EMG sensors. This will allow the prosthetic device to interface with both current and future control methodologies.

Chapter 4

Research Approach

As discussed in Section 2.4 (Prosthetic Hand Designs) there are challenges facing research into prosthetic hands for children. The key challenge is to increase acceptance of the devices, and thus prevent rejection. To do this, this research has focused on developing a highly functional humanoid prosthetic hand that is lightweight. The biggest limitation to the research (as faced in all other prosthetic research for children) was the constraints on the size and mass with the requirements for robustness; these influences will be seen throughout the presented solution.

Due to the multi faceted nature of a prosthesis, the research is structured into distinct sections. These sections are; Fingers, Metacarpophalangeal (MCP) Joint, Thumb, Thumb Metacarpophalangeal (tMCP) Joint and Palm. Chapter 2 highlights that modularity is a key consideration in the design of modern prosthetic devices; these sections provide natural modules and therefore will be considered as such. Figure 4.1 shows how these modules combine to provide a complete prostheses.

Although these modules are distinct, they are intrinsically co-dependent. This thesis aims to discuss each of these sections individually, however, this is not always possible due to the interdependence of the modules. The finger design determined that of the MCP, whilst the tMCP and the MCP drove the shape of the palm. Figure 4.1 identifies the modular breakdown of the hand and how the module reuse has been implemented.

The modularity of the research is beneficial to the aim of increasing the acceptance of prosthetic devices, which can be identified in three key areas. Firstly, it allows for the configuration of the device to be altered during fitment and in use, providing customised prostheses that are suited to the individual users. Secondly, the reuse of components and modules means that the device is low cost, this allows for more regular replacement cycle, which prevents the out growing of a prosthesis. Finally, it allows for greater accessibility to prosthetic devices; variants can be produced, which satisfies the requirements of multiple markets, for example, lower cost or greater functionality.

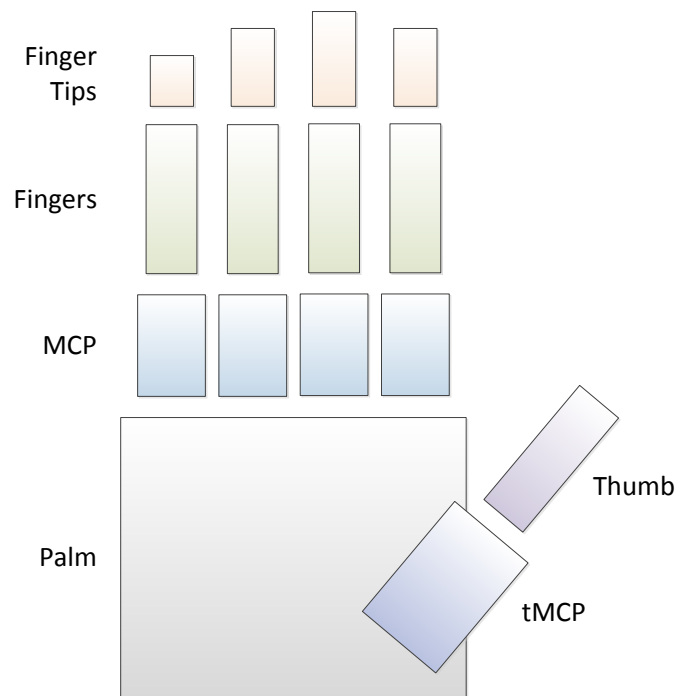


FIGURE 4.1: Model of the Degrees of Freedom in the Human Hand.

As discussed in the introduction (Chapter 1), there are multiple novelties presented in this thesis. They are focused on improving device function and acceptance, with the aim of reducing prosthetic rejection; this is the major issue with pediatric prosthetics. This thesis presents the first prosthetic hand designed for children that has individually actuated fingers, and separately, is the first to be fitted with a driven opposable thumb. These advancements to the state of the art mean that the presented device has the capabilities of the most advanced adult commercially available devices, such as the iLimb and BeBionic hands discussed in Section 2.4. Also presented is a novel modular finger that provides a natural curling motion, whilst providing suitable fingertip speed and force.

Multiple areas have been identified to aid in improving children's acceptance of their prosthesis. These have been represented in the development of each of the modules. Individual actuation of the fingers has been primarily facilitated by the development of the MCP (Chapter 6). Multiple iterations have been developed to produce a robust design that could be integrated with both the Hybrid Finger as well as the Palm. The Hybrid Finger has been designed to produce the humanoid closure trajectory that is lacking from the existing designs in Section 2.3, whilst maintaining the ability to apply fingertip forces equivalent to current commercially available devices.

To increase the acceptance of the hand, a thumb with driven opposition and closure was investigated. This development has allowed the device to offer many different humanoid grips, for example, the Key, Pinch and Power grips. This is a functionality that is

not available with any current prosthetic devices for children. Therefore, acceptance is increased, through increased functionality.

The contributions are separated into four chapters Design and Analysis of Finger Mechanism, Design of Metacarpophalangeal (MCP) Joint, Design and Analysis of Palm and Thumb Mechanism and System Controller. The first three discuss the mechanical implementation and advancements, whilst the fourth presents the supporting electronics and control system.

Novelties are presented in each chapter. Chapter 5 (Design and Analysis of Finger Mechanism) presents a hybrid finger design, the first curling finger that is fitable to prosthetic devices designed for children. Chapter 6 (Design of Metacarpophalangeal (MCP) Joint) outlines the facilitating module that allows for individually actuated fingers, whilst accommodating a drive system that provides fingertip forces equivalent to the common commercial hands for children. Chapter 7 (Design and Analysis of Palm and Thumb Mechanism) describes the thumb and palm combination. This is the first thumb design presented in prosthetic hands for children with both driven closure, as well as opposition. Finally, the first fully modular control system for prosthetic devices is presented in Chapter 8 (System Controller).

Furthermore, this research has aimed to pioneer the use of rapid prototyped materials in prosthetic construction and customisation, as discussed later in this chapter. The use of this material and manufacturing method is low cost and quickly manufactures components, whilst allowing for the consideration of individually customised components.

4.1 Requirements Specification

It has been identified that there is a gap in the field of advanced upper body prosthetics for children. This thesis aims to improve the state of the art in this area. To ensure that this need is met a requirements specification was created, which outlines the key performance characteristics of the device. These requirements focus on the device form and function, as well as specifying the characteristics of the wearer of the prosthesis. They have been drawn from the conclusions and discussions in the Literature Review and the Technical Discussion (Chapters 2 & 3).

When outlining a requirements specification language definition is essential. In this case shall will be used to denote a mandatory requirement and, should to denote a non-mandatory provision. This allows clear differentiation between the requirements.

1. The device shall be the size of a typical five year old's hand. As outlined by the normal measurement of a 5 year old child's hand, (Table 3.3).
2. The device shall have a hand length of 125.0mm.

3. The device shall have a middle finger length of 52.5mm.
4. The device shall have a palm length of 72.0mm.
5. The device shall have a palm width of 57.0mm.
6. The device shall have a ratio of palm width to hand length of 82.5 %.
7. The device shall have a ratio of palm length to middle finger length of 42.35 %.
8. The hand should have a mass of less than 200g. The hand shall have a mass of less than 250g
9. The device shall be designed to be attached to a standard prosthetic socket. This shall transmit electrical power as well as input signals. No provision shall be made for the connection of the socket.
10. The device shall be able to be fitted to patients who have amputations above “Transradial”, and should be able to be fitted to patients above “Wrist Disarticulation”.
11. The system, shall not be dependent on a specific control methodology.
12. The system controller shall have a standardised input communications method. This should be in the form of Inter-Integrated Circuit (I2C) communications.
13. The device shall used direct current (DC) electric motors to provide the actuation.
14. The device should use worm wheels to transfer motion to the fingers.
15. The hand shall have four individually actuated fingers.
16. The device should be able to position all fingers independently.
17. Each finger shall be able to apply a maximum fingertip force of 5N.
18. The closure/opening time of a finger shall be below 2s and should be less than 1s.
19. The hand shall have an opposable thumb.
20. The thumb shall have actuated closure.
21. The thumb should have powered opposition.
22. The fingers shall close with a humanoid trajectory.
23. THe thumb should close with a humanoid trajectory.
24. To adhere to prosthetic convention the hand shall be powered from a 6v source. For the benefit of the research it shall be considered that the power source ideal source with infinite power.

25. The power supplied to the hand shall be regulated by an on board power management system.
26. The hand shall be able to be manufactured on a rapid prototype printers. The hand should be able to be manufactured on low cost rapid prototype printers.
27. The device should be able to withstand the force applied by the weight of an average 5 year old (186N).
28. When manufactured in low volumes (less than five devices), the device should cost less than £1,000. In these volumes the device shall cost less than £1,500.

4.2 Rapid Prototyped Materials

To fully realise the potential as a prosthetic hand for children this device must fulfil two major requirements in terms of materials. The first is that it must be able to withstand the rigours of use, the second, that it is low cost enough to be replaced regularly. Typically engineering plastics are used in these situations, however to be cost effective they must be produced in high quantities. To produce low volume, low cost components another material or manufacturing technique must identified. From the research it can be seen that an additive manufacturing technique such as 3D printing could satisfy these requirements.

A feasibility study was completed investigating the advantages of using an Objet Connex 3D Printer to prototype the hand and as a production material. This method was found to be invaluable in the prototyping stage. When comparing components constructed in this manor to those machined from plastic in traditional material removal process, they could be made more complicated, quicker and at a fraction of the cost. A comparison showed that this process cost approximately one tenth of that of the traditional methods. This is attributable to the automated nature of the process, once the design has been uploaded and the manufacture started the only interaction required is to remove the final product from the machine and clean it. To evaluate this process all of the components for the designs have been constructed from this process. The Objet FullCure720 Material was found to have the best properties of the single resin materials since it has the lowest water absorption and the highest tensile strength. The Objet process was chosen as the preferred method for a couple of reasons the first was at time of printing they were able to provide the lowest resolution features and therefore the best finish. The range of materials gave some of the best performance characteristics. The final advantage is that the machine is able to deposit two materials simultaneously, by varying the mixture of these materials the properties of the component can be altered, this means that up to ten different material can be produced from the two base resins.

The initial study found that the rapid prototype material has the required mechanical properties for the construction of most of the prototype. Although as discussed later (in Section 6.3.1) it was decided that the axles were incompatible with this process as the final products were not fully circular and they experienced a high level of wear becoming misshaped. This study also highlighted that some characteristics of the printer were not fully understood and warranted further investigation.

The characteristics that were of greatest interest are the long term stability and the anisotropic properties (inconsistency of the material properties in different orientations). The second of these properties is not discussed in any of the Objet documentation however it was felt that due to the layered nature of the technique there would be an inherent anisotropic nature. To investigate this experiments were conducted by Barlow (2012) at the University of Plymouth, Mechanical Department for fulfilment of his final year project. Three separate materials (White Fullcure 720, Grey DM7230Transblack and Vero Clear 810) in their untreated state were tested. The Elastic Modulus of the materials and therefore the tensile strength was found to vary depending on the orientation of the materials. When stressed in either the X or Y-directions, the material performed within the tolerances given in the data sheets. When stressed on the Z-direction it was found that the Elastic Modulus was approximately 17% lower than stated in the manufacturers literature.

There are two new Objet materials RGD525 and RGD5160-DM. These materials are both designed to have thermal post treatments to increase their mechanical strength and melting points to be in line with common engineering plastics. An advantage of this post treatment is that the anisotropic properties that have been highlighted are minimised. The first material RGD525 has the greatest tensile strength and modulus of elasticity as well as a heat deflection temperature (HDT) greater than it could be expected to be exposed during fitment. However this material has a relatively high hardness which could make it brittle. This assumption is supported by the low elongation at break. The second material is the ABS-like Digital Material (RGD5160-DM) available only for the Objet Connex as it uses a two part resin. As implied by the name, the properties of this material can be compared to those of ABS plastics. ABS is an engineering plastic that has good impact resistance and toughness. It is used in many products ranging from car bumpers to Lego bricks, as well as in existing prosthetic devices. Although this material has a lower tensile strength it is the impact resistance that would be highly desirable in a prosthetic designed for children.

As discussed, the long term stability of the material is of interest. The manufacturing process of the Objet machines relies on stereolithography (SLA) a process by which resins are cured (made to set hard) with UV light. It has been seen that some materials produced with this process, when exposed to light for extended periods they can become brittle (Proto Labs, Inc., 2009). A qualitative assessment of the long term material properties was conducted. The assessment involved leaving four similar MCP joints

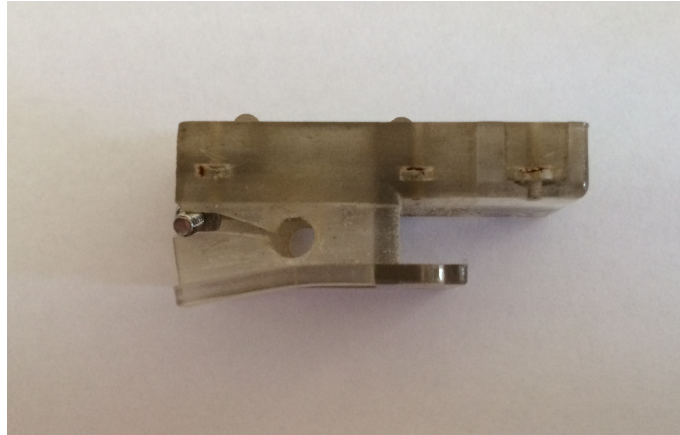


FIGURE 4.2: Image showing the brittle failure of an SLA material due to ageing

made from different materials (Tango Black, Vero-White, FullCure 720 and ABS-like) in view of the sun for period of five months. At the end of this period they were each inspected. It was found that some of the materials had been affected by the exposure. The Tango-Black and FullCure 720 materials had both become noticeably brittle, to the extent that the components could no longer be considered fit for purpose. As well as this the Vero-White and Full Cure materials showed high levels of discolouration. The ABS-like component showed no noticeable changes from the exposure. The exposure to these factors could be managed by the addition of a Ultra-Violet (UV) resistant coating or cover, however this would be likely to affect cost. This evaluation of the materials further supports the conclusion that the ABS-like material would be the best choice.

An aim of the project it to continue using rapid prototyped materials for the majority of the construction. However, the exact material that is used can be altered. The hand had been made stronger than the previous design with the use of the Objet ABS-like Digital Material (RGD5160-DM). This material is stronger than the FullCure720 and also has a lower density, the full material properties can be seen in Table 4.1. This would make the hand lighter and more robust.

An effective method of assessing the likelihood of failure caused by stress is safety factor analysis. This method compares the stress in each location to the yield strength of the material producing a ratio. A result of greater than one means that the device under test will withstand the force. It is common for a design to have a safety factor above two, this suggests that the product could withstand up to two times the applied force. This method is useful because it shows both the locations of highest stress and also the likelihood of the failure occurring at these points.

Analysis shows that using RGD525-DM will increase the safety factor in a full weight scenario from 2.14 to 2.55. This is a 16% increase in the strength of the product without redesigning or adding mass, which is a significant improvement that will prevent issues caused by failure and fatigue. See Figures 4.3 and 4.4 for details of the exact Safety

TABLE 4.1: Objet High Temperature Material (RGD525) Properties. Adapted from data sheet Objet Geometries Ltd. (2010).

	Units	Data Given	Assumed Value
Tensile strength	MPa	70-80	70
Elongation at break	%	10-15	10
Yield strength	MPa	?	59.5
Modulus of elasticity	MPa	3200-3500	3200
Poisson's Ratio		?	0.350
Water absorption	%	1.2-1.4	1.4
Polymerized density	g_{cm^3}	0.97-0.98	0.98
Heat deflection temperature after treatment	$^{\circ}C$	75-80	75
Shore Hardness (D)	Scale D	87-88	87
Rockwell Hardness	Scale M	78-83	78

Factor distribution. Figure 4.3 shows the situation where force is applied to the MCP through the finger, simulating the child pressing downwards fully with one finger. Figure 4.4 models the situation where force is applied to the front of the MCP, simulating the child resting on the knuckle of the device. When force is applied to the front of the MCP casing the safety factor would also be increased.

TABLE 4.2: Objet ABS-like Digital Material (RGD5160-DM) Properties. Adapted from data sheet Objet Geometries Ltd. (2010).

	Units	Data Given	Assumed Value
Tensile strength	MPa	55-60	55
Elongation at break	%	25-40	40
Yield strength	MPa	?	33
Modulus of elasticity	MPa	2600-3000	2600
Poisson's Ratio		?	0.350
Heat deflection temperature after treatment	$^{\circ}C$	82-90	82
Shore Hardness (D)	Scale D	85-87	85
Rockwell Hardness	Scale M	67-69	67

It can be seen in Table 4.2 that the ABS-like material does not have the same Tensile strength as the RGD5160-DM material however, due to it having a greater elongation at break and a lower hardness, this material would be less brittle and therefore could better handle transient loads. This would present a more robust material for a product designed for use by children.

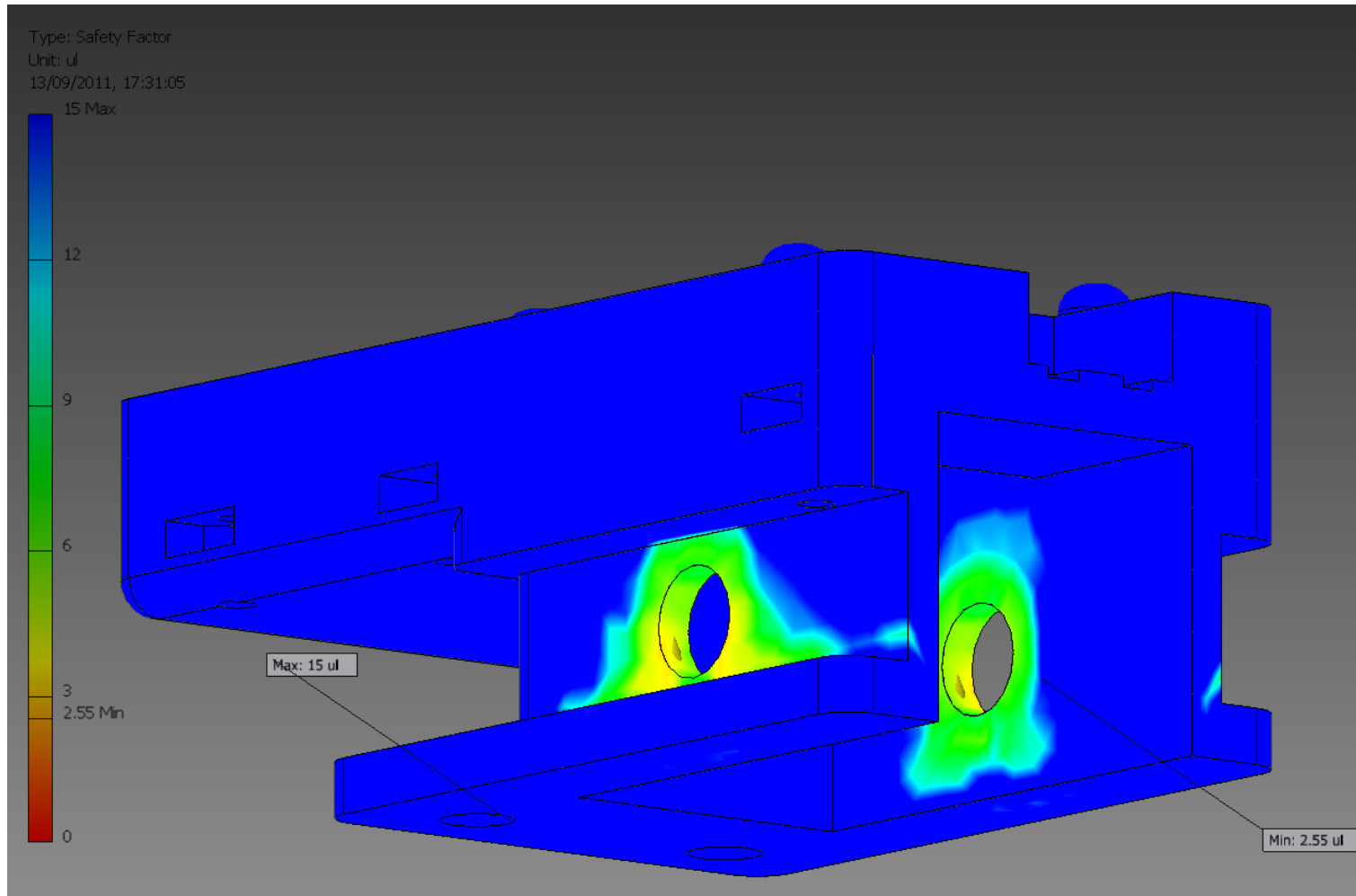


FIGURE 4.3: Safety factor analysis of the MCP Joint V2.4 constructed from Objet High Temperature Material (RGD525) subjected to a 186N force on the axle. The axle is not shown in the Figure but is between the two holes where strain is visible (yellow and green areas)

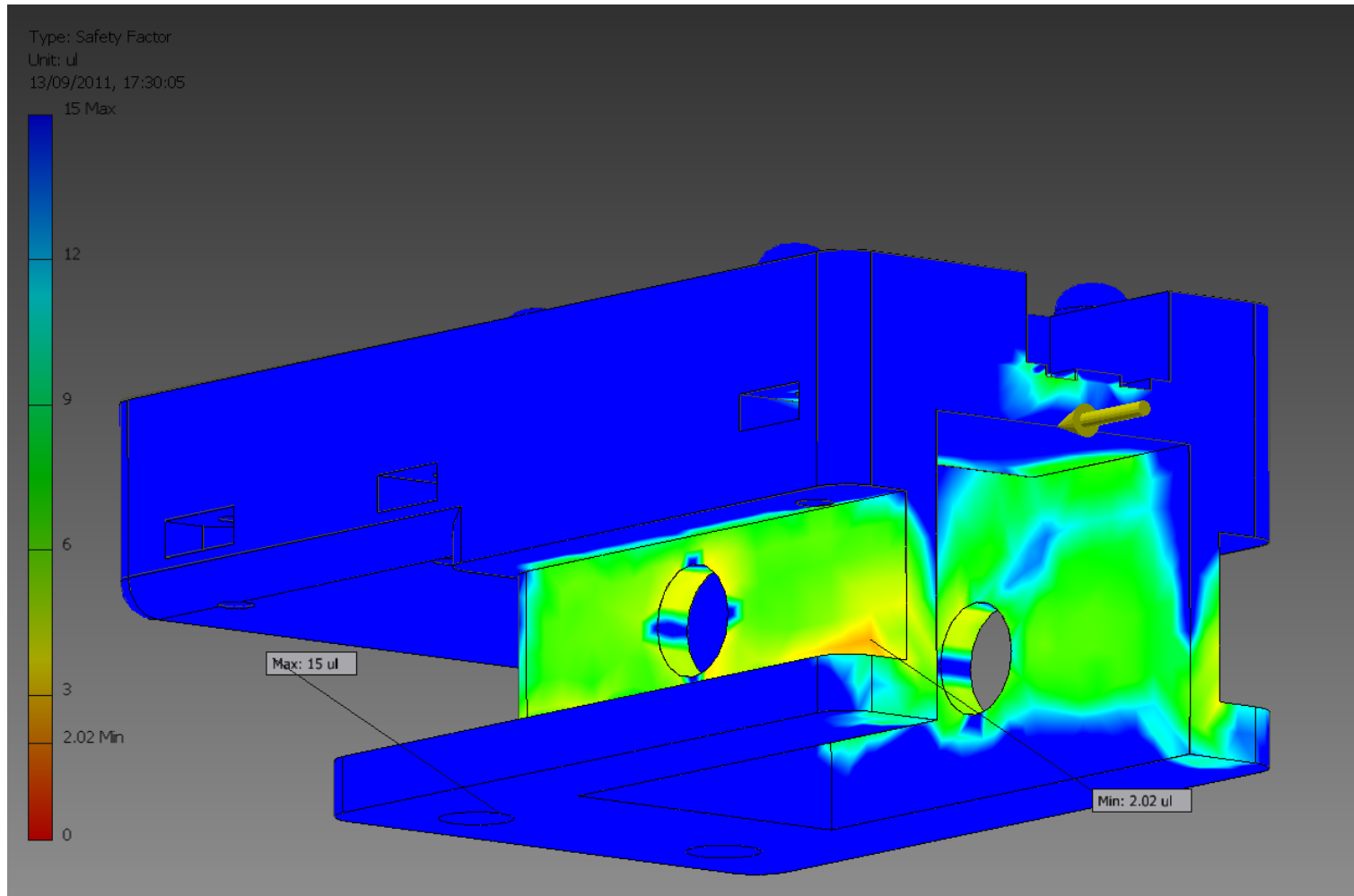


FIGURE 4.4: Safety factor analysis of the MCP Joint V2.4 constructed from Objet High Temperature Material (RGD525) subjected to a 186N force on the front. Arrow indicated location and direction of the applied force.



FIGURE 4.5: MCP Printed Using Fused Deposition Modelling Printer

This research suggests that with the correct design and material choice that the rapid prototyping would be a viable and cost effective method to produce components for the hand. The Objet rapid prototyping method and materials are both compatible with the design of parts for prosthetic hands, allowing the construction of parts for a fraction of the cost that conventional low volume manufacturing can achieve.

Another method of rapid prototyping was used towards the end of this research (as seen in Figure 4.5). Fused Deposition Modelling (FDM) uses an extruded plastic to draw sequential layers to construct a component. This technology had been discounted initially as it was unable to produce sufficient resolution to form the smaller features or to provide bearing surfaces. Newer printers and a revised design has meant that this is a viable printing method. From the initial trials using this material it provided similar material properties at substantially lower cost; the raw material is between ten and twenty times cheaper. This indicates that the hand could be manufactured from twenty pounds of material, using a printer costing approximately five hundred pounds.

4.3 Design Iterations

In Tables 4.4 to 4.7 are listed all of the design variants that have been designed in this research. They have been split into the different modules of the hand and are accompanied by a brief description of the version. These multiple versions are due to the iterative nature of the research and the design of one module changing to accommodative changes in others. There are four versions of the MCP joint. Version 1 of the MCP is the original design produced in the feasibility study. Version 2 of the MCP involves the initial research into the suitability of the rapid prototyped material as well as assessing possible assembly methodologies. The design of the Hybrid Finger meant that the Version 3 was created to allow coupling of the Supporting Link to the MCP. Finally, Version 4 which

was created, as the design of the interface between MCP and Palm was changed to improve the strength of the coupling.

Version	Finger Compatibility	Palm Compatibility	Description
MCP V 1.0	F V 1.0	P V 1.0 - P V 5.0	GDP design
MCP V 2.0	F V 1.0	P V 1.0 - P V 5.0	Suitability of the rapid prototyped material
MCP V 2.1	F V 1.0	P V 1.0 - P V 5.0	Black Design
MCP V 2.2	F V 1.0	P V 1.0 - P V 5.0	Hexagonal Axle
MCP V 2.3	F V 1.0	P V 1.0 - P V 5.0	Split Lid
MCP V 2.4	F V 1.0	P V 1.0 - P V 5.0	Positional feedback
MCP V 3.0	HF V 1.0	P V 1.0 - P V 5.0	Hybrid finger prototype block
MCP V 3.1	HF V 1.0	P V 1.0 - P V 5.0	Hybrid Finger
MCP V 4.0	HF V 1.0	P V 1.0 - P V 5.0	Altered MCP-Palm connector + encoder
MCP V 4.1	HF V 1.0	P V 6	With slots for PCBs
MCP V 4.2	HF V 1.0	P V 6	For Maxon Motor

TABLE 4.3: Table showing the iterations of metacarpophalangeal (MCP) joint

Version	Description
F V1.0	Solid Finger
HF V1.0	Hybrid Finger

TABLE 4.4: Table showing the iterations of finger designs

Version	Description
TH V 1.0	Non-opposable GDP Thumb
TH V 2.0	Thumb with 1016 motor
TH V 3.0	Open sided case
TH V 4.0	Split Case 1215 motor
TH V 5.0	Open ended
TH V 6.0	Split Middle
TH V 6.1	Split Middle - Bearings
TH V 7.0	End pivoted

TABLE 4.5: Table showing the iterations of the thumb metacarpophalangeal (tMCP) joint

Thumb Version	Palm Version	Palm Lid Version	Palm Description
TH V 1.0	P V 1.0		GDP Sheet palm
TH V 2.0	P V 1.1		Moulded Palm
TH V 3.0	P V 2.0	PL V 2.0	Metal Lid
TH V 4.0	P V 3.0		
TH V 5.0	P V 3.0		
TH V 6.0	P V 4.0		
TH V 6.1	P V 4.0		
TH V 7.0	P V 5.0	PL V 5.0	
TH V 7.0	P V 6.0	PL V 5.0	PI V 6.0 & MCP V 4
TH V 7.0	P V 6.1	PL V 5.1	Mouldable version

TABLE 4.6: Table showing the iterations of the Palm and Lid

Version	Thumb MCP Compatibility
T V 1.0	TH V 1.0
T V 2.0	TH V 2.0 - TH V 5.0
T V 3.0	TH V 6.0
T V 4.0	TH V 7.0

TABLE 4.7: Table showing the iterations of thumb designs

4.4 Final Modules

Table 4.8 shows the final version of each module for the hand (Multiples of some modules are needed to populate the hand).

Component	Version
Finger	HF V 1.0
MCP	MCP V 4.2
Palm	P V 6.1
Palm Lid	PL V 5.1
Palm Arms	PA V 1.0
Thumb MCP	TH V 6.0
Thumb	T V 3.0

TABLE 4.8: Table of the modules on final design

4.5 Discussion

This chapter has outlined the design approach of this research. It begins with a discussion of the design intent of this research, highlighting the key research areas and what

the research aimed to investigate. Then a specification for the hand is presented, this specification was laid out to guide the development of the research and to ensure that the novelties were developed so to be fitable to children aged five. These were outlined to ensure the technical impact of the research and to facilitate the conclusion of this research to advance the state of the art in the paediatric prostheses.

An investigation into rapid prototyped materials has been presented. This concludes that there are materials from the Objet Digital Material range that are suitable to manufacture a prosthetic device for children from.

Finally this chapter details the multiple research iterations of the individual modules and how the dependencies between the modules influenced each other. Table 4.8 shows the versions of each module that form the final device presented.

Chapter 5

Design and Analysis of Finger Mechanism

At present there are two distinct designs for prosthetic fingers: a rigid finger which is a simple solid design and a linked design. The advantage of the simple finger design is that it is low cost and robust. However the design has several drawbacks such as the range of movement which limits the achievable grips. The second design that has been presented is that of a six bar linkage, it uses a lever mechanism which, during actuation provides the finger with a humanoid closure trajectory. This curling motion suffers from a high level of mechanical disadvantage providing significantly reduced tip forces. Hands fitted with these linked fingers are usually heavier due to the larger motors needed to provide a sufficient grip force and therefore suffer rejection due to their weight. Due to these disadvantages of both of these hand designs are likely to suffer rejection. Research into rejection of prosthetic devices has shown that the unnatural closure and heavy devices both, can cause distress to the wearers promoting rejection.

5.1 Rigid Fingers (VF1.0)

This is a simplistic design that was designed as part of the first prototype child's hand. The only axis of movement is at the base (from the MCP joint), the rest of the design in a solid link that has fixed bends at the PIP and DIP joints to mimic the shape of an at-rest human hand. There are two main features that can be observed in this design. The first is a slot (yolk) to allow for a strong and effective coupling to the wheel gear. The second is the curved section designed to allow the finger to align with the MCP joint when straight; this allows the hand to lie flat when fully extended.

In child prosthetics individually actuated rigid fingers is a novel concept, and although this design is functional, allowing for effective pinching and grasping, it has an unnatural

closure trajectory. As discussed in Section 2.3 (Users' Perspective) many prosthetic wearers list an unnatural closure as one of the reasons for rejection. This suggests that this design is likely to introduce a compromise for the user and therefore could experience the many of the issues of rejection seen in existing designs.



FIGURE 5.1: CAD image of Finger V1.0 (Scale in centimetres (cm))

5.2 The Hybrid Finger

This design was proposed after analyses of the six-bar linked finger presented as part of the Southampton Hand presented by Kyberd et al. (2001); Light and Chappell (2000) taking into account the comments of Doshi and LeBlanc (1998). “That the DIP joint can be made solid without significant loss of the curling action provided by a multi linked design.” The Southampton Hand design has a good closure however suffers from a high mechanical disadvantage that is due to the six-bar linkage. It can be modelled as two crossed four-bar linkages that share a common link; therefore any mechanical disadvantage caused by the first linkages is multiplied by the second.

The hybrid design removes this first linkage and replaces it with a solid section, not dissimilar to the tip of many rigid fingers. This produces a design that has a crossed four-bar linkage in place of the proximal phalanges, that actuates the PIP joint and a rigid section forming the intermediate and distal phalanx. The design has most of the closure trajectory presented by six-bar linked designs however produces a fraction of the mechanical disadvantage and therefore can be driven by a motor that is markedly smaller.

5.3 Finger Trajectory Analysis

An effective method for evaluating the design of a finger is to calculate the force transmission characteristics. This is the ratio of the input torque to the perpendicular fingertip force across the range of input angles. Fingers such as the rigid version presented in

this report which have a single link can be modelled as a single lever which is rotated around a pivot, with a torque (turning moment) (Figure 5.2). Equation 5.1 shows the magnitude of the normal force (F) force, where τ is the magnitude of the torque, r is the length of the lever arm and Θ is the input angle.

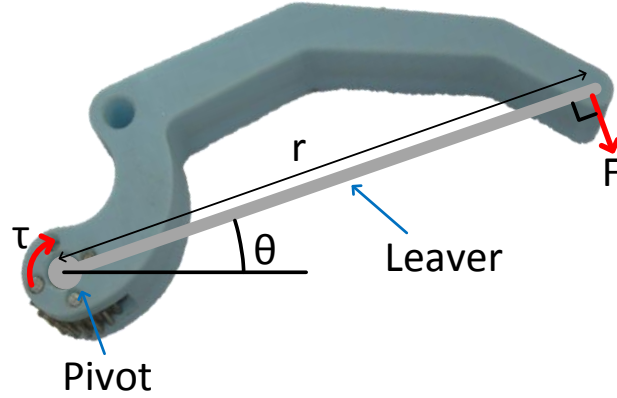


FIGURE 5.2: Diagram showing visualisation of rigid finger equations

$$\tau = rF \quad (5.1)$$

Since the force is always normal to the beam and is unaffected by the input angle Θ , therefore the force transmission ratio is constant throughout the input angles. Meaning that the length of the finger determines the force transmitted. The rigid finger presented with a length of 55mm (0.055m), when driven with a nominal input torque of 1 unit of force will provide an output of 18.18 units of force.

For a dynamic system such as the hybrid finger there are multiple links that have variable relative positions therefore varying force transmission. This causes varying contact angles of the links and therefore causes the force perpendicular to the surface of contact to alter as the relative positions change and thus affect the output. Due to the crossed four-bar linkage in some situations one link can be transmitting a negative force and working against the output. The calculation of the transmission ratio of the hybrid finger, with a crossed-four bar linkage, is split into two discrete problems. The first is the orientation of the link BC relative to the origin (O) and the second is the force transmission.

Figure 5.3 shows the hybrid finger represented in a diagrammatic form. The driven link and the support link are Lob and Lac respectively whilst, Loa and Lbc are the corresponding parts of the MCP and fingertip. The two links shown by the dashed lines are imaginary links used during the orientation calculations. All angles are shown measured anti-clockwise from the positive X-axis (also referred to as Normal of A) to adhere to the conventions of the Cartesian coordinate system.

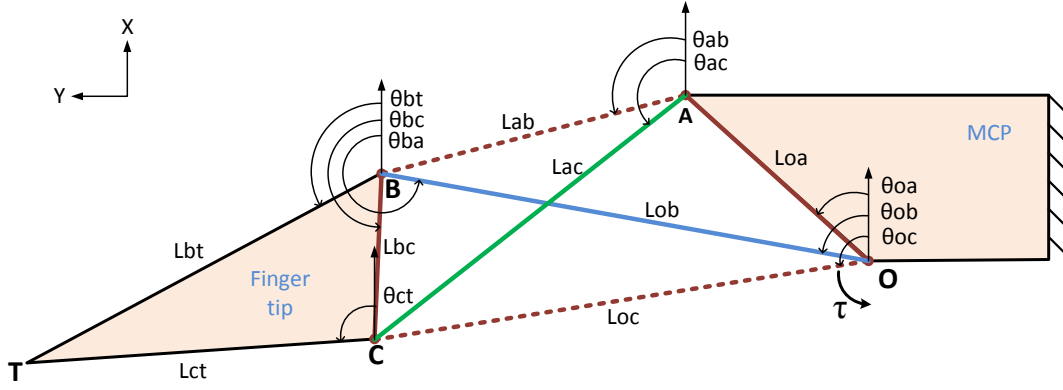


FIGURE 5.3: Hybrid Finger Diagram.

Since all links are set lengths and there are two fixed pivots (O, A) a discrete range of positions exist that can be achieved. The pivot that is labelled O is considered the origin and the angle of the link Lob to the origin (Θ_{ob}) is the input angle. Due to the design, each input has its own exclusive output. The X Axis is referred to as the Normal of

The first step to calculate the orientation is to find the distance between A and B. For simplicity this has been modelled as an theoretical link Lab:

$$Lab = \sqrt{Lob^2 + Loa^2 - (2 * Lob * Loa * \cos(\Theta_{oa} - \Theta_{ob}))} \quad (5.2)$$

Then to calculate the angle from the Normal of pivot A to pivot B, where, $xLob$ and $yLob$ are the Cartesian references for the pivot B; found with trigonometry using Θ_{ob} and Lob . $xLoa$ and $yLoa$ are the X and Y design distances between the origin and pivot A:

$$\Theta_{ab} = \pi + \arctan\left(\frac{yLob - yLoa}{xLob - xLoa}\right) \quad (5.3)$$

where x and y denote the X and Y components of the respective links.

This allows the angle from the normal of pivot B to Lbc to be calculated:

$$\Theta_{bc} = \Theta_{ab} + \arccos\left(\frac{Lac^2 - Lab^2 - Lbc^2}{2 * Lab * Lbc}\right) \quad (5.4)$$

The X and Y distances from the origin to point C are found using the X and Y distances from O to B and from B to C. These are labelled $xLoc$ and $yLoc$.

$$xLoc = xLob + (Lbc * \cos(\Theta_{bc})) \quad (5.5)$$

$$yLoc = yLob + (Lbc * \sin(\Theta_{bc})) \quad (5.6)$$

The angle between Lab and Lac is defined as:

$$\Theta_{abac} = \arccos\left(\frac{Lac^2 + Lab^2 - Lbc^2}{2 * Lac * Lab}\right) \quad (5.7)$$

Then to calculate the angle from the normal of A and point C:

$$\Theta_{ac} = \Theta_{ab} + \Theta_{abac} \quad (5.8)$$

Then calculate the angle between the links ob and oa:

$$\Theta_{Oob} = \Theta_{ob} - \Theta_{oa} \quad (5.9)$$

Define the angle between the links origin and point C:

$$\Theta_{Oac} = \Theta_{ac} - \Theta_{oa} \quad (5.10)$$

The second section is to calculate the transmission ratio. Since rotational power around a fixed point is equal to the product of torque and angular velocity:

$$P = \omega * \tau \quad (5.11)$$

If zero power loss is assumed across the system then:

$$P_{in} = P_{out} \Rightarrow \omega_{in} * \tau_{in} = \omega_{out} * \tau_{out} \quad (5.12)$$

Therefore the transmission ratio is, where Θ_{in} and Θ_{out} have been defined as Θ_{ob} and Θ_{oc} respectively:

$$R(\Theta_{ob}) = \frac{\dot{\Theta}_{in}}{\dot{\Theta}_{out}} = \frac{\omega_{in}}{\omega_{out}} = \frac{\tau_{out}}{\tau_{in}} \quad (5.13)$$

The final stage is to calculate the change in input and output angle.

$$\begin{aligned} \dot{\Theta}_{in} = & (Lob * Lac * \cos(\Theta_{Oob}) * \sin(\Theta_{Oac})) - Lob * Lac * \cos(\Theta_{Oac}) * \sin(\Theta_{Oob}) \\ & - Lac * Loa * \sin(\Theta_{Oac}) \end{aligned} \quad (5.14)$$

$$\begin{aligned} \dot{\Theta}_{out} = & Lob * Loa * \sin(\Theta_{Oob}) + Lob * Lac * \cos(\Theta_{Oac}) * \sin(\Theta_{Oob}) \\ & - Lob * Lac * \cos(\Theta_{Oob}) * \sin(\Theta_{Oac}) \end{aligned} \quad (5.15)$$

TABLE 5.1: Inputs for hybrid finger analysis

$\Theta_{ob_{begin}}$	79.72	deg
	1.39	rad
$\Theta_{ob_{end}}$	134.72	deg
	2.35	rad
Θ_{oa}	47.73	deg
	0.83	rad
x_{Loa}	10.00	mm
y_{Loa}	11.00	mm
L_{ob}	29.73	mm
L_{ac}	23.79	mm
L_{bc}	10.00	mm

MatLab was used to create a graph showing the absolute output force as a percentage of the absolute input force (Figure 5.5). These show a near linear increase of the ratio ($R(\Theta d)$) between 0.61 at 78° and 2.3 at 120° . The ratio then becomes large at 130° , rising to 45.05. This shows that across a small range of 10° the finger transmits more force than at other occasions. However this is during the end of the pinch where more force could ordinarily be needed. This occurs because links L_{ob} and L_{bc} have become aligned meaning that the entire force applied by L_{ob} is converted into rotational force around pivot C and no force is lost in the moving of C.

To analyse the maximum force that can be transmitted by the finger tip, the turning moment around pivot C needs to be calculated. This is done with a rearranged and adapted version of equation 5.1 that takes into account the changing transmission ratio due to the input angle Θ_{ob} .

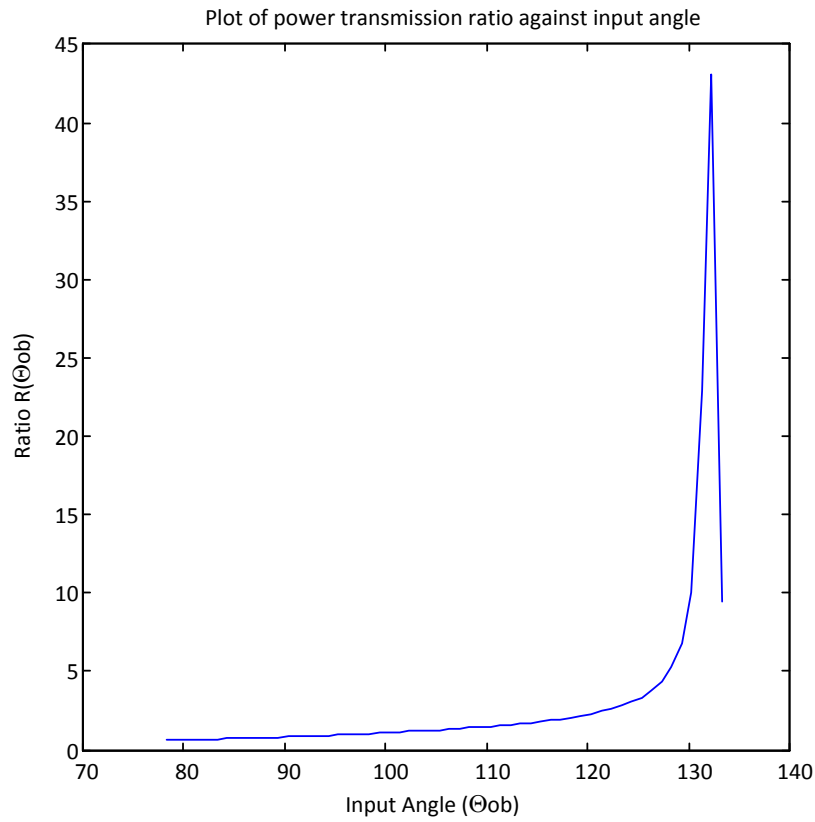
$$F(\Theta_{ob}) = \frac{\tau * R(\Theta_{ob})}{r} \quad (5.16)$$

Where r is the length from C to T (L_{ct}) these lengths are shown in Table 5.2.

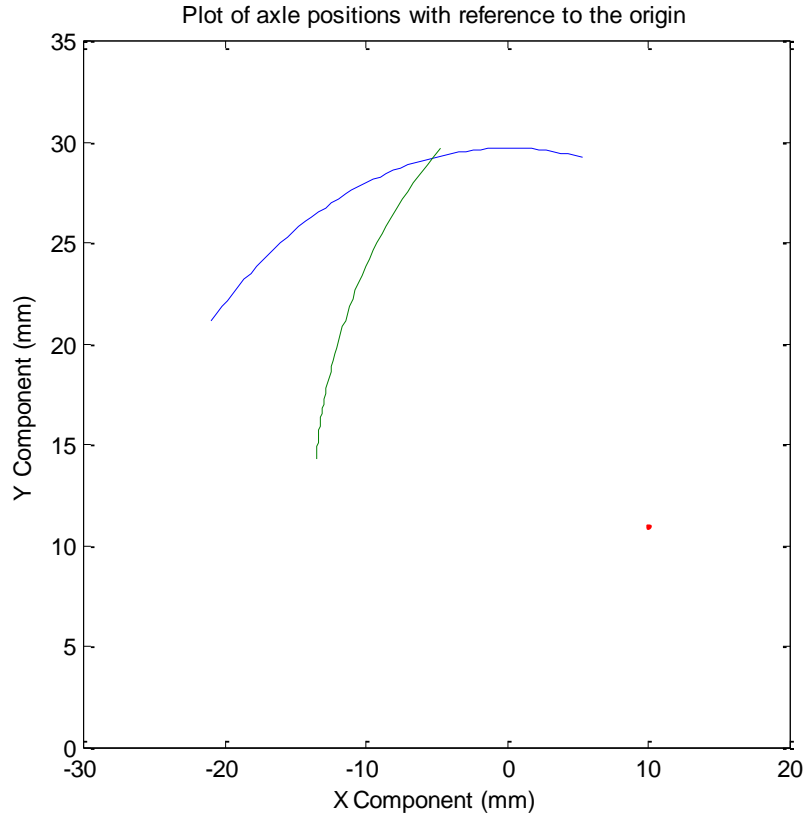
TABLE 5.2: Lengths for L_{ct} on the hybrid finger

First Finger	24.92	mm
Second Finger	27.90	mm
Third Finger	24.92	mm
Fourth Finger	21.10	mm

The highest and lowest values for the ratio are 0.61 and 43.05 respectively and the maximum torque that the Maxon RE10 motor produces is 1.5 mNm. When applied to the finger through a 64:1 gearbox the predicted output force at the finger tip and effective weight are shown in Table 5.3.

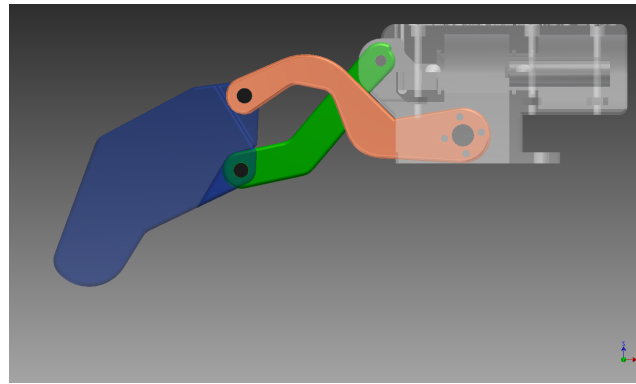


(a) Plot of the power transmission ratio (%) against input angle

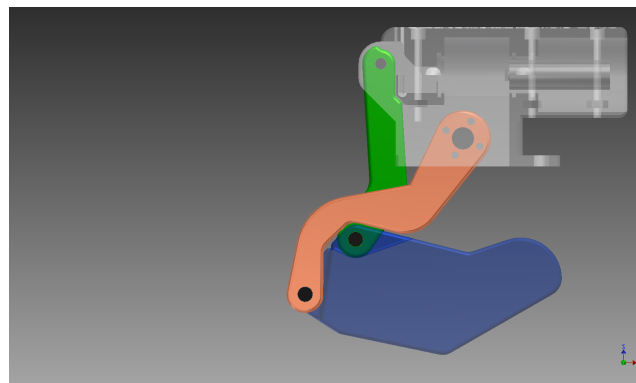


(b) Plot of axle positions with reference to the origin (0,0). The red dot at 10,10 represents pivot A. The blue trace represents the trajectory of pivot B whilst the green trace represents the trajectory of pivot C. (Diagram not to scale)

FIGURE 5.5: MatLab plot of the force transmission ratio and finger link trajectory



(a) Open



(b) Closed

FIGURE 5.6: CAD image of Hybrid Finger VH1.0

four-bar linkage. The final piece is the MCP. All of these have two axle holes in them to allow each to be attached to the others.

Driven Link: As suggested by the name, this link transfers motion from the gear of the worm-wheel to the finger and on to the fingertip, it is shown as the orange link in Figure 5.6. It is essentially two separate parallel links that allow the Support Link to move between them. It is made into one component by joining them at points that does not prevent the movement of the Support Link. This adds strength and helps to prevent twisting when force is being applied. The link has a S-like shape to allow for the crossover of the links. As it can be seen in Figure 5.6 the exact shape of the link is determined by the components it must avoid. When in the open position the top must have a flat section to avoid contact with the MCP (Figure 5.6(a)). In the closed position, it must curl around the fingertip (Figure 5.6(b)). The last feature to note is the four holes in the MCP end of the component these are to allow the insertion of pins to couple its motion to that of the wheel.

Fingertip: The fingertip is designed to be the equivalent length of the intermediate and distal phalanx of an average five year old child with approximately a 40° bend in the DIP joint between them, to provide a humanoid shape. The tip is rounded to provide

the largest possible pinch contact surface with a flat top surface to replicate the side profile of a human finger created by the fingernail.

Support Link: The Support Link is the last component of the finger design, shown as the green link in Figure 5.6. It is bent to minimise the possible contact with the driven link and also has a small section removed at the MCP end to avoid contact with said component. The second reason for this thinning is to cause it to be the weakest-link in the design, if too much force is applied to the finger it will break without transferring excessive forces through to the expensive drive components. This link was designed to be the point of failure as it is the least complicated component and therefore the most practical to replace.

There are four axles that hold the design together. They are different sizes dictated their different roles, the two axles in the fingertip have a 2.0mm diameter as this is a suitable stock size. The drive axle has a diameter of 3.0mm as it will experience added lateral forces applied by the turning of the worm-wheel. The final axle is only 1.5mm in diameter, this is designed to provide an increased load stress on the supporting link ensuring that it is the sacrificial component.

The initial proportions of the finger were chosen arbitrarily to fit within the size and shape requirements of a child aged five and around the existing components in the MCP. The force transmission characteristics of this design are evaluated in section 5.3 and proved to give an effective solution.

5.4 Input-Output Equations

To allow the controller to determine the position of the finger, it requires a relationship between the input angles and the fingertip positions in Cartesian space. Using the dimensions of the finger (Table 5.1) and the input angle of each driven link (Θ_{ob1-4}), then the fingertip location with respect to its MCP can be mapped to a space model. The equations presented above allow the Cartesian location of pivot B (x_{Lob} and y_{Lob}) to be found. This allows the computation of L_{ab} and Θ_{ab} and in turn Θ_{bc} .

Using Θ_{ob} and Θ_{bc} along with the geometry of the finger tip (Table A.1), the tip location with reference to the the origin (X_{ot} and Y_{ot}) can then be calculated. Here, θ_{tcb} is the angle between the imaginary links L_{bc} and L_{bt} .

Since:

$$x_{Lob} = L_{ob} * \cos(\Theta_{ob}) \quad (5.17)$$

$$y_{Lob} = L_{ob} * \sin(\Theta_{ob}) \quad (5.18)$$

$$\Theta_{bt} = \Theta_{bc} - \Theta_{tcb} \quad (5.19)$$

And using Θ_{bt} (Equation 5.19) gives Equations 5.22 and 5.23 which identify the location of the finger tip with reference to pivot B:

$$x_{Lbt} = L_{bt} * \cos(\Theta_{bt}) \quad (5.20)$$

$$y_{Lbt} = L_{bt} * \sin(\Theta_{bt}) \quad (5.21)$$

Combining the Equations 5.17 and 5.20, and 5.18 and 5.21, gives the positional reference from the MCP origin:

$$\begin{aligned} x_T &= x_{Lob} + x_{Lbt} \\ &= (L_{ob} * \cos(\Theta_{ob})) + (L_{bt} * \cos(\Theta_{bc} - \Theta_{ct})) \end{aligned} \quad (5.22)$$

$$\begin{aligned} y_T &= y_{Lob} + y_{Lbt} \\ &= (L_{ob} * \sin(\Theta_{ob})) + (L_{bt} * \sin(\Theta_{bc} - \Theta_{ct})) \end{aligned} \quad (5.23)$$

Summary: In this chapter a novel a prosthetic finger has been presented. It brings together the designs of six bar linkages and solid fingers to deliver acceptable speed and force characteristics for prosthetic hands. To provide a natural curling action; as discussed in Section 2.3 the lack of a natural curling action is a driver for rejection. This design has been mathematically modelled to gauge the expected properties. It can be seen in Figure 5.7 that the finger tip follows a smooth path which arcs in towards the hand. As the finger follows through the arc it can be seen that the spaces between the points become smaller. This suggests that when in the extended position, the finger travels faster than in the closed section of the arc. This was the design intent, which allows for faster closure of the finger whilst providing for control when finer movements are required.

The computed trajectory was then compared against the curling nature of a human hand. It was found that during closure of the human hand the fingertip would naturally follow the computed path of the hybrid finger. Examples of this comparison can be seen in Figure 5.8. It can be seen that the human fingertip lies on the trajectory path at both the open (Figure 5.8(a)) and closed (Figure 5.8(e)) positions. As well as, through out the movement (Figures 5.8(b), 5.8(c) & 5.8(d)). Figure 5.9 shows an overlay of the different finger positions against the computed finger trajectory. This analysis found that the design of the hybrid finger provides the natural humanoid closure that is discussed in Section 2.3.

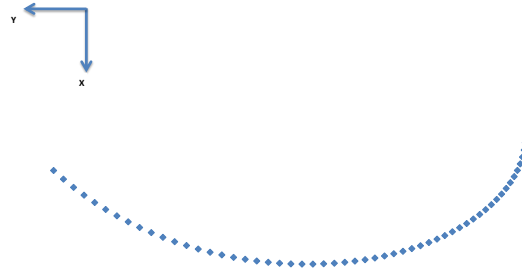


FIGURE 5.7: Trajectory of the tip of the first finger. Computed using Equations 5.22 and 5.23

With these equations the location of each finger to be mapped to the input angle of the driven link. Running these equations on a microchip would prove to be computationally intensive, due to the number of trigonometric functions that are involved. However, there is a discrete output for each input angle (Θ_{ob}), therefore the solutions can be pre calculated and accessed from the memory of a microcontroller. Table A.1 in Appendix shows the mapping of the fingertip with regards to a normalised input angle, for each of the fingers.

There has also been an investigation into the force transfer characteristics of the finger mechanism. This analysis shows that the fingertip applies the greatest force when the finger is in the closure region of the action; this is the area where higher fingertip force would be desired. The results from this force analysis shows a linearity in most of the profile, however there is the sharp increase as discussed. By mapping fingertip force to the fingertip location, the output force can be controlled to provide a smoother force profile when maximum force is not required.

TABLE 5.4: Dimensions of the hybrid fingertip. Where O_{tcb} is the angle between links L_{bt} and L_{bc} .

	O_{tcb} ($^{\circ}$)	L_{bt} (mm)
First Finger	35.3	32.40
Second Foinger	36.9	35.24
Third Finger	35.3	32.40
Fourth Finger	33.5	28.70

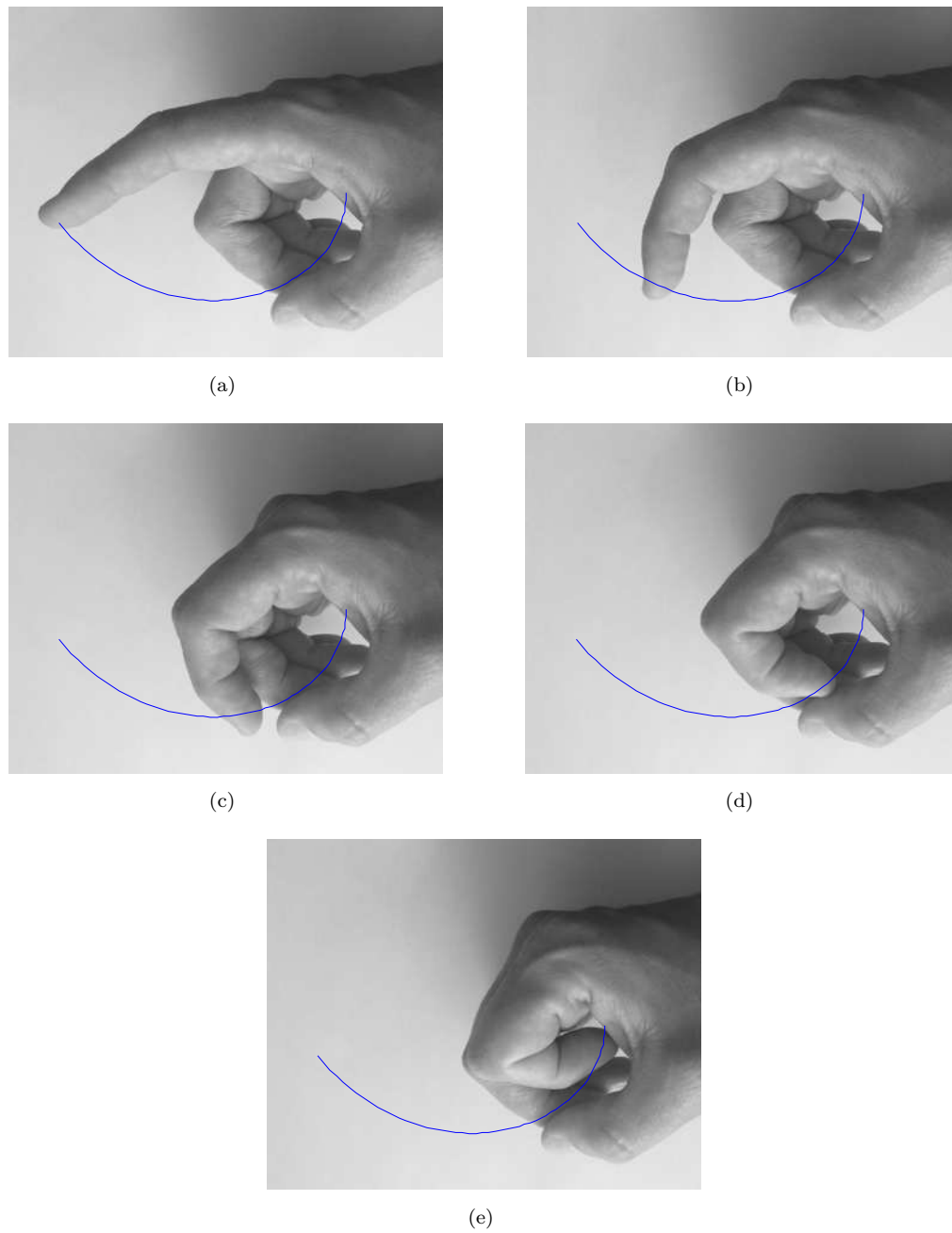


FIGURE 5.8: Trajectory path of the first fingertip projected onto a closing human finger. Computed using Equations 5.22 & 5.23

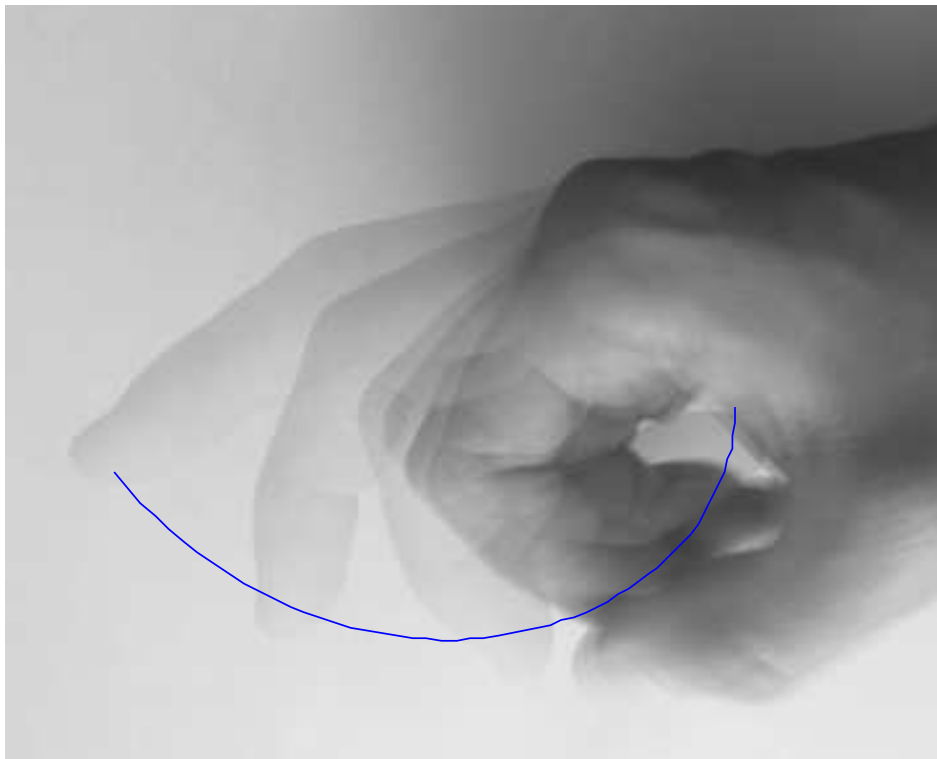


FIGURE 5.9: Overlaid image of a closing human finger against the trajectory of the hybrid finger. Trajectory computed using Equations 5.22 & 5.23

Chapter 6

Design of Metacarpophalangeal (MCP) Joint

The MCP joint is the most important single component in the hand as it houses all of the moving components for each of the fingers. The final version contains the motor drive system, a worm-wheel, four bearings as well as mounting points for the finger and palm. To implement the design intent as outlined in earlier chapters the MCPs are designed to be completely modular and interchangeable, allowing for quick servicing, repair and configuration; this is facilitated by standardised slots in the palm for all of the fingers. The main constraint for this component is the width, it must be narrow enough to be able to fit four across the $57mm$ palm, whilst being strong enough to withstand any forces exerted on the finger.

There have been multiple iterations of this component since the original prototype. The changes have included; a reduction in mass, the addition of bearings on the major drive axles and a two changes of motor. In addition there have been changes to both of the MCP-Finger and the MCP-Palm interfaces. These alterations have facilitated a light and robust design that incorporates a more powerful drive-system, alongside an improved sensing ability.

6.1 MCP Version 1 (MCP V1.0)

This is the design from the feasibility study (Redman et al., 2011) it showed that making a hand for children aged five with five actuated DOF was possible. However, it is heavy and required a large amount of machining which in turn made it expensive. When evaluated, the design was found to have several design features that were considered non optimal. These were;

- The motor power
- The lack of axle bearings
- The brass retaining plate
- The motor securing method
- The length of the worm wheel
- Incorrect worm-wheel separation

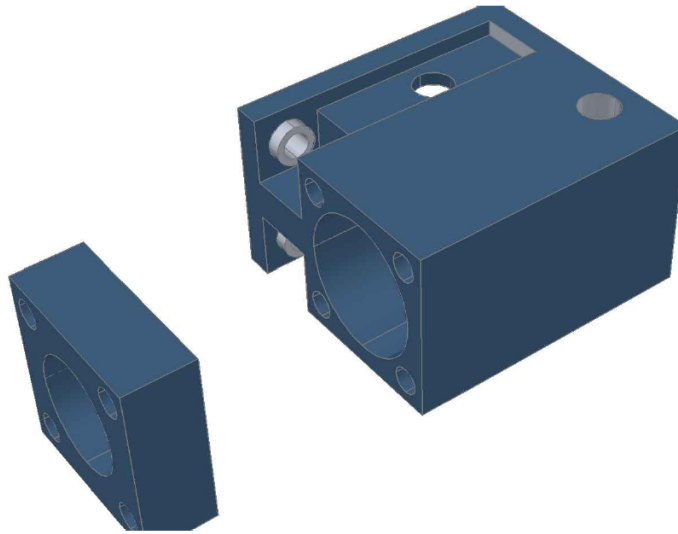


FIGURE 6.1: CAD image of MCP V1.0

6.2 MCP Version 2 (MCP V2.0)

This version is a copy of the design of MCP V1.0 however it was produced on the Objet rapid prototyping machine. The sole purpose of this design was to complete the investigation into the suitability of the rapid prototyped material for all of the features on the design. The results showed that the design could be produced from Objet materials and that no other constraints are introduced by using this material. This also confirmed that this manufacturing technique was able to produce a comparable component for a fraction of the cost, and in a quicker time.

6.2.1 MCP V2.1

Version 2.1 was the first prototype to display alterations from the original design. These were in the choice and method used to secure the motor, the total mass and the worm-wheel separation. Two of the interfaces (MCP-Finger and MCP-Palm) were standardised from the original MCP. Standardisation was adopted to ensure the modular nature of the hand. As discussed, it is felt that modularity is key to producing a low cost, adaptable and serviceable hand. The first interface to be standardised was the fastening between the MCP and the finger, the second was between the MCP and the palm. These specific connectors were chosen because they have to mesh with other components on the device. In doing this it means that all versions of a component will be able to be fitted to the corresponding receptor.

Motor Power: In the original design the Fauhauber minimotor 0816 was used with a 64:1 reduction gearbox. At stall torque this drive system produced a force at the fingertip (Length = 55mm) of 2.17N and a 90° closure time of 1.95s. These characteristics are not optimal, meaning that the force produced and the speed of closure are both below the target to provide a sufficient grip. This motor was replaced with a Fauhauber minimotor 1016, with a 64:1 reduction gearbox. The new drive system gave a predicted output of 6.96N at the finger tip with a 90° closure time of 1.67s.

This represents a 320% increase in the fingertip force as well as a 14% reduction in the closure time.

Motor Securing: In the original design the motor is secured by the tightening of a single screw causing a pinch on the motor case. This design also causes the motor-gearbox to become slightly offset from the centre of the axle. This in turn would cause unnecessary pressure on the bearings of motor-gearbox causing added friction, therefore increased levels of wear. To address this problem a split case design was adopted. The design has a partial lid to allow the top of the motor surround to be secured and removed by 4 screws. Meaning that pressure is applied across the motor casing and motor misalignment was corrected.

Mass: After analysis it was decided that there were features in the MCP joint that could be removed or altered to reduce the weight of the design. The main points that were highlighted were the worm wheel and end plate. The worm wheel was longer than was necessary and therefore could be shortened. By doing this the length of worm-wheel was reduced a further 6.5mm to 8.5mm, this represents a 43% reduction in length and weigh from the first MCP and a 110% reduction compared to the original worm wheel. As well as the reduction in mass this also allowed the MCP to be shortened saving space for other components. The end plate and securing pin has a mass of 4.27g. These components were removed and replaced with a slot above the worm-wheel. This design allowed for the insertion without affecting the functionality of the hand. This mass is not entirely reduced since the space is filled with other materials; although these are significantly lighter than the metals used in both the end plate and the worm wheel.

Worm-Wheel Separation: This was a trivial problem that was causing significant backlash in the finger movements and a weakening of the gears. The issue required an alteration of the meshing distance of the worm and wheel. In the original design the axle separation was incorrect and needed to be changed from 9.5mm to 8.5mm. By correcting this the backlash was almost entirely removed and caused the full face of the gears to be touching.

Evaluation: This design addresses several of the issues that were present. Motor alignment has been corrected whilst still providing sufficient securing. The power and speed are increased with the inclusion of a bigger motor, although this motor caused an increased mass. The 0816 motor and gearbox has a mass of 8.1g as opposed to 14.5g for

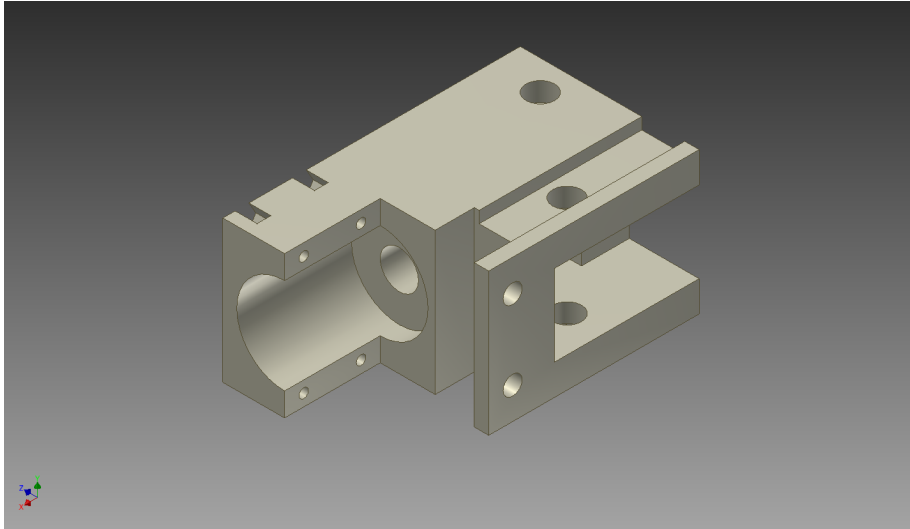


FIGURE 6.2: CAD image of MCP V2.1

the 1016 motor gearbox, meaning an increase of 6.4g per MCP. This increase in mass was completely counterbalanced by the other reductions discussed above, therefore the additional power was delivered without the cost of increased mass. The unrecognised problem caused by this design is that there is no viable method to attach the worm to its drive axle. The initial solution was to glue the axle to the worm during insertion however after investigation this causes the worm to become glued to the case. This issue meant that V2.1 was a non functioning design a faulty design.

6.2.2 MCP V2.2

This is a design that was never produced as it involved using a hexagonal shaft to provide the connection to the worm wheel shaft. It allowed for the worm to be dropped into the top of the box and the axle to be inserted from the back afterwards. Producing a worm with this type of bore would be prohibitively expensive and therefore the design was infeasible. If not for the cost this would have provided a reliable and mechanically sound solution for the coupling.

6.2.3 MCP V2.3

The approach used to solve the worm axle insertion was to split the case entirely down the middle. This allows the worm to be glued to the axle before fitment and then placed into the design. As well as this, the split case allows for the addition of bearings either side of the worm. This arrangement allows for less friction and less wear on the axle shaft.

Split Case: It was decided that a split MCP design would improve the ease of assembly and would allow the bearings and worm to be easily inserted into the design. To secure

the two sections two additional features needed to be added to the design. The first is the use of alignment lugs (these can be seen in Figure 6.4), they are stepped sections at the front to keep the lid straight and a sloped section at the rear to prevent it from moving backwards. The second features are six recesses for M1.0 bolts and their associated nuts. These are designed to minimize the space requirements of the MCP and so not to hinder attachment to the palm. The recessed holes for the nuts are designed to be hexagonal to aid assembly.

Axle Bearings: It was found that the digital material created by the rapid prototyping machine did not have good bearing properties and therefore caused significant inefficiency in the transmission. This is due to the uneven surface caused by the 17 micron steps between the layers of material. To increase the efficiency of the transmission, bearings for either end of the main axle were created from Tuffset plastic. This is an engineering plastic which has a similar density to the digital materials, however it also has self lubricating properties that make it suitable as a bearing. See Figure 6.3. The bearings are 1.5mm thick and have a 6.0mm diameter with a 4.0mm hole for the worm axle. Each end has 0.5mm indent with a diameter of 5.0mm to prevent lateral movement.

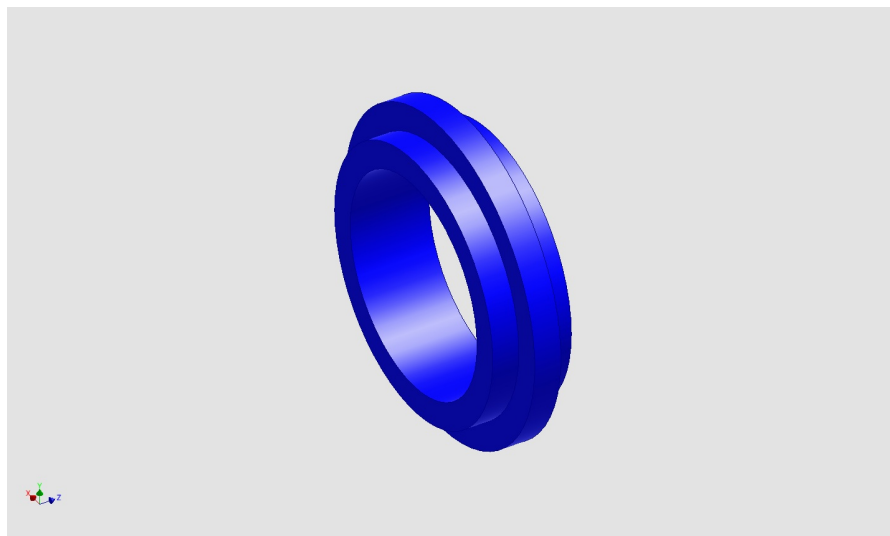


FIGURE 6.3: CAD image for axle bearings

Evaluation: This design was never produced because of the simultaneous development of V2.4 however this design was the first design to be fully fundamentally operational. The split case allows for easy construction whilst reducing the complexity of construction. The addition of the bearings reduced the losses due to friction in the MCP and therefore has improved the reliability and smooth operation of the hand.

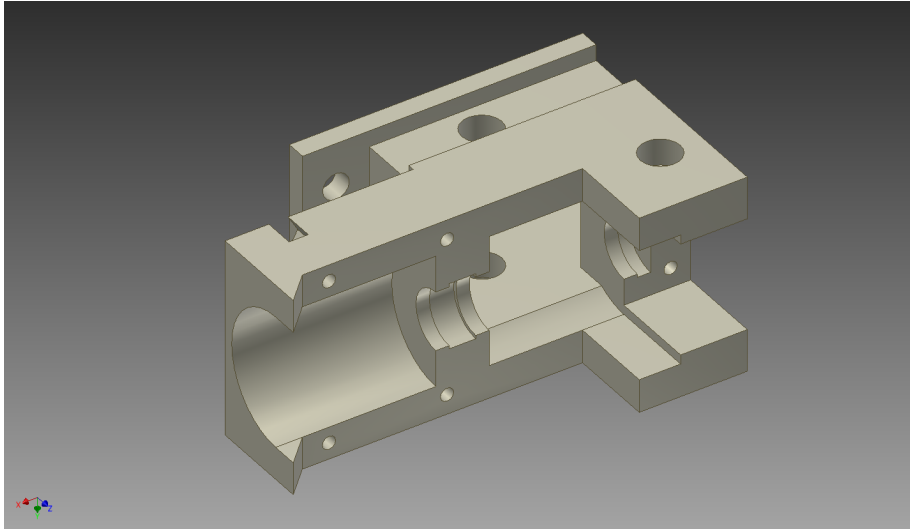


FIGURE 6.4: CAD image of MCP V2.3

6.2.4 MCP V2.4

Position sensing is an important factor in advanced prosthetic control. To be able to form gestures with a prosthetic hand, it requires the ability to detect the position of the fingers. This version was the first that attempted to solve this issue and add positional feedback to the device.

Position Sensing Encoder: From the first prototype of the hand it was found that one of the limiting factors was that there was no position sensing encoders on the fingers. This meant that the controller had to work using an open loop control methodology, using the stall of the motors to detect contact with an object. This limits the functionality of the hand and prevents the hand from forming effective gestures (non-gripping finger positions) such as pointing. The standard encoders that were designed for the Faulhaber 1016 motors are both too large and too heavy for the hand. Another technique is to attach an encoder or potentiometer to the axle shaft of the finger. In this case due to size this option was more viable than the motor encoders. Also the mass of the potentiometer is significantly less than an encoder. Although this was the preferred option, there is little to no space between the axles to allow this design to be implemented and therefore necessitated the use of a miniature potentiometer.

The final design incorporated a multi turn potentiometer on the axle of the worm wheel. This design allows for a small and light weight component to be placed inside the MCP joint; in space that was previously unused. To implement this, the minimum number of turns that worm would turn during closure, and thus the potentiometer, needed to be calculated. The maximum angle that the finger and therefore the wheel would turn is 120° . With a reduction of 20:1 between the worm and wheel. The worm would turn approximately seven times during flexion of the finger. The potentiometer that was chosen was an eleven turn 10K potentiometer produced by Murata Manufacturing.

This was chosen due to its size ($5.1\text{mm} \times 4.8\text{mm} \times 3.9\text{mm}$), it's relatively large change of resistance from end to end and the suitable number of turns. It also has the benefit of being sealed, protecting it from dust and particle interaction. Preliminary evaluation showed that this component could fit into the MCP joint and provided a measurable value for the position of the finger.

The design uses an adapted worm-axle to turn a miniature multi-turn potentiometer, which then outputs a voltage proportional to the position. The advantages of this specific design over those with a potentiometer mounted on the finger axle, is that it does not make the design wider. This means that this version is the same thickness as previous versions and therefore still the equivalent size of a five year old child's hand. The modifications to add the potentiometer to the MCP were limited to a few minor points. The front bearing had to be reduced to a thickness of 1 mm as well as the addition of four locating lugs to replace the previous alignment features. Also a meshing feature had to be added to the worm wheel axle to interface with the potentiometer. This is in the form of a rectangular extrusion similar to that of a flat headed screwdriver.

Other alterations that are evident in this design are filleted edges for a smoother look and side inserts for the securing nuts that provided a more robust fixing. It was also decided that it was necessary to emboss the version on the top to aid in the identification of different component versions.

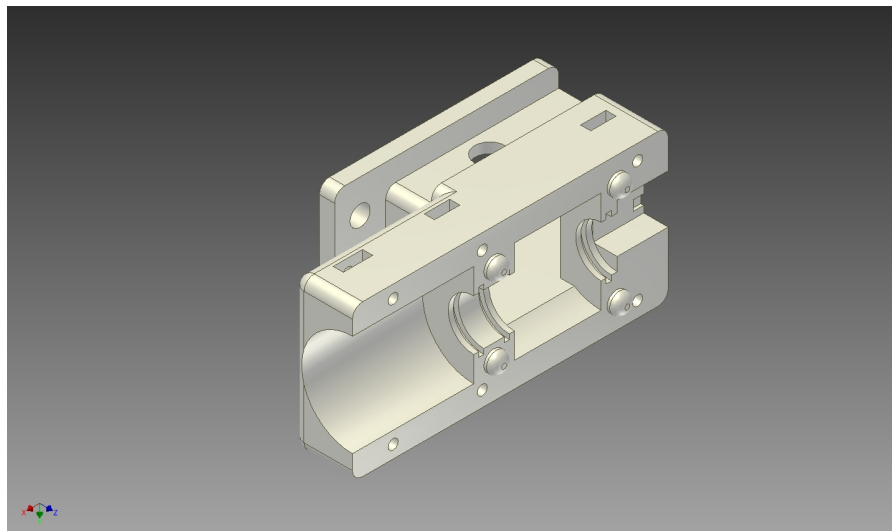


FIGURE 6.5: CAD image of MCP V2.4

Evaluation: The addition of a positional encoder to the finger joint means that the device has the potential to form gestures as well as functional grips, providing greater functionality than any child's device and match some of the most advanced adult devices such as the iLimb touch and BeBionic v2. This design extends the functionality of the design without adding weight, size, altering the position of major components or compromising the strength of the product.

6.3 MCP Version 3 (MCP V3.0)

The development of the hybrid fingers (Described in Section 5.2) meant that the existing design (MCP V2.4) required an alteration, as did the interface between the MCP and Finger. This was because the design of the hybrid fingers requires a second attachment point on the MCP for the supporting link. To facilitate this the front of the MCP was extended past the potentiometer and a hole added to accommodate the extra axle. Due to the already tight space constraints in this area of the design, several components needed to be placed within $0.5mm$ of each other. This does not affect the performance or the structural integrity of the MCP, however for manufacture and assembly this is closer than desirable. The new MCP-finger interface was first manufactured in isolation on a representative MCP block (V3.0) to verify the position of the links and their movement.

6.3.1 MCP V3.1

Once MCP V3.0 was used to verify the hybrid finger, the new MCP-Finger interface was transferred onto a working MCP design. Due to the extension of the MCP it was necessary to include of three $0.5mm$ holes in the lid to allow for the connection to the potentiometer.

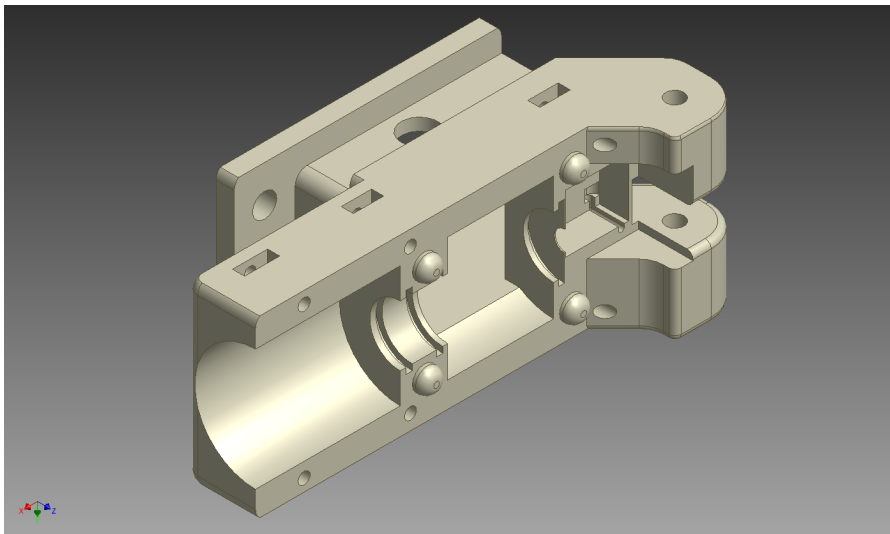


FIGURE 6.6: CAD image of MCP V3.1

To test the accuracy and repeatability of the potentiometer encoder, a key was produced that was able to replace the motor and drive the worm. With this key it was possible to control the rotational input of the worm to within 10° , therefore allowing 0.5° control of the finger position. During this testing it was found that there was a hysteresis in the positional measurement from the encoder, that could allow up to 6° of unmeasured movement in the finger. It was found that this hysteresis was caused by backlash in the meshing of both the worm-wheel and the axle-encoder. In addition, there was an

inherent hysteresis in the potentiometer of over 60° . This meant that with this design and components the best achievable accuracy in the measurement of finger position would be $\approx \pm 3^\circ$. When tested this was found to be insufficient to control the finger at the speed necessary to fulfil the specification requirements. In this testing the MCP was driven with the use of the motor controller implementing a closed loop control methodology. When driven at lower speeds ($\approx 5s$ for 90° closure) the finger could be controlled smoothly, if this speed was increased then the finger would oscillate and became unpredictable.

At this milestone the MCP was subjected to more in-depth mechanical evaluation tests than its predecessors. The drive system was tested over a hundred cycles and the MCP was subjected to loading through the finger. A kilogram weight was placed on the finger when it was in different positions. The finger was closed fully onto a solid object applying full torque to the object. Finally the driven link was closed onto itself at full power. During this evaluation of the design it suffered failures which highlighted the following underlying faults requiring alterations.

MCP walls: During the closure tests it was found that the MCP cracked around the wheel axle mounting. This was attributed to lateral loading of the component during the test and highlighted that this area of the MCP did not have the strength to withstand the normal forces applied to it. Due to the interfacing of the MCP with the driven link and the palm, there was a fundamental limit to the wall thickness of the MCP at this point. This limit was the reason that the wall was not able to withstand the forces applied during gripping.

Axles: It was found that all of the axles and mounting holes experienced a high level of wear, which, allowed the wheel axle to float, this in turn caused excessive backlash in the finger. To overcome this wearing the materials needed to be strengthened or substituted, it was decided to switch the printed axles for metal ones. To reduce wear and increase strength.

Smoothness: Before the wear became apparent, it was noticed that the drive axle suffered from high levels of friction, caused by the two printed surfaces running against each other. As the decision had been made to change the axle material to metal, it was felt that this issue would have been overcome.

Evaluation: The alteration of the specification for the MCP-finger interface is backwards compatible, allowing the hybrid MCP joints to be fitted with either the rigid or hybrid fingers. The addition of the Hybrid Finger performed as expected and axle holes placed on the MCP were in the correct position. That aside, the subsequent tests highlighted that the current design was not fit for purpose: The potentiometer gave insufficient resolution and the MCP case had developed multiple mechanical faults.

Using the potentiometer at the limit of its accuracy the finger could not be controlled to provide either the speed or repeatability required. The size constraints mean that a more accurate potentiometer could not be implemented. The proposed solution to this was to build a custom light gate based encoder built into the MCP; printing the encoder as part of the worm axle.

The mechanical faults were all centred around the MCP-Palm interface and the restrictions that this imposed on the corresponding features. There are two possible solutions, the first is to reinforce this section of the design with another component. This is not feasible as the component is already at the limit of its thickness due to its placement which is between the palm and the finger interfaces. The second option is to alter the MCP-Palm interface. This would mean that all previous designs would become obsolete and that the palm would require updating. However, as discussed in Section 7.1.7 (TH V4.0) the MCP-Palm interface is likely to produce further failure issues; meaning that altering the standard was the most logical solution.

6.4 MCP Version 4 (MCP V4.0)

Following the first prototype inspired from the Southampton hand, all of the MCP designs had interfaced with the palm with a slot which slid around the palm from the front, and then retained using two screws. As discussed above and in Chapter 7 (Design and Analysis of Palm and Thumb Mechanism) this interface methodology provided insufficient mechanical strength for a prosthetic device. As a result the methodology needed revising. To preserve the modular nature of the device this interface needed to be removable whilst providing a stable mechanical connection. The solution that was chosen was one where the MCP is designed to slot into the palm from above. This overcame the problem of separation with two altered features. The first is the retention feature at the front of the palm interface, this prevents the MCP from pulling out of the slot. The second is the alteration of the retention screws, which have been moved so that they are screwed down from the top into the palm. Passing through features in the MCP that prevent forward movement, the screws were also increased from M2 to M3 to further strengthen the design.

This version of the design was manufactured to test the integrity of the new MCP-Palm interface and to layout the space requirements for the light gate encoder. The final addition to this design variant was the addition of four miniature stainless steel roller bearings to replace the Tuffset ones used previously and to support the wheel axle. The removal of the potentiometer and the thickening of the MCP side wall allowed for their inclusion.

The area around the wheel axle bearing has been domed to improve stress distribution in the component when loaded. This alteration was made following the lessons learned during TH V5.1 (Section 7.1.6)

Evaluation: It was found that this new interface was more robust than the previous models. By increasing the wall thickness from $1mm$ to $2mm$, the component was stiffened and allowed the space to include bearings. The increased stiffness of the finger mounting combined with the improved attachment to the palm, provided a more stable solution. When subjected to the same forces that produced failure in the previous model (MCP V 3.1) this model was unaffected. The addition of the bearings and metal axles on the finger joints reduced the friction seen in the drive system, improving the smooth running of the system and reduced wear. The one drawback of these additions was that the wheel axle needed pressing into the bearings, increasing the complexity of assembly.

6.4.1 MCP V4.1

This version of the MCP was never manufactured as it was superseded by MCP V4.2 before the design was completed. The design features a remodelled encoder enclosure, to give better sealing around the PCB for the optical encoder, which it was hoped would improve the encoder detection sensitivity. Also, slots had been added to accommodate the PCB that would house the encoder electronics in the MCP. As discussed this design was surpassed, this was because an alternative motor became available, which included an encoder, rendering this design obsolete.

6.4.2 MCP V4.2

MCP version 4.2 can be seen in Figure 6.7. After discussions with a motor supplier (Electro Mechanical Systems Limited). It was found that there was a new $\varnothing 10mm$ motor manufactured by Maxon Motors (RE10) which had been reduced in length sufficiently to be fitted into the hand; it had previously been too long. There were three benefits to adopting this motor;

- It provides 1.5 times more torque than the Faulhaber equivalent, that was previously being used.
- The length of the motor meant that it could be fitted into the hand with an encoder, which, removed the risk of implementing a custom encoder.
- The Maxon motor-gearbox and encoder was lower cost than the Faulhaber motor-gearbox.

The alterations for this design were subtractive. The features that had been added to facilitate the embedded encoder, were removed; such as the PCB slots, the light guides and wire channels. These alterations meant that there was more freedom on the placement of the bearing at the front of the MCP. By moving the bearing towards the back, closer to the worm, the worm axle could be shortened and complexity of the surrounding features reduced.

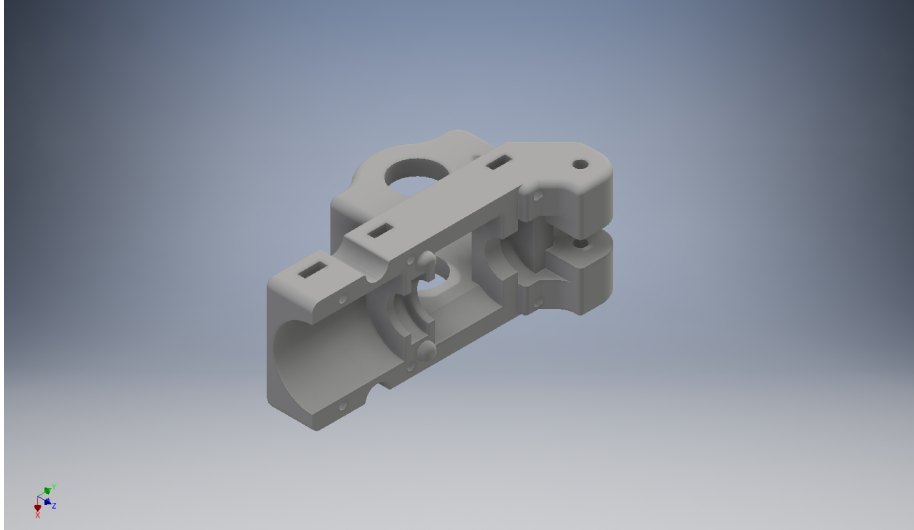


FIGURE 6.7: CAD image of MCP V4.2

Evaluation: By replacing the Faulhaber motor with the Maxon RE10, the MCP has higher output power, a simplified design and a lower unit cost; as well as a simplified design. With no apparent drawbacks this modification increases the capabilities of the hand and almost doubles the output power of each finger, when compared to the Faulhaber powered MCPs.

From inspection of this part, it became evident that the M1 bolt could be removed from the design. This would increase serviceability and reduce cost; these are precision manufactured parts that are expensive. With that exception this part is fully functional, the key component in delivering a lightweight prosthesis with multiple actuators.

6.4.2.1 Other Components:

This final design contains five other components; a drive shaft, two axles, a worm-wheel combination, four bearings and six enclosure screws. The bearings and the screws are standard components, whereas the two axles and worm-wheel are purchased components that have been modified. The drive shaft is a custom component that has been printed in the same material as the case. Below is a description of each of these parts, the order codes and the alterations made.

Bearings: There are two types of bearing in the MCP one for the finger axle and another type for the work axle. Simply Bearings - 7-0x4-0x2-0 MR74 and the Simply Bearings - 6-0x3-0x2-0 MR63 respectively.

Screws: The MCP final design is secured together using six M1 by 10mm micro-screws and the corresponding nuts (M1x10 Screws (A840110), M1 Nuts (A93401)). Due to their small size these screws are made from stainless steel and supplied by Precision Technology Supplies Ltd. (PTS-UK). It has been suggested that these screws could be removed from the design however this has not been tested.

Worm-wheel: The worm and wheel are both modified parts supplied by HPC Gears Ltd. The 0.4MOD, 1 start worm (PN: W0.4-1 (HPC Gears Ltd, 2011)) is nominally 25mm long, this has been reduced to 8.5mm. This reduces the worm to its minimum length, defined by the teeth in contact with the wheel. As discussed in MCP V2.1, this alteration means that the component is lighter and has a reduced the space requirement.

The wheel is a 0.4MOD 20 toothed gear (PN: PM0.4-20 (HPC Gears Ltd, 2011)), this part has four 1mm holes drilled into it, mm from the centre at 0°, 90°, 180° and 270° respectively. These holes allow the yolk of the driven finger link to be attached to the wheel.

Axle: There are two axles on the MCP, the driven link (or wheel) axle and the supporting link axle. These are manufactured from stock hardened steel Ø1.5mm and Ø3.0mm rod that has been cut to the correct length (14.9mm and 12.5mm respectively). Hardened steel rod was chosen for these components as the increased stiffness makes assembly easier.

Drive shaft: The drive shaft is a custom component specific to each MCP version; It is printed in the same material as the rest of the hand. The drive shaft that fits MCP V4.2 has a nominal diameter of 4mm. There are features at either end. The motor end has a feature to accept the motor shaft and at the other there is a collar that helps prevent movement of the axle.

Summary: The design for the MCP has passed through multiple iterations since the original variant. In this process there have been improvements to maximise the reliability, output power, weight, manufacturability and cost. The final design met the requirements as outlined in Section 4.1 for force transmission, size and cost. Whilst, permitting the individual actuation of each finger and supporting the capability for curling fingers. Both interfaces to the fingers and the palm have been modified. The finger interface has been upgraded to be able to accept the hybrid curling fingers. Whilst, the palm interface has been remodelled to improve coupling between the MCP and palm; increasing serviceability and reliability. The motor has been twice upgraded from the Faulhaber 0816 to the Faulhaber 1016 and then the Maxon RE10 this has increased the

recommended motor-gearbox torque and speed from 9.6mNm and 140rpm to 54mNm and 125rpm. The modular MCP unit presented in this research facilitates the functionality of multiply driven fingers lacking in all upper body prosthetics developed for children to date.

6.5 Computer Aided Design (CAD) Analysis

Using Autodesk Inventor Professional 2011 Autodesk, inc. (2011), the effects of stress on the hand were analyzed in the event of a child's weight being applied at different locations. To do this several assumptions of material properties had to be made. This was because the data sheet for the Objet FullCure720 has missing data and instead of a single value a range is often stated. When a range was given the worst scenario was chosen (Table 6.1). There were, however, two values that were not specified in the data sheet. The first of these is the yield strength, however the tensile strength (50MPa) and the elongation at break (25%) are specified. Assuming Hook's Law (stress is proportional to strain) this means that a value of 37.5MPa can be calculated; this is 75% of the tensile strength. The second was the material's Poisson's Ratio, assumed to be 0.350, similar to many other engineering plastic materials such as ABS Plastic, Nylon-6/6 and Acetal Resin who have values of 0.380, 0.350 and 0.350 respectively.

	Units	Data Given	Assumed Value
Tensile strength	MPa	50-65	50
Elongation at break	%	15-25	15
Yield strength	MPa		37.5
Modulus of elasticity	MPa	2000-3000	2000
Poisson's Ratio			0.350
Water absorption	%	1.5-2.2	1.15
Polymerized density	g_{cm^3}	1.18-1.19	1.19

TABLE 6.1: Objet FullCure720 Material Properties. (Adapted from data sheet Objet Geometries Ltd. (2010).)

The final factor that was required for the analysis was an applied force on the component. It was decided that the maximum force that the hand and therefore the components should be able to withstand would be the weight of the user; in this case five years old. To calculate a force Newton's Second Law was used. A five year old child has an average mass of 18.96Kg (Disabled World (2008)). The force on the hand supporting this mass is 186N (Full Weight Scenario). It was decided that the entire mass of the child would be placed on the hand during normal operation. This is a realistic force that the hand could be expected to withstand. The analysis focused on this force being applied in three different circumstances, the first two were both upwards and downwards on the finger axle location Figures 6.8 and 6.9. This would simulate the user putting their mass and therefore force on the finger. The third location was on the front of the MCP this would

simulate the application of force onto the knuckle of the hand Figure 6.10. The units on the plots are safety factor values and show where there are large and small strains in the component. Low values show where there are high strains and the component is likely to fail.

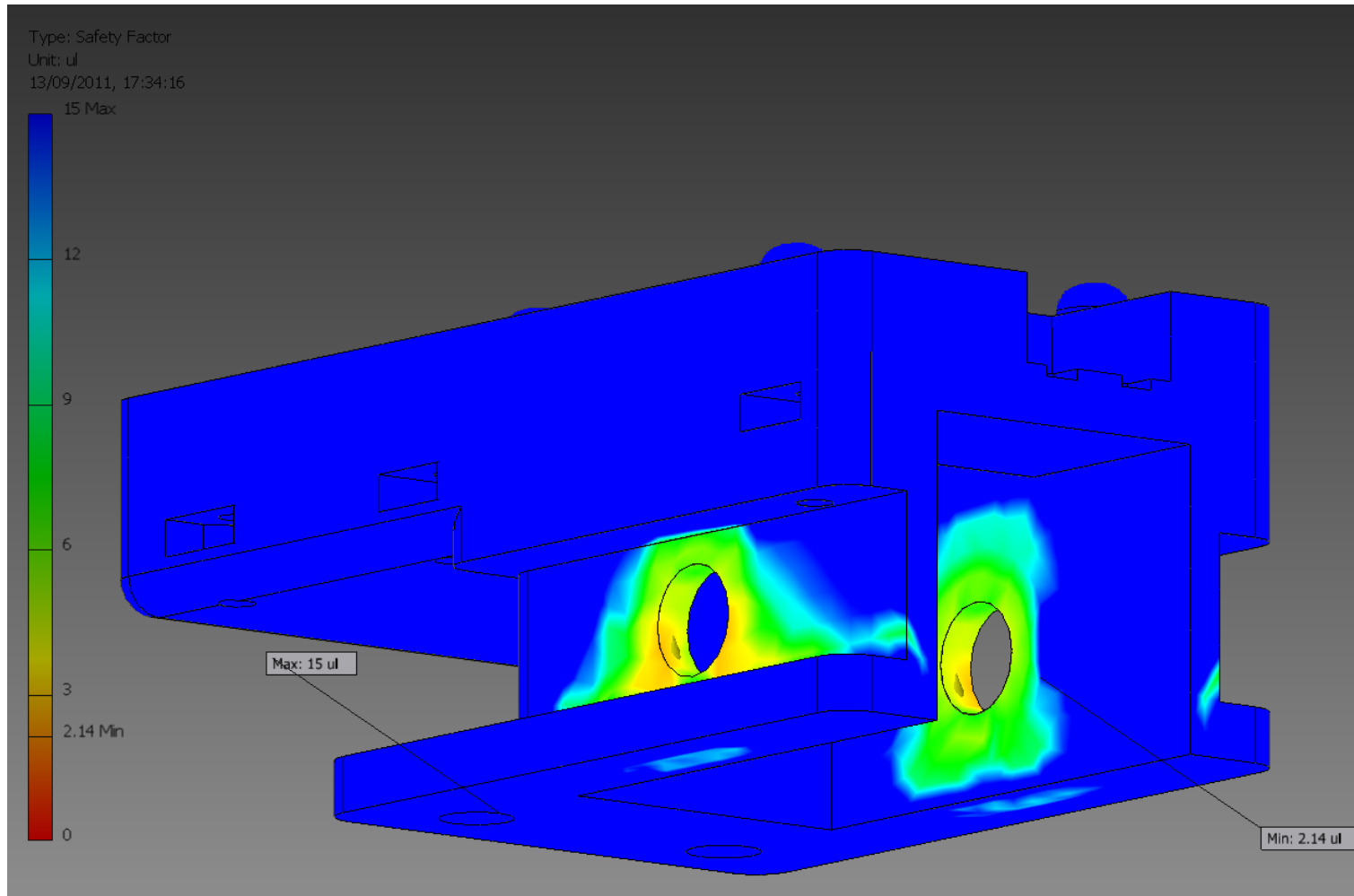


FIGURE 6.8: Safety factor analysis of the MCP Joint V2.4 constructed from Objet FullCure720 subjected to an upwards 186N force on the axle. The axle is not shown in the Figure but is between the two holes where strain is visible (yellow and green areas).

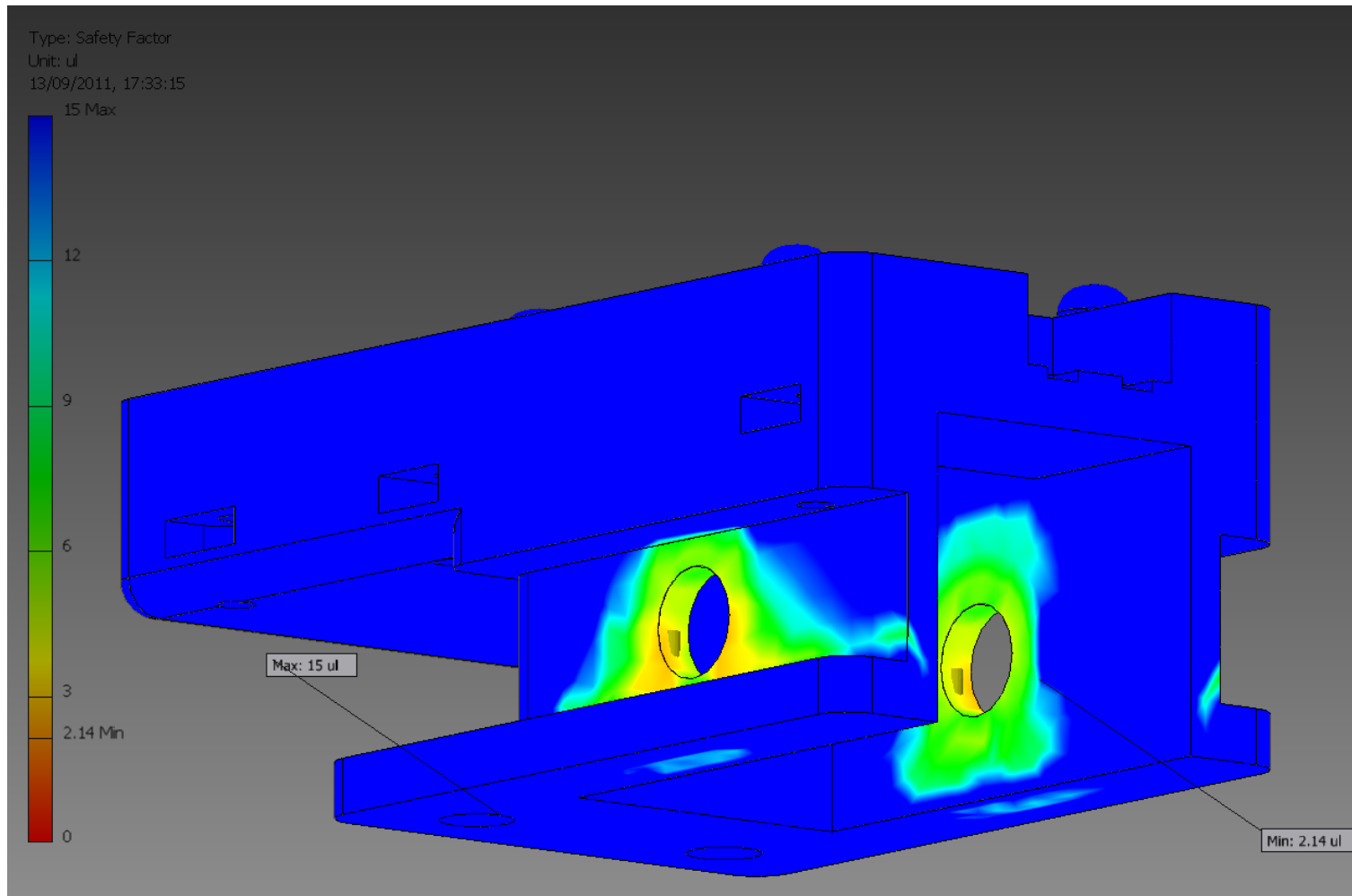


FIGURE 6.9: Safety factor analysis of the MCP Joint V2.4 constructed from Objet FullCure720 subjected to a downwards 186N force on the axle. The axle is not shown in the Figure but is between the two holes where strain is visible (yellow and green areas).

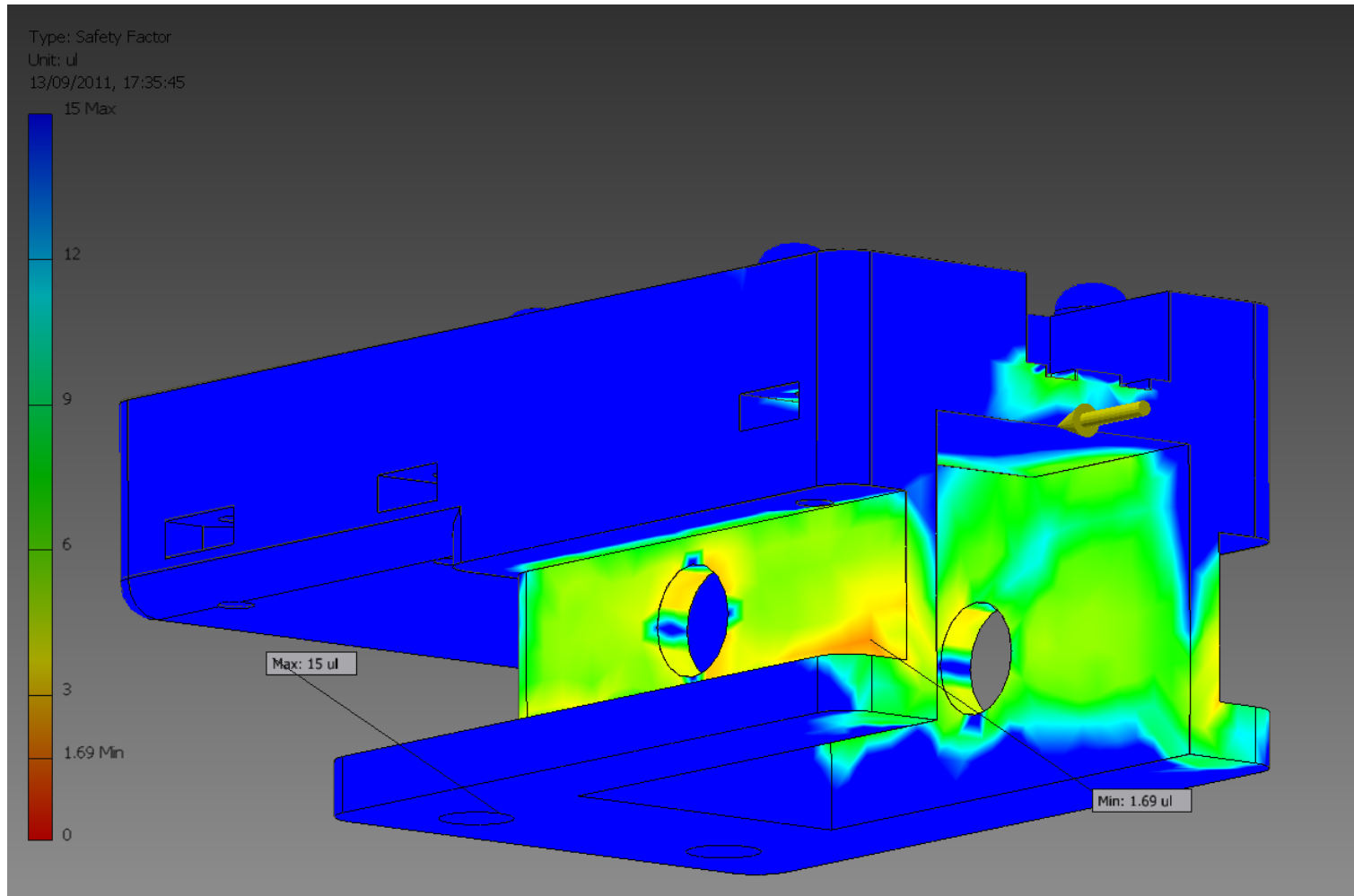


FIGURE 6.10: Safety factor analysis of the MCP Joint V2.4 constructed from Objet FullCure720 subjected to a 186N force on the front. Arrow indicated location and direction of the applied force.

Chapter 7

Design and Analysis of Palm and Thumb Mechanism

7.1 Opposable Thumb MCP and Palm

Light and Chappell (2000) suggest that it is common clinical consensus that at least 50% of the functionality of the human hand is attributable to the thumb. Therefore, having a prosthetic device with the full functionality of the human thumb is desirable. It is felt that the development of an opposable thumb could outweigh the development of individually actuated fingers. This view is supported by the fact that the latest OttoBock Michelangelo Hand has a powered opposable thumb over individually actuated fingers. Many other prosthetic hands possess a thumb that has actuated closure. However the thumb is rotated manually in these designs. This research aims to include two driven axes to provide a fully actuated opposable thumb.

In this section the palm will be discussed alongside the design of the thumb, this is because their designs are codependent alterations to the thumb MCP (tMCP) will affect the shape of the palm. This shape is an important factor in determining the different grips that the device can achieve. This specifically determines which and where individual fingers will intersect. The design of this hand will aim to allow the first and second fingers to make a pinch grip with the thumb. However it will not aim to allow the thumb to cross to the other fingers.

Studies into task specific prosthetics have found that they significantly increase the ability to complete the specified task (Walker et al. (2008)). With the modularity designed into the hand it would be possible to create task specific palms that the user could easily fit with their MCP modules. This would greatly increase both user choice and functionality. An investigation into developing different palms to provide varied functionality to the user is not within the scope of this research however, the development

of non-anthropomorphic and task specific palm designs that utilise modules from this research could be completed, once an anthropomorphic hand is developed.

7.1.1 TH V1.0

As the most incomplete section of the feasibility study, the palm and tMCP are underdeveloped. The palm is a flat sheet machined from plastic with four standardised interface features for accepting the fMCP joints along the front edge. Whilst, the thumb is a fixed block that is screwed to the palm using four locating holes. It provides no opposition capabilities, purely closure. Although limited, this design provided the final component for a light and functional hand that could perform both pinch and power grips with the first finger.

This design did provide the basis for the MCP-Palm interface specification (detailed in Figure 7.2). The $14.9mm$ total width allows for four finger MCPs to be placed on the hand within the $59.85mm$ total width requirement of a child's hand (Table 3.3 and Section 4.1). This specification allows for the insertion and retention of the MCP in the palm. The required cut-out is outlined with the maximum overlap permitted by the MCP guides. The mechanical interface between the components is maintained by a U-shaped channel on the MCP and two M2 screws, that run through the MCP into the palm.

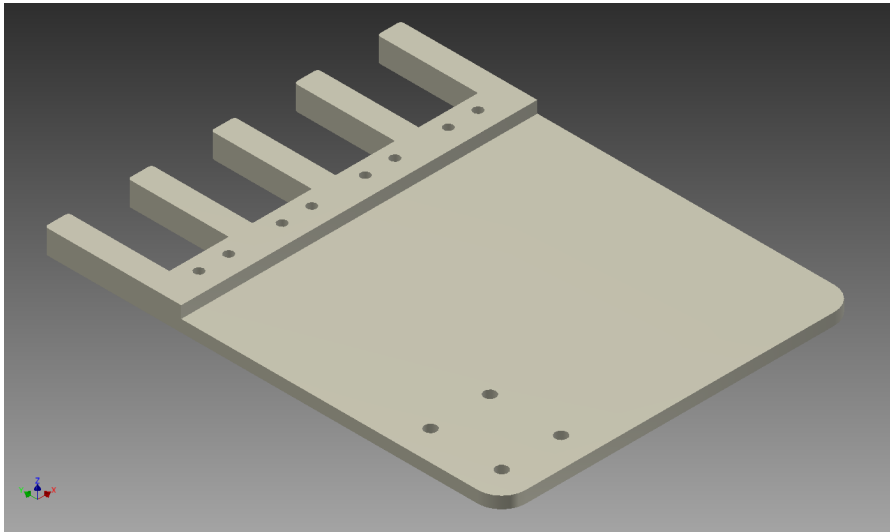


FIGURE 7.1: CAD image of the palm TH v1.0

7.1.2 TH V2.0

This design focused on the mounting of the drive system of the thumb opposition motor. The palm is an adaptation of the original design (P v1.0) that has been made thicker to accommodate the thumb closure motor. This motor and the drive gears have been

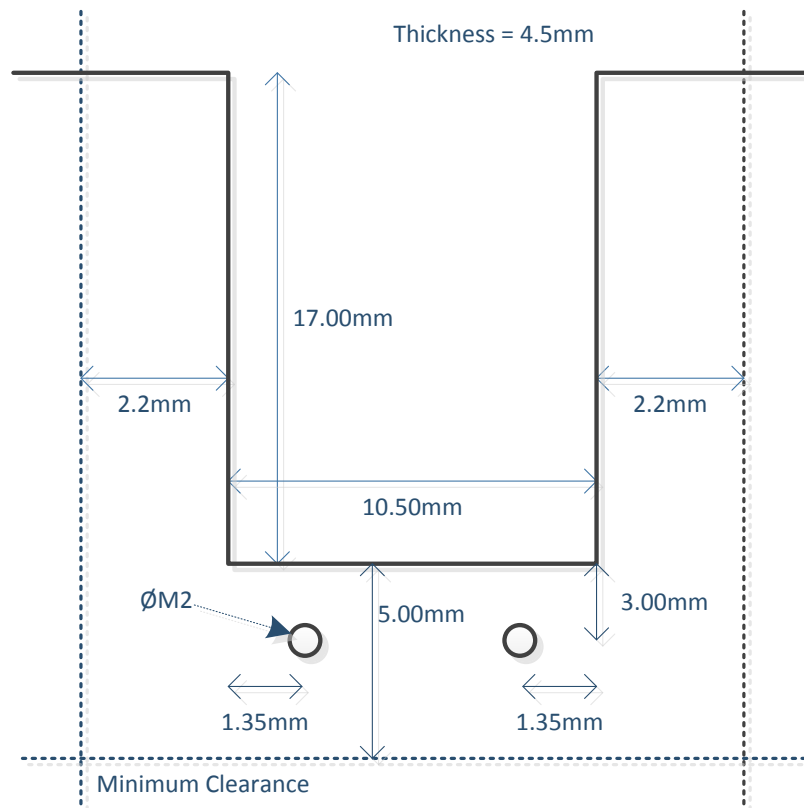


FIGURE 7.2: MCP-Palm Interface Specification v1.0

fitted into a cut-out in the palm, with a cover that fits flush to the rest of the design. A design decision was to build the axis of rotation of the tMCP close to the centre of mass. this was aimed at minimising the inertia needed to be overcome during opposition and therefore reducing the necessary power requirements of the motor assembly.

To drive the closure of the thumb, the tMCP uses the same Faulhaber 1016 DC motor-gearbox that has been used to actuate finger closure since MCP V2.1. As with the MCP joint, closure is transmitted from the motor through a shortened worm-wheel to the thumb.

Due to the low inertia and the assumption that no force would be applied to the thumb during opposition a smaller Faulhaber 0615 DC motor drives the opposition. The smaller motor helps minimise the total mass. Opposition is actuated via a spur gear that is hollowed out to allow it to sit around the Faulhaber 1016 motor of tMCP. The advantage of this is that it reduces the length of the component, however it does increase its diameter.

The design for the tMCP and therefore palm was never completed as it became apparent that a drive gear large enough to fit around the motor would be too large to be accommodated within the centre of the palm and therefore the design was not feasible.

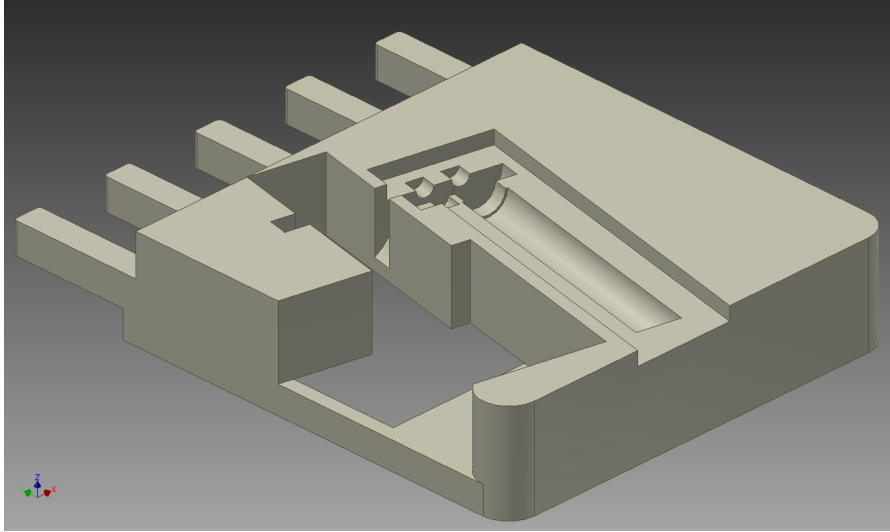


FIGURE 7.3: CAD image of the palm TH-V2.0

7.1.3 TH V2.1

Building on from TH V2.0, this was the first complete design for the palm and tMCP. It features a similar layout to the previous design, however the drive gear has been moved forward towards the fingers to allow for a smaller gear and therefore a reduced thickness. The palm in this design is a direct alteration from the design presented in TH V2.0.

tMCP: The tMCP is based around a main section that houses all of the components and an end plate that holds the worm in place after insertion. It is fully open on one side to minimise the thickness of the palm. This slot is used to insert the motor which, is then retained by a bearing that is pressed in before the worm is inserted. This end-plate fits onto the back of worm-wheel section, it allows the worm wheel to be inserted and it is held in place with four M1 screws.

An issue highlighted in the previous version was the length of the tMCP, this assembly boasts several notable features aimed at reducing its length. The first is the worm axle which is flared from $\varnothing 6.5mm$ at the end to fit over the motor drive shaft collar and then reduces to a $4mm$ diameter to fit through the worm. The second feature is the main opposition axle that doubles as the bearing and support for the worm axle. Both of these features are aimed at reducing the overall length by fitting components inside of each other and present a saving of approximately $2.5mm$; which accounts for a 10% reduction in length.

The last feature is an oval slotted gear mounting at the end off the design (this can be seen bottom right of Figure 7.4). It provides meshing between the opposition gear and tMCP without the need for additional fastenings.

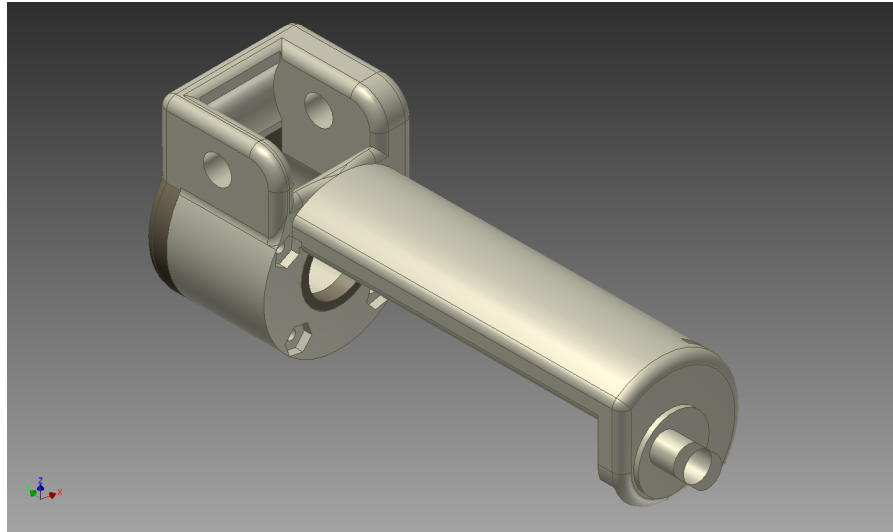


FIGURE 7.4: CAD image of the palm TH-V2.1

Palm: The palm had been altered from TH V2.0 to allow the fitment of the new tMCP; the opposition drive system was moved and the slot to allow the oversized gear required or the previous design was removed. Other modifications to the design included the shelling of the solid material to reduce the mass and provide a location to mount the PCBs. In addition an aluminium lid was added to the prototype to add strength around the tMPC cut-out, which it was felt lacked strength.

Evaluation: Since TH V2.0 there are several areas of this hand that are designed to reduce length, although these are successful solutions, after evaluation it was felt that there would be considerable friction on the modified axle and which would require alteration.

Once the design was assembled with the fingers in the CAD package it became evident that the design was too long. This was due to two oversights the first was because the palm had been designed to be the length of the hand of a five year old child without the consideration that the fMCPs would overhang. The second was due to the development of the hybrid fingers. Their curling action means that they make contact in a different location than the previous design, this results in inefficient pinching and the need for a thumb that is almost double the length of an humanoid thumb. This means that a shorter design is required for the palm, and therefore the tMCP.

There are two features that deserve merit. First, the slotted gear mount provides a low cost and efficient method of mechanically coupling the two parts together, without adversely affecting the strength of the component for this application. Also, the end-plate used to insert and support the worm, provides an efficient method of assembly.

7.1.4 TH V3.0

The current design for the tMCP could not be reduced in length without choosing a different motor. As the smallest Faulhaber DC minimotor only provides a reduction in length of $1mm$, therefore, a completely different approach was required. This came in the form of the Faulhaber 1512 flat DC-Gearmotor. They have slightly lower torque and speed characteristics than the comparable 1016 motor as well as having a slightly larger diameter however this power difference is small and they are two thirds shorter. The other difference between this motor and the last is that the motor drive shaft is no longer concentric; this means that the tMCP has to be shaped to accommodate this offset.

This version is a two-part design that is split down the middle, into a left and right section. This split requires the use of locating lugs as well as four screws to ensure integrity. This includes two sets of tabs at either end to provide fixing locations. Both of the sections are almost mirrors of each other, although they have opposite alignment features. The oval slotted gear mounting and Tuffset axle bearings seen in the previous version have also been incorporated into this design.

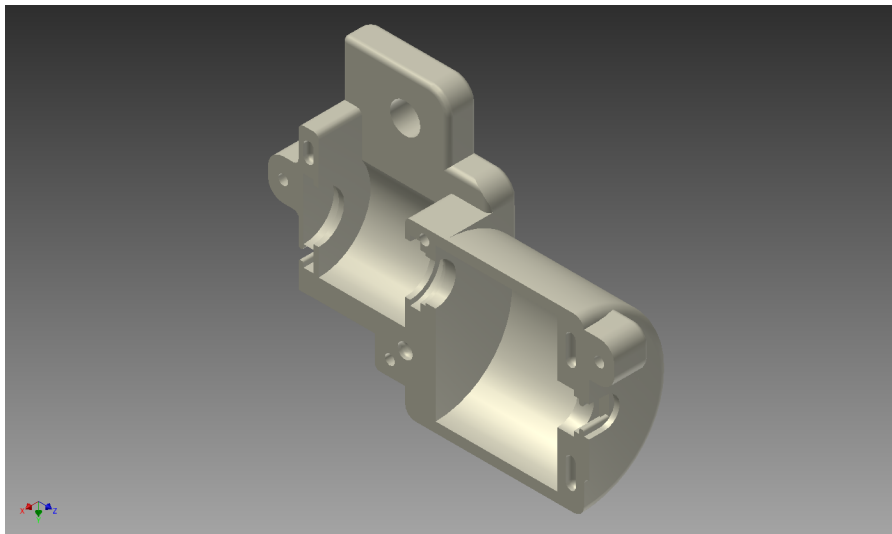


FIGURE 7.5: CAD image of the palm TH-V3.0

Evaluation: This design encountered multiple problems. The complex nature of the design would mean that it will be expensive to produce with additive manufacturing processes, and the curved nature means that it requires large amounts of support material. The tabs that hold the design together required the removal of a large amount of material in the palm, causing stability issues. Finally, the whole design is too high due to the offset drive shaft of the 1512 motor, making the palm too thick. The flat DC-Gearmotor is still the preferred option however it needs to be fitted in a different orientation. If the motor was placed with the drive shaft at the bottom it would reduce

the height of the design but would required a shaped thumb to avoid collision with the top of the tMCP.

7.1.5 TH V3.1

TH V3.1 was another intermediary step where the design was never fully matured. As suggested in the evaluation of the last design, this uses the 1512 motor rotated so that the drive shaft is at the bottom, meaning that this tMCP is not as high as the previous one (TH V3.0). This is the first design to make use of an elliptical form. Figure 7.6 shows how this shape permits a larger object can be rotated through 90° between two parallel planes, without interfering with the space above or below. This allows the design to accommodate securing tabs to screw the design together whilst still minimising the height of the palm. The drawback of the elliptical form is that mirror copies of the components are needed to make the right and left handed versions.

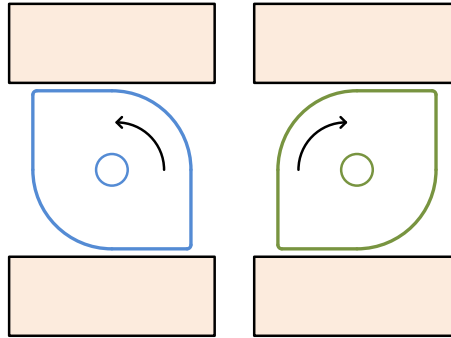


FIGURE 7.6: Diagram detailing 90° rotation of an elliptic object

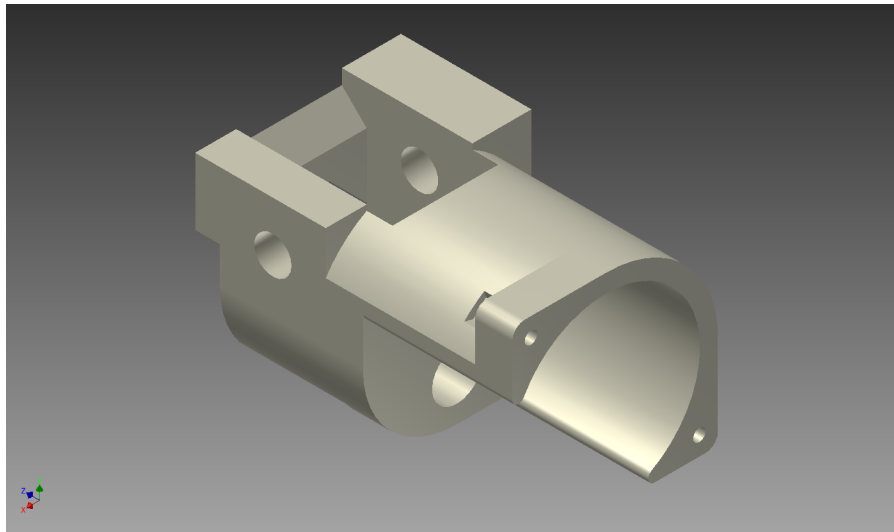


FIGURE 7.7: CAD image of the palm TH-V3.1

Evaluation: This version of the tMCP proved the concept for an elliptical form and the rotated motor position allowed for a much reduced palm thickness, therefore guiding

the final form of this component. However, the integrity of the part relied on 45mm^2 of material with a nominal thickness of less than 1.5mm . This would hold the motor in place and supported load transmission through the thumb. After the initial CAD modelling it was clear that this would not be sufficient and would cause this part to be prone to failure.

7.1.6 TH V5.1

In this version several previously unseen features are added. These are miniature ball bearings, wire threaded inserts and structural reinforcing. The first of these is to address an issue that has yet to be encountered; the fMCP designs developed in parallel with this research have shown high levels of friction and wear on the axles. It can only be assumed this is due to high radial forces during gripping causing large amounts of friction and wearing. To counteract this MCP Version 4 (MCP V4.0) added miniature ball bearings to provide a smooth action and better reliability. Therefore the design for the tMCP will also include bearings.

The second two features are included as a response to the issue of strength, as highlighted in the previous design. To add reinforcement, two M2 metal screws are inserted down both of the elliptical edges of the tMCP. The screws distribute most of the applied stress across the part, reducing the forces at any specific point. To reinforce the threads for these screws wire threaded inserts were added. Figure 7.8 shows how these metal sprung threads are wound into a pre-existing hole and provide a strong metal thread for a screw.

The advantage these are that they can handle higher loads without stripping the thread from the hole. This is because they spread the shearing force across the top and bottom of the threads of the original hole. As well as this the wear resistance of the thread is increased as the metal-on-plastic wear becomes metal-on-metal.

tMCP: This is the first design for the tMCP that fully encases the motor. The elliptic form is retained however it is split into two distinct parts, the motor housing and, the worm-wheel housing. The end plate is considered part of the worm-wheel section.

The motor housing is a hollow piece that slides over the top of the motor and has the oval slotted gear mount on the end. This piece is designed to be ambidextrous and therefore can be fitted to either hand. As mentioned previously, most of the structural rigidity is provided by the securing screws. This allows the reduction in the thickness of the walls around the motor to minimise size. The worm-wheel section is not dissimilar to the design from the previous section, except the addition of bearings to support the drive axles. One alteration is that the end plate and the main axle have been incorporated to produce one component. This allows space for the bearing supporting the worm axle to be placed within the end plate.



FIGURE 7.8: Wire Thread Insert

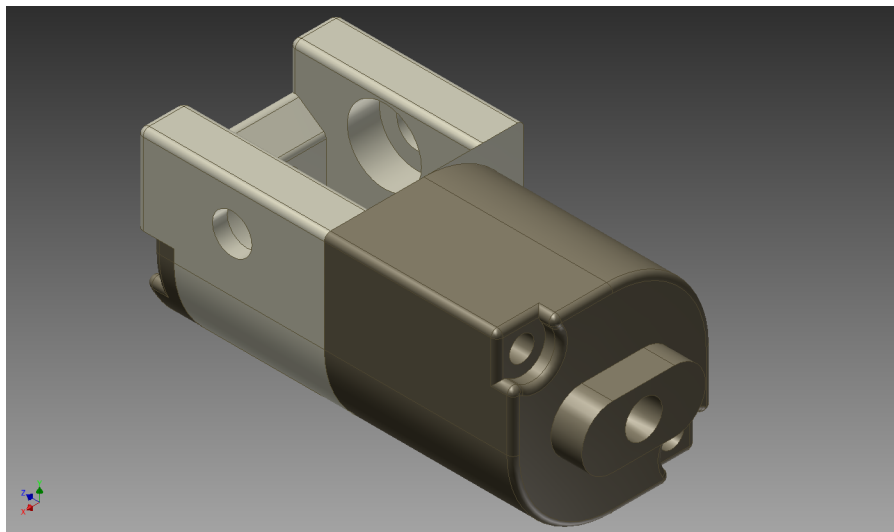


FIGURE 7.9: CAD image of the tMCP TH V 5.1

Evaluation: The addition of the new features increased the complexity and therefore the overall cost burden, however this is small when compared to the expected increases the reliability and serviceability. The use of M2 screws with wire inserts, over the M1 screws and nut used previously adds strength to the component, as well as reducing the reliance of the hand on speciality components. An initial evaluation of the use of bearings showed an increased smoothness of actuation and reduced signs of friction (faster and quieter actuation).

A fault was discovered with the design of the thumb axle support. The material that was removed for the thumb axle bearings had caused a weakening in the top of the design that caused cracking when the bearings were inserted. This requires the addition of material above the bearing fitting, to transmit the loads more effectively.

This design is less than 33mm long and can fit between a space that is less than 16.5mm wide. However, this still consumes more space than is available within the palm. Initial evaluation of the palm shape for this tMCP showed that with the associated drive train, the palm could become weak due to too much material removal. Also, due to the length of the tMCP, it would interfere with the locating of the finger joints.

This analysis suggested that with all possible reductions in length of the thumb joint that it would be too long to fit into a palm that is able to support multiple fingers. This necessitated a review of the mounting methodology of the thumb. This considered the solution is robust, low cost and light, which are all essentials in prosthetic products.

7.1.7 TH V4.0

Up to now, to achieve opposition, all of the designs for the thumb have rotated around the same axis as the worm-wheel, to minimize the inertia. This version takes a completely fresh approach to the design. The motor has been stood on its end, making it part of the metacarpal. This means that the space required within the palm is instantly reduced. As with TH V5.1, this design has screws to provide reinforcement and wire inserts in all of the screw holes. In addition it has bearings on all the joints and gears.

This section has been split into the three main components of the design. These are: the tMCP, the palm and the thumb.

tMCP: This is a two piece design which, is fundamentally similar to that of the previous version (TH V5.1), however, there have been additions to the design and due to the reorientation. These changes were centred around the mounting locations of the main axle that were moved from either end to the front and back of the motor housing. Unlike the previous tMCP versions, 5mm main axles were designed to be integral to the motor housing. This merging of components reduces the total component count and allows for space reduction as no room is required for main axle bearings on the tMCP. These are placed into the palm. The rear axle also incorporates the slotted gear mounting, seen in previous designs.

The other alterations that were made to the tMPC were the rounding of the base so that it follows the shape of the palm, the addition of a slot to allow the egress of the motor cable and the addition of support material above the thumb bearing. The altered profile on the base of the motor housing was to add reinforcement around the axles and to prevent debris from becoming lodged underneath it. Since the motor is asymmetric, the position of the channel for the motor cable was dictated by the cables location on the motor and the motor position. Fortunately the path runs through the thickest edge of the tMCP, therefore, the addition has little effect on the structural integrity. As discussed in the evaluation of tMCP version 3.2 the area around the thumb axle bearing

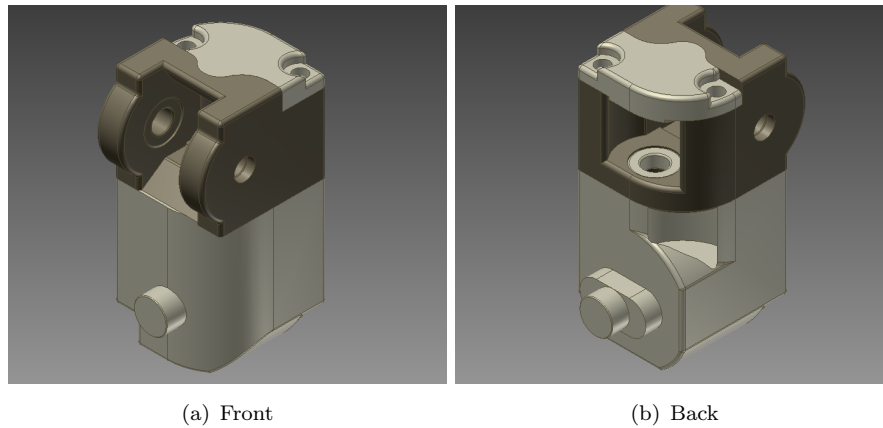


FIGURE 7.10: CAD image of the tMCP TH V4.0

needed to be strengthened. To overcome this issue the material around the hole was increased to form an arc with a radius of 6.5mm .

Palm: Like the first version (P V1.0) of the palm this design continues to have four finger locations that are in a straight line across the front of the part. However this is the end of the identifiable similarities. Due to the inclusion of the thumb and its associated opposition gear, it was required to make this piece thicker. It has been increased to a nominal thickness of 15.7mm up to 18.6mm around the thumb joint. This component has two notable features; the thumb mounting and, the opposition drive mounting. As with the tMCP the thumb mounting it designed to minimise debris build-up between the tMCP and the palm as well as maximise the structural integrity of the bearing locations. This is achieved with a curved form underneath the tMCP and with a slot to allow the largest opposition gear to rotate freely. There are three opposition gears which have been chosen to create the largest gap permissible between the tMCP and the motor whilst, giving a large ratio across them so to prevent unwanted movement by creating a self locking situation. The gears chosen for this application have 30, 58 and 80 teeth gears respectively which gives a gear ratio of $3/8 : 1$ from the gearbox to tMCP. In the reverse direction this is $2, 2/3 : 1$ and when coupled with the $64 : 1$ from the motors planetary gearbox gives a ratio $170, 2/3 : 1$ between the tMCP and the motor. From the perspective of driving the tMCP, the inertia of the motor rotor is increased by over 170 times. To manually move the tMCP a relatively large force is required and therefore, it seems locked.

The lid is open above the tMCP to allow it to rotate from an opposing grip to a pinch grip. The motor mounting opposition motor and associated gears in place. The notable point is that due to the length of the motor it is almost the length of the palm casing. At 31mm this represents the fourth shortest Faulhaber DC motor configuration possible and the first that is able to provide the suitable power requirements (25.6mNm) to oppose the tMCP. The length means that the electrical connectors must protrude into

the are under the fMCP sockets. This causes no interference problems, however it does mean that the design would not be waterproof.

Thumb: Although there is a anthropomorphic bend in the shape of the thumb, it is purely a functional design. It is dictated by the different points of contact that it is required to make. The tip has a rounded section so to be able to form stable pinch grips. The pad of the thumb is flat to allow for the formation of the lateral grip along the side of the palm. The final feature is the standard finger connection to mesh with the tMCP. Although this design is functional, there is an allowance to make it thicker. As the current design is the same thickness as the fingers and an anatomical thumb would be thicker. Widening the thumb could help increase the stability of the grips.

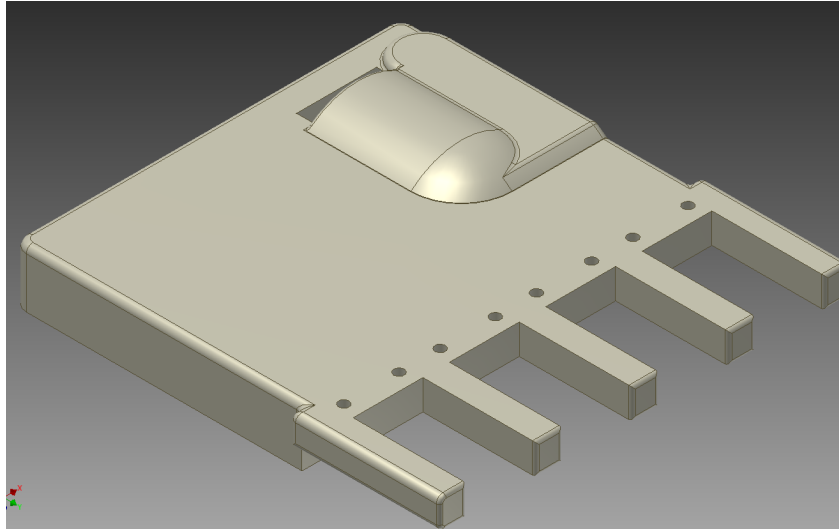
An area of concern for the hand is the interface between the MCP and the palm. When the hand is carrying or pulling something, the interface provides little protection to the MCP pulling from the hand. To test a palm and fMCP, they were loaded twenty times and the response of the design to these loads was assessed. As discussed in Section 6.5, the force caused by the weight an average 5 year old child 184N. If the child was hanging from both hands and assuming equal weight distribution the then this would apply 23N to each of the four fingers of each hand.

The test set-up consisted of a palm (P v 4.0) and MCP (MCP v 3.0) (Seen in Figure 7.14), note the oversized screw used to attach the mass to the finger. The palm was then clamped to a desk with the finger pointing vertically downward. Then the mass was attached to the finger and the joint was inspected with and without the mass applied. It was observed that, when loaded, there was deflection in the interface. At the end of the experiment it was apparent that the retention screws had loosened, which allowed the MCP to slide back and forth within the interlace by 0.14mm. This movement was removed after re-tightening the screws, however reappeared when the test was run a second time.

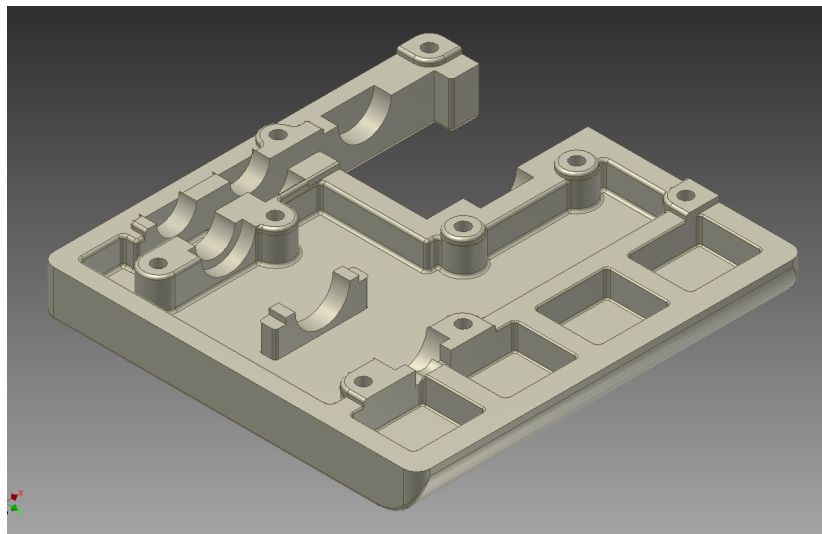
From this test it could be concluded that the interface relied on the integrity of the screws when mass was applied to the MCP. It was also established that the cyclical loading caused the retaining screws to loosen. This leads to the assumption that repeated loading would cause the screws to loosen, which could cause failure of the screws. This, it turn would allow the MCP to slide from the hand.

Evaluation: This is the first prosthetic with a fully powered opposable thumb designed for children. Since the reorientation the design has the added benefit that the tMCP joint takes the place of the human Metacarpal becoming part of the thumb. Therefore, the thumb need only be the length of the Proximal and Distal phalanx. This means that the motion looks more natural than it would have otherwise.

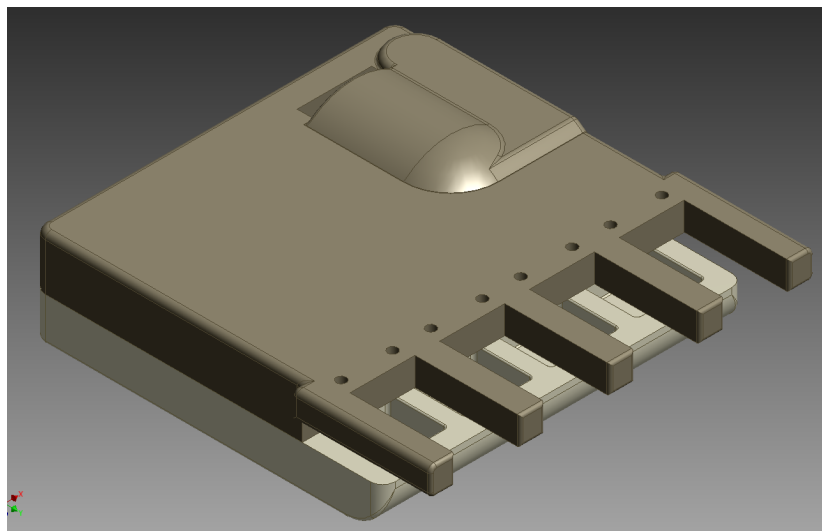
Although this is a working design there are areas that could be improved. As previously mentioned increasing the width of the thumb could aid grip stability and increase the



(a) Base Top

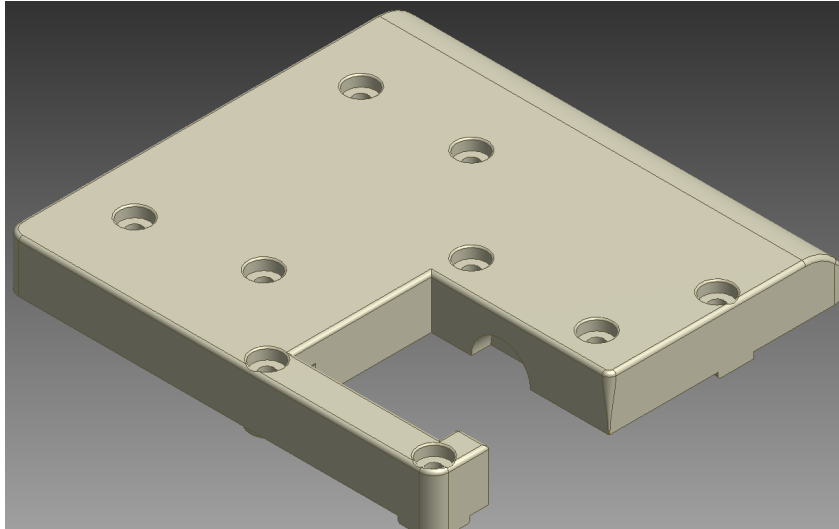


(b) Lid Bottom

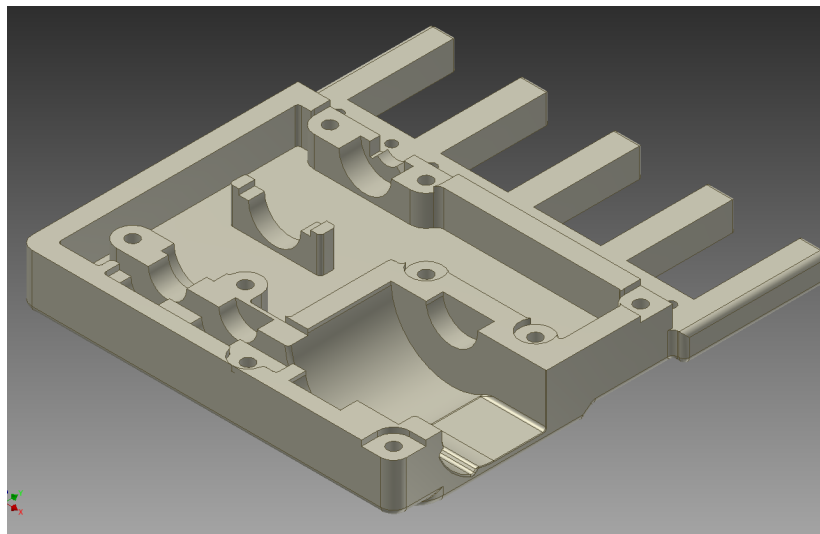


(c) Assembled Palm

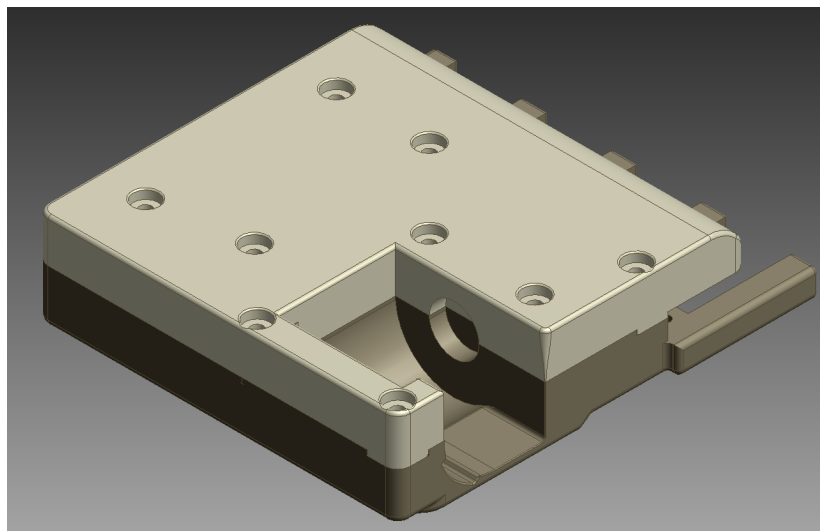
FIGURE 7.11: CAD image of the base and lid of the palm for TH V4.0. Viewed from the top.



(a) Lid Top



(b) Base Bottom



(c) Assembled Palm

FIGURE 7.12: CAD image of the base and lid of the palm for TH V4.0. Viewed from the underneath.

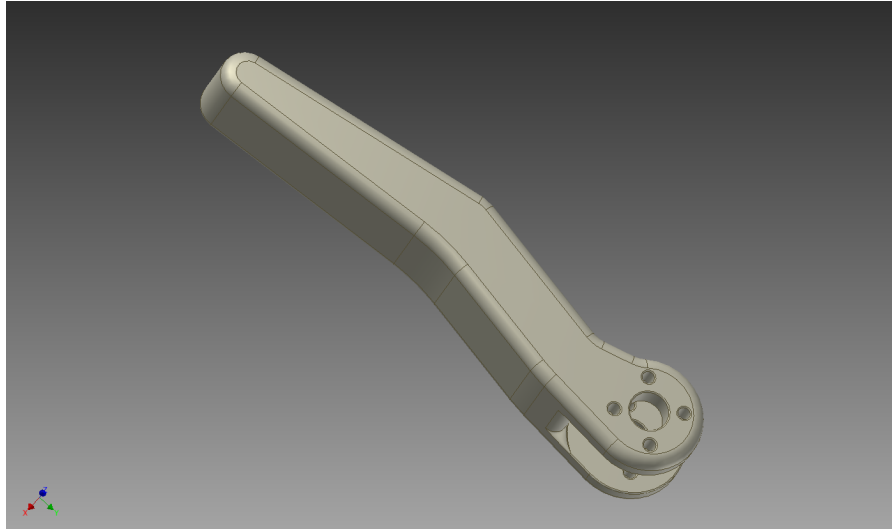


FIGURE 7.13: CAD image of Thumb T V4.0

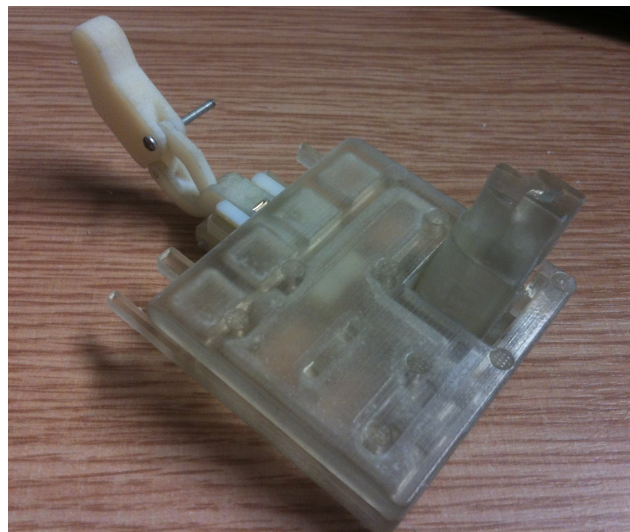


FIGURE 7.14: CAD image of Thumb (T V4.0) test rig

anthropomorphic nature. The motor cable is the only component that bridges between the palm and the tMCP. It is made from a ribbon cable that allows some movement but the amount required when the joint moves may mean that it is susceptible to breaking or snagging. To overcome this a mobile cable tidy or rotary electrical contacts could be used however neither solution is without its own drawbacks.

One element that was omitted from this design that is required in a final product is a position sensing unit for the tMCP opposition. If a small encoder is employed it could be added either on the main opposition axle or on the axle for the middle gear.

The current design for the palm lid could be made almost $3mm$ thinner. This would mean that the fingertips would not touch the palm when fully closed. However the Be-Bionic hand brochure RSL Steeper (2011) identifies fourteen functional hand positions

none of which require the contact of finger tip and palm. This suggests that this functionality is not required and therefore mass and the thickness of the product could be reduced.

The findings from the investigation into the MCP-Palm interface show that it is necessary to change the design of this interface, as it is not fit for purpose. To fix the issues that have been highlighted, the screws could be made bigger or they could be bonded with an adhesive. However, failures in the MCP described in Section 6.3.1 made the appropriate decision to alter the MCP-Palm interface design.

7.1.8 Palm V6.0

A new specification was needed for the MCP-Palm interface, to correct two issues. The first is pulling out of the MCP and the second was to allow the strengthening of the driven axle support on the MCP. To achieve this, the space between the interface has been increased, allowing for the MCP to be strengthened. To prevent the interface from pulling apart when loaded, the screws have been increased and moved to sit within channels in the MCP and retaining lugs added at the front. This new specification can be seen in Figure 7.15.

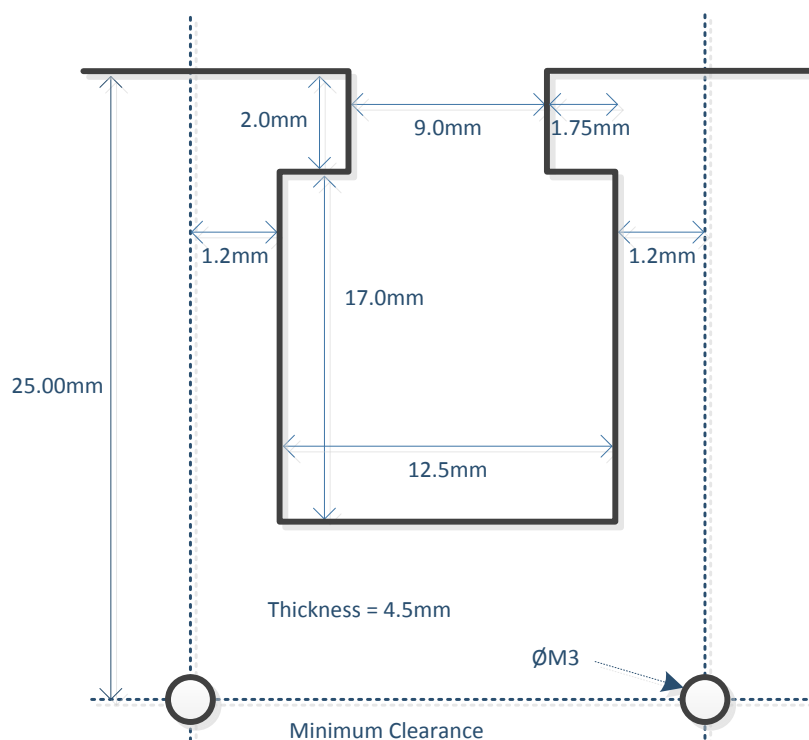


FIGURE 7.15: MCP-Palm Interface Specification V2

7.1.8.1 Palm V6.1

The palm needed redeveloping to accommodate the new specification for the MCP-Palm interface. To improve strength and serviceability the palm (v6.0) was separated into two sections. The existing body of the palm and an interface section; these components were fastened together using four M3 screws which screwed into threaded holes in the interface section.

The palm had the existing interfaces removed, and a flat surface developed for the interface section to mate onto. The driving motivation behind the addition of the interface section was the ability to upgrade the interfaces to a metal, if the plastic variants were found to be too weak. It is a flat component that holds the four fMCPs, it was designed to allow quick removal of either the individual fingers, each fMCP is held by 2 screws, or removal of the finger unit, which is held by four screws.

The palm underwent one further version (V6.1) this was to remodel the design so that it was able to fit an encoder onto the middle transfer gear and therefore provide positional feedback on the opposition position of the thumb. During the re-model it was felt that it would be an advantage to adapt the design so that it could be injection moulded as well as 3D printed. Allowing for more flexibility in the manufacturing process, this creates a more versatile system.

The addition of an encoder onto the thumb opposition joint means that all six driven joints on the hand have positional feedback, therefore the controller has the ability to produce gestures and complex grip patterns. With the correct control profile this provides the device with the equivalent functionality of the most advanced multi-actuated adult hands discussed in Section 2.4.2.

7.1.9 Proposed Device

There have been several iterations of the research that have culminated in a device aimed at bridging the gap between child and adult prosthetics. The final hand has, individually actuated curling fingers and, a driven opposable thumb. In addition, it also achieved the goals of a low cost, modular system. The final prototype hand has the same form factor as discussed in the Research Approach (Chapter 4).

It can be seen in Figure 7.12(c) that at present the palm is flat. This does not provide assistance when gripping objects that do not have a flat face. Features may need to be added to give the hand a concave anthropomorphic shape to aid in object stability during gripping.

7.2 Modelling

To be able to control the hand the controller must understand the position of the fingers and thumb in a spacial context. The relationship between the position of a finger tip with relation to its input angle was discussed in Section 5.3. Here the trajectory of the thumb will be calculated. Allowing for a whole hand model to be discussed.

The spacial area of the thumb is defined where, x denotes back to front, y across the palm, and z the height above the palm.

A model of the accessible space in which the tip of the thumb can actuate can be computed as it consists of two rotational joints and two fixed length links. Therefore the position of the tip of the thumb relative to the base of the tMCP can be calculated with Equations 7.1, 7.2 and 7.3.

$$x = L_2 * \sin \theta \quad (7.1)$$

$$y = L_1 * \cos \alpha + L_2 * \cos \alpha * \cos \theta \quad (7.2)$$

$$z = L_1 * \sin \alpha + L_2 * \sin \alpha * \sin \theta \quad (7.3)$$

Where: Length of tMCP, $L_1 = 30mm$,

Length of thumb, $L_2 = 52mm$,

Opposition angle, $90 > \alpha > 0$,

Closure angle, $110 > \theta > 0$.

To model the entire hand the Origin of the Hand (the 0,0,0 position) must be defined, this was selected to be the bottom corner of the palm opposite the tMCP, chosen as it would likely be the point of attachment of the hand to the socket.

The top of the palm is a flat surface that is parallel to the XY plane offset from the main axes of rotation of the thumb by $7.0mm$, and the side of the hand is a flat surface parallel to the XZ plane, main axes of rotation of the thumb by $14.7mm$. The area underneath these planes is defined as inaccessible.

Using the equations above, the thumb can be inserted into a whole hand model, giving the equations for the thumbs position as:

$$xTH = L_2 * \sin \beta + xTH_0 \quad (7.4)$$

$$yTH = L_1 * \cos \alpha + L_2 * \cos \alpha * \cos \beta + yTH_0 \quad (7.5)$$

$$zTH = L_1 * \sin \alpha + L_2 * \sin \alpha * \sin \beta + zTH_0 \quad (7.6)$$

Where xTH_0 & yTH_0 & zTH_0 denote the offset of the rotational axes of the tMCP from the origin of the hand.

The fingers can be introduced into the whole hand model by calculating their position with relation to the Origin of the Hand, using Equations 5.22 and 5.23 to get xT and yT .

This requires a mapping transformation the between the reference frame of the MCP (as denoted in Section 5.3) to that of the whole hand. In this mapping the x-axis of the finger maps onto the negative z-axis of the hand and the y-axis of the finger maps onto the x-axis.

Applying this mapping and calculating the position with reference to the Origin of the Hand gives the generic Equations 7.7, 7.8 and 7.9 to describe position of each fingertip with relation to hand.

$$xF_n = xF0_n + yT_n \quad (7.7)$$

$$yF_n = yF0_n \quad (7.8)$$

$$zF_n = zF0_n - xT_n \quad (7.9)$$

Where,

n is the finger reference (1-4),

F denotes the fingertip position with reference to the Origin of the Hand, in the x , y and z axes,

$F0$ is the offset of the MCP from the origin of the hand in the x , y and z axes.

Since xT and yT are dependent on θ . it can be seen that the orientation of the a grip can be defined with the knowledge of only six variables; α , β , θ_1 , θ_2 , θ_3 , θ_4 . All of these equations are discrete, for a specific input they only have only one possible output position. As well as that the device has the ability to measure all of these in real time, therefore the hand is able to continuously calculate its grip pattern.

Chapter 8

System Controller

This research aims to improve the state of the art of prosthetic hands for children. To increase a users acceptance of their device. To benefit from the advancements of the novel fingers and thumb, a system needed to be developed to control the hand. As this research aims to increase the level of choice and adaptability when fitting a prosthetic device, a control system needed to be developed that is equally modular and flexible. This controller must be able to control the individual actuation of the fingers and thumb whilst enabling the flexibility of the device provided by the modularity of the device.

This controller must accept control signals from an input source, interpret the desired command and then individually position each of the fingers. The final control system is presented in Figure 8.1. It can be seen that it is a master-slave system where each finger has its own controller and motor driver that manages actuation. The thumb has different controller for opposition and closure.

This controller is required to interpret an input signal from a range of sources and then individually position the fingers using selection of control methodologies. The best method of implementing this was with a master-slave control system, where each finger actuator has an identical control board that is then centrally managed by another of the devices; programmed to be the master. The slaves are then linked via a communication bus allowing for any number to be connected or disconnected at one time. The system has also been designed to support multiple analogue and digital feedback sensors from the finger.

For this purpose a miniature PCB needed developing that is able to communicate with other devices, drive a motor, read an encoder, detect and prevent a motor over-current situation, as well as have analogue capability to measure analogue force and temperature sensors. The design allows the board to be used as any of the slave motor drivers as well as the master. This provided the additional requirement to be able to read digital and analogue inputs on all of its pins. Hence this would allow the master to handle multiple different inputs.

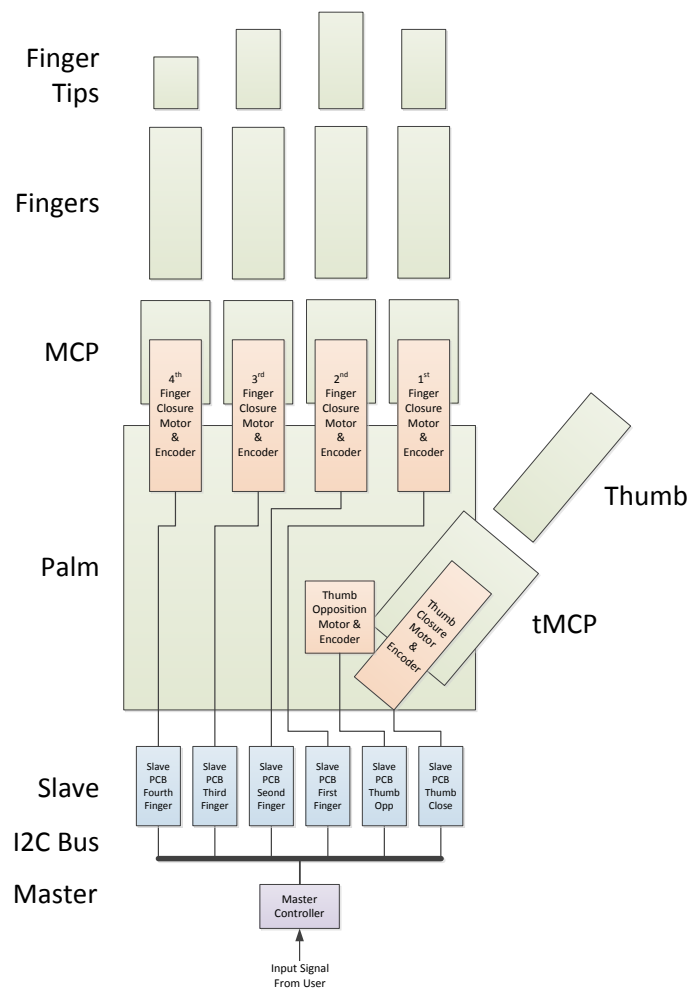


FIGURE 8.1: Diagram of the Control System for the Hand

Table 8.1 shows the specification requirements for the controller boards. This covers aspects from the physical dimensions which have been chosen to fit on the palm around each motor, to the required external connections. It can be seen that the specification allows for a motor with higher supply needs than the chosen motors, this allows the motors to be upgraded if a better alternative becomes available. The other advantage of having an overrated motor driver is that it produces less heat, meaning there is no need for cooling.

It was decided that each of the motor drivers should have their own low power linear regulator to provide 3.3V for the chips. This means that there would only need to be one main 6V power supply for the hand, and would allow for less connectors between boards. As well as this, it acts as a buffer for the microcontroller removing spikes caused by the motor switching. The regulator that was chosen was the Texas Instruments TPS79933, which has a low quiescent current and a small footprint. These are then supplied

by a single 6V switch mode regulator (Section 8.1.2) that supplies power to the entire hand.

Pulse Width Modulation (PWM) is a common method used to control the average power to an electrical device. It uses a modulated rectangular waveform where the pulse width (duty cycle) can be adjusted to vary the total high time of the pulse. By adjusting this the average voltage, and therefore the power seen by the load, can be controlled. To avoid interference the switching frequency of the PWM must be chosen to be high enough so that it is not seen by the load.

When running a unidirectional DC motor with PWM there are some additional requirements for both motor and circuit protection. To give the optimal input response during switching an inductor is required. The size specified in Table 8.1 was recommended by the manufacturers during personal communications. Clamping diodes to the supply and ground have been specified to protect the motor driver from the back EMF produced as a motor is stopped. The final aspect of the protection is the inclusion of two capacitors ($22\mu\text{F}$ & $0.1\mu\text{F}$) used to remove any voltage spikes that can cause interference within the circuit.

TABLE 8.1: Final Specification for Controller PCB

Parameter	Typical Value	Variance	Units
Length (L)	25	Max	mm
Width (W)	15	Max	mm
Height (H)	10	Max	mm
Step Height (H1)	5	Max	mm
Step Length (L1)	15	Max	mm
Number of Motors	1		
Maximum Motor Voltage	10	$\pm 10\%$	V
Maximum Motor Current	500	$\pm 10\%$	mA
Motor Inductor	200	$\pm 10\%$	μH
Motor Protection			
Programming Header	1		
LED	1		
User Input Button	1		
No. Analogue-Digital I/O Pins	4		
Number of External 3V3 pins	1		
Max Current on Ex 3V3 pin	150	$\pm 10\%$	mA

8.1 PCB Design

8.1.1 Controller

The allegro A3906 H-bridge motor driver is able to comfortably supply the required power to the motor, however it was primarily chosen because it has inbuilt over-current protection. It uses a small resistor to continuously monitor the current, then limit the power when it detects the current is too high. The resistor for the current detection is placed in the circuit between the H-bridge and ground. The value then must be chosen to cause a 0.2V drop across the resistor when the current is at the desired limiting value. Using Ohm's law the required protection resistor for the three motors can be calculated (Table 8.2):

TABLE 8.2: Required protection resistors

	Max Current (mA)	Desired Resistor (Ω)
Maxon RE10	300	0.69
Faulhaber 0810	120	1.67
Faulhaber 1215	130	1.57

The resistances specified in Table 8.2 are not exact resistor values, the closest available alternatives need to be found. Resistors that are greater than the optimum need to be chosen to ensure that the over-current cut-off is below the maximum value, allowing for a margin of tolerance. Values that are approximately 10% higher than required were chosen. The resistor values and the resulting maximum motor currents can be seen in Table 8.3. Since the Faulhaber-0810 and the Faulhaber-1215 motors require similar values, it was decided that they should use the same resistors to increase the level of component reuse.

TABLE 8.3: Available protection resistors

	Available Resistor (Ω)	Set Max Current (mA)
Maxon RE10	0.75	270
Faulhaber 0810	1.80	110
Faulhaber 1215	1.80	110

This motor driver arrangement provides a robust solution to protect the motors whilst also reducing the number of components needed in the circuit and the processing demands on the microprocessor. The driver is also able to comfortably handle the power requirements placed upon it, which will limit chip overheating, removing the need to cool the circuit.

The Texas Instruments MSP430TM microcontroller family was chosen because it was able to support all the required functions. As well as this, they are designed to be super low power, are low cost and have a familiar architecture. The exact chip chosen was the MSP430G2332IRSA16 as this was the smallest and lowest cost MSP430TM that was able to support all of the requirements. It is a 16 pin square package, with four pins dedicated to power and one for programming, it leaves nine mixed signal (digital and analogue) Input/Output (IO), one digital IO and a single programming pin that can be configured as a digital input. Of these, two pins are required by the Inter-Integrated Circuit (I2C) module, two are required by the PWM module and, one to detect the over-current interrupt from the motor driver. Due to the implementation of the digital input pin it is best used for the user input button.

Finally there are four mixed signal IO pins. On the slave there will be two for the encoder and the two for the sensors. On the master these will act as general input pins to connect a variety of input/control devices. This leaves one remaining pin for both the motor driver sleep pin and the LED. It was decided to implement both; the LED is mainly necessary for testing and programming whereas the sleep mode would be used during normal operation (therefore with a header it is able to switch between the two functionalities).

8.1.2 Power supply

As stated previously the power supply designed for the motors is a switch mode supply. The circuit is specifically designed to be able to handle the power demands from all of the motors at once whilst still having a small physical size.

The first consideration is that the power demand needs to be estimated. Each of the Maxon RE10 finger motors consume 290mA. The thumb has two motors the Faulhaber 1512 and the Faulhaber 0810 these consume 113mA and 45mA respectively. This totals 1,318mA (1.3A), allowing for a 10% safety factor means that a supply able to provide approximately 1.6A is required. Although the design must accommodate for the situation when all motors are driven spontaneously, it is not expected that this will be the case. Therefore the actual operating safety factor will be higher than 10%.

The circuit for the final design presented here was designed using the Texas Instruments WEBENCH® Power Designer (<http://www.ti.com/lstds/ti/analog/webench/power.page>). The design provides a 6V output with at a continuous 1.5A current when supplied with a 7.5V input voltage. The circuit includes reverse polarity protection in the form of a P-Channel MOSFET. With the MOSFET drain connected to the power supply, the gate connected to ground, and the source connected to the load. In this configuration when the battery is connected properly the gate is held at a lower voltage than the source and therefore the MOSFET conducts, powering the circuit. If the battery is

reversed then the gate will be held at a higher voltage than the source, meaning that the MOSFET will not conduct, protecting the circuit. The switching regulator has a shut down facility that would allow the master to put it into a mode where the quiescent current is only $10\mu\text{A}$ allowing the motor drivers to be turned off whilst not in use.

8.2 Controller Code Implementation

There are two programs used to control the hand, the master code and the slave code, that are loaded onto the appropriate control boards. These implement the functionality defined in the Requirements Specification (Section 4.1) point 10. The master code is not designed to have a specific control methodology. The slave code has been implemented in depth; the different codes explanations are accompanied by a flowchart that details the complete logic flow for each device.

Table B.1 (in Appendix B) shows and defines all of the symbols used in these flowcharts. The decision block and the switch function are fundamentally quite similar, they both choose a specific path due to the outcome of an argument. The difference between them is that a decision block only has a true or false output, meaning that it best suited to logical arguments such as “greater than”, “less than” and “equal to” arguments. In contrast the switch function will go to one of multiple states and can be visualized as an option based decision. Therefore it is much more suited to a situation where multiple output paths are permitted. In operation the switch statement causes the logic flow to be diverted from the main path, and therefore requires a break to terminate.

8.2.1 Slave Functionality

The slave code has been developed to fit the modular nature of the design and therefore the same code is implemented on all of the finger controllers. The I2C address assignment is loaded separately and is used to differentiate each finger. Figure 8.2 shows the main operation of the slave code.

Once through the set-up stage, the code operates around a main loop which completes four processes. Firstly the code updates the known finger position from the count encoder counter. Then it checks for a completed I2C communication from the master, by analyzing whether the last of the communication buffers is nonzero. Both the finger position and the I2C are operated by interrupt routines that are described in Figure 8.3. If there is new data from the master then the code enters an processing routine that updates the slaves function and settings before continuing. The code then enters the main stage of the code that performs the motor operations. It is based around a switch statement dependent on the mode. The device has three control modes (speed, position and force), plus a default idle state. In speed mode the desired motor settings

are loaded into the PWM module (using the PWM Set subprocess detailed later and in Figure 8.7), the controller stops motor power when the motor stalls and triggers an over-current situation. The other two slave modes (position and force) both have their own subprocesses to determine the exact motor settings and end point, before entering the PWM Set subprocess. The three operational modes, speed, position and force, each have the facility for a control algorithm to be added before PWM Set is called.

Finally the code checks if it has encountered any errors, if so it sends them to the master, before returning to the beginning, to update the finger position.

Before the processor starts the main code it performs a set-up operation. This goes through various stages to initiate the device. In the first stage the core is calibrated, setting the clock frequency and functions. Secondly the peripherals that control the I2C, the motor encoder and the motor PWM control are turned on, with the initial output conditions set. Finally the user the LED and button are configure.

Motor Encoder Code

The Maxon MR TypeS 16 encoder Max (2013) has two outputs, labeled EncoderA and EncoderB respectively, with a 90° phase shift between the waveforms. In this arrangement when the signal changes on one of the channels, the direction of rotation can be detected using the state of the other. EncoderA is monitored via an interrupt handler, that is initiated in the start-up process. Due to the microprocessor only being able to detect either a rising or falling edge of a signal and not both, the appropriate mode must be detected and set in start-up.

Once initiated, the handler runs as shown in Figure 8.3. The interrupt routine takes one of two paths, one for a rising edge and the other a falling edge. Both then check the state of EncoderB to decide the direction of rotation, clockwise adds one to the Encoder Counter and the anticlockwise subtracts one. In this setup one complete turn of the motor will cause 32 counts. Therefore accounting for the gearbox (1:64) and the worm-wheel (1:20), 0.5° closure of the of the finger will cause 20,480 counts. Therefore, 90° closure will cause 3,686,400 pulses. This is outside the range of a single memory block in the microcontroller and thus a scaler (of 64) is required for it to fit into one memory block.

Only 0.5° accuracy of control is needed, which relates to approximately 0.5mm at the fingertip. Therefore 0.1° finger position measurement accuracy is more than accurate enough. This allows for a much larger scaler (4096) to be used.

Slave I2C Processing

Figure 8.4 details the Slave I2C Processing sub-process. Once a communication is completed the slave will have new commands. The I2C processing subprocess is used to decrypt the information that it has received and to implement the required action. This is done with the use of a switch statement that is directed using the first piece of data from the communication; the I2C command. There are five commands; Speed, Position, Force, Sleep and Error return. The first three commands work exactly as their namesakes in the main slave code switch function, however they update the relevant registers before an equivalent routine is completed. The error return command does one of two things dependent on the request it, either resets all existing errors or causes the slave to send any present errors back to the master. The sleep command sets the mode to idle and returns to the main code to await another command. The final section of this switch statement is the transmission error block, the code defaults to this state if no recognizable command is received. If this happens an error flag is set and the chip continues with its previous actions. Once the switch string is completed the subprocess returns to the main code.

Motor Control

In both the force (Figure 8.5) and positional (Figure 8.6) finger control subprocesses a short algorithm is needed, to determine the required direction of travel. This is dependent on the current and desired states. In both cases the computation is based around an “if greater”, “else-if smaller”, “else equal” decision flow. Where the direction of finger motion is set as forward, reverse or stationary accordingly. Apart from the input data the two subprocesses are very similar. There are two differences, the force mode begins by acquiring the finger tip force using the analogue to digital converter (ADC). The second difference, in position mode once the desired position had been reached, the controller stops the motor and enters an idle mode.

PWM Setup Architecture

The largest subprocess that runs within the slave code is the PWM setup algorithm. The flow diagram for this subprocess is shown across two figures 8.7 and 8.8. It can be perceived as two parts, a verification section and an implementation sections. The verification section checks for an over-current event flag, if present it identifies the direction of the previous over-current. Continuing the drive the finger in the the same direction could cause motor damage therefore to prevent this the code will, stop the PWM, enter idle mode and exit the subprocess. If the finger has changed direction the error flag will be reset along with its counter and the code will continue. To conclude the verification

the input values are analysed, to ensure the PWM will run correctly by checking that the PWM period is longer than the pulse width.

The implementation begins by loading a new period into the PWM settings, if it is required. Before the speed is set dependent on the direction; forward, reverse or stationary. Both forward and reverse have the same process except they set different registers. If there is a change of direction the code stops the motor and delays, to prevent instantaneously switching direction and stressing the motor. Finally the width settings are loaded and the PWM is restarted, before the subprocess ends. The stationary setting is the main method of stopping the motor, by clearing the forward and reverse PWM width registers and setting the outputs low, this ensures that a residual setting will not inadvertently drive the motor. There is also a mode that the code will default to if the direction has not been set correctly, if this happens an error flag will be set and the motors are stopped in the same process as the stationary protocol.

8.2.2 Master Functionality

The main function of the master controller is to interpret a range of input signals and issue the appropriate commands to the slave drivers. The master has been designed to be flexible and therefore allows for several different operational modes to be implemented. Such as, proportional and digital control schemes, computer operated, as well as driving the fingers individually, in groups or all together. This module is not mature however the slave controllers can interpret commands from a computer that mimics this functionality.

8.2.3 Discussion

When used alongside this controller the factor limiting the functionality of the prosthetic hand developed in this research is the number of functional inputs that can be acquired. It has been shown that the controller is able to individually manipulate all six axes simultaneously in real time. As discussed in the literature review (section 3.4), a person fitted with a traditional dual channel EMG system, has two viable inputs. Therefore they would find it difficult to fully realize the potential of a six DOF system. The advancement of the hand design and the control system that has been presented in this research has exposed the limitation of conventional EMG detection methodologies.

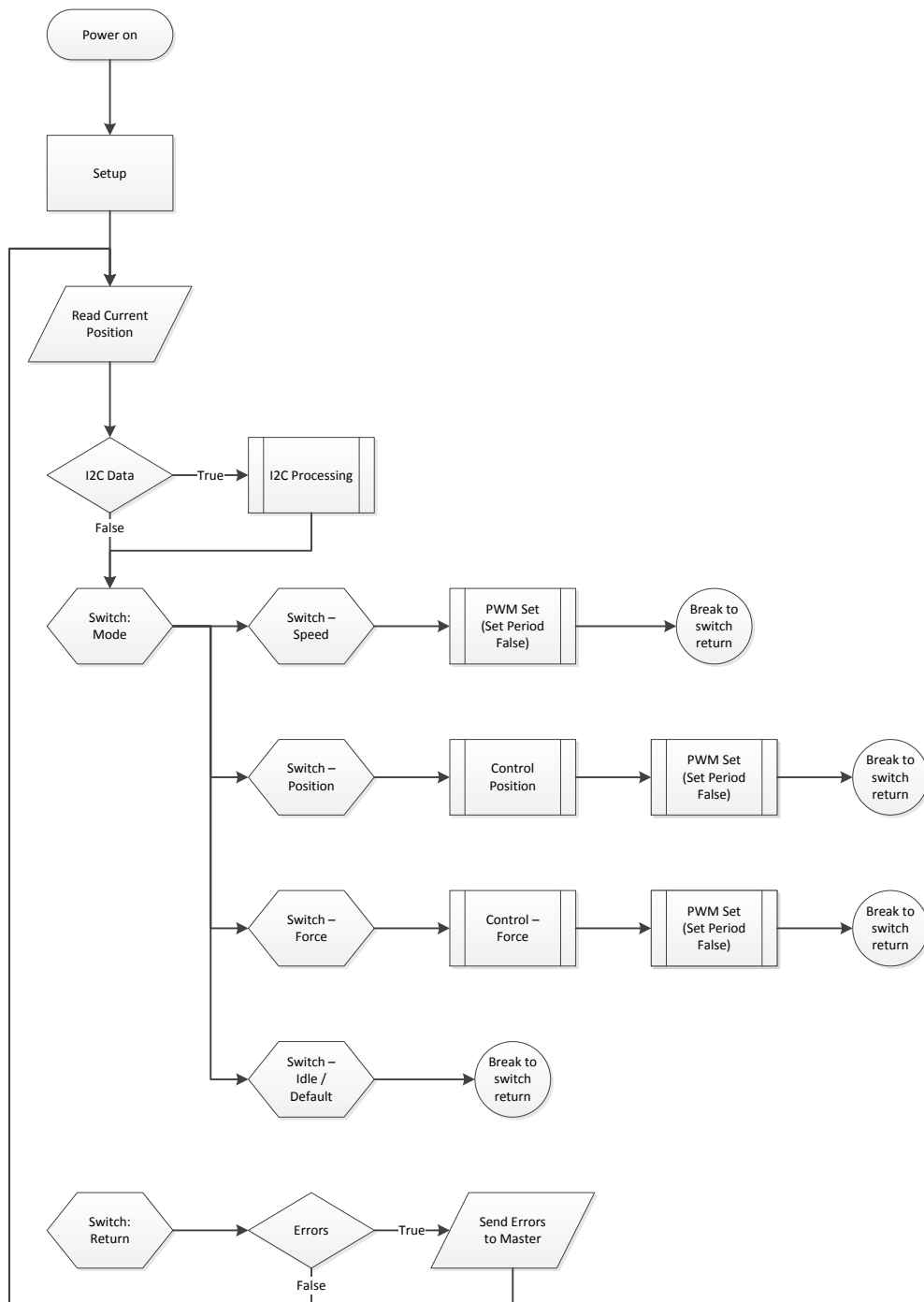


FIGURE 8.2: Flow diagram of the slave controller main loop

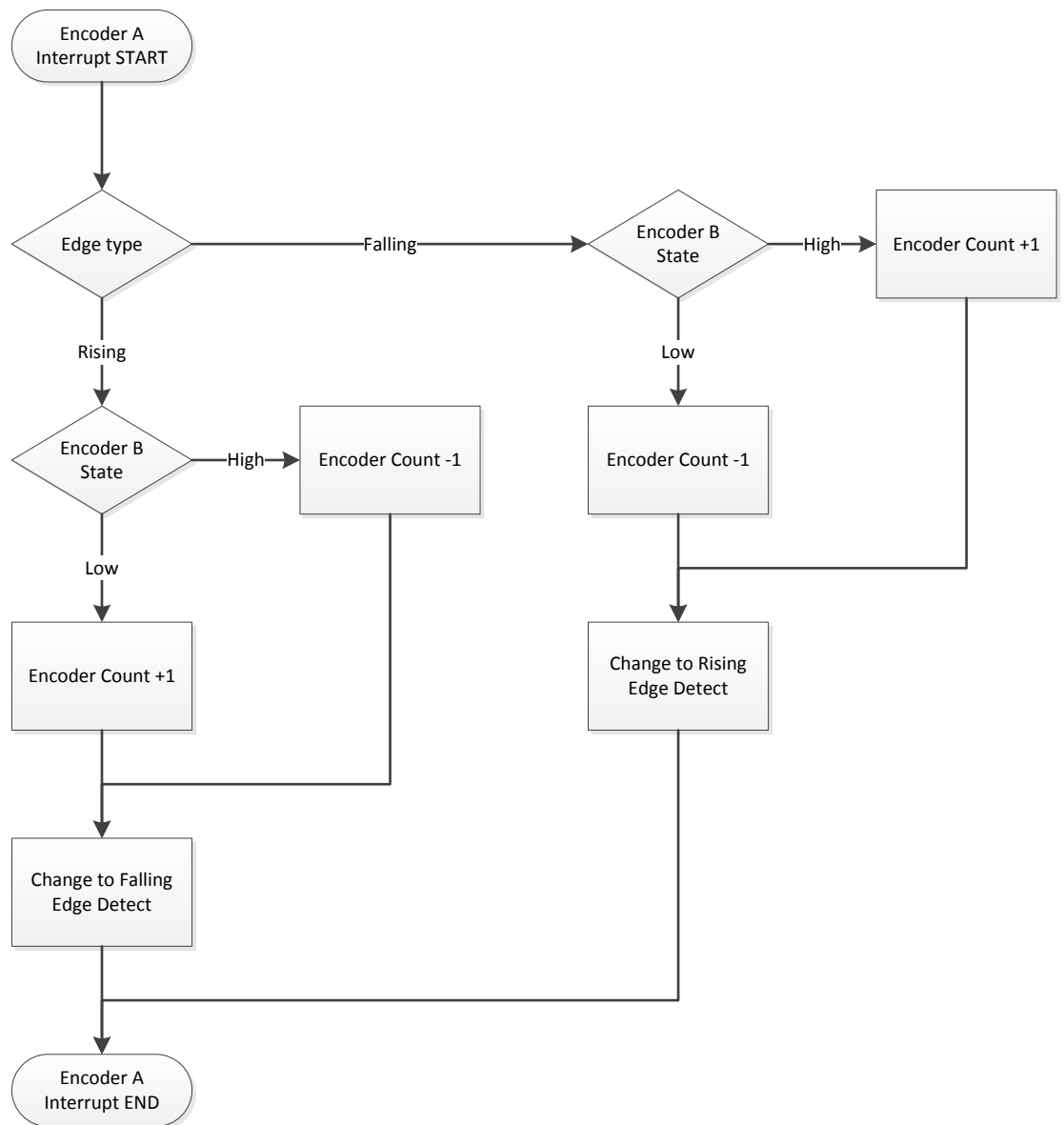


FIGURE 8.3: Flow diagram of the slave controller encoder counter routine

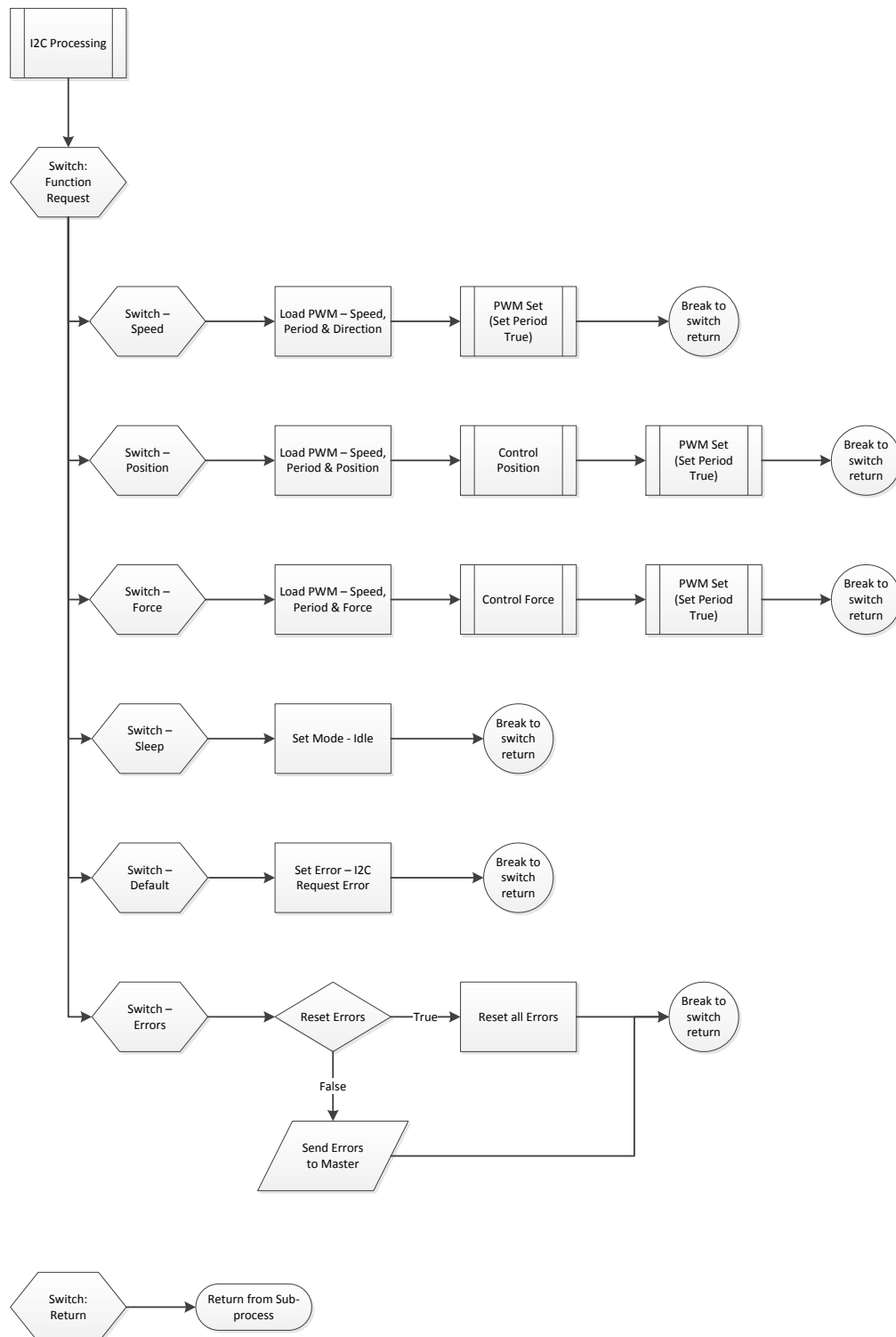


FIGURE 8.4: Flow diagram of the slave controller I2C processing protocol

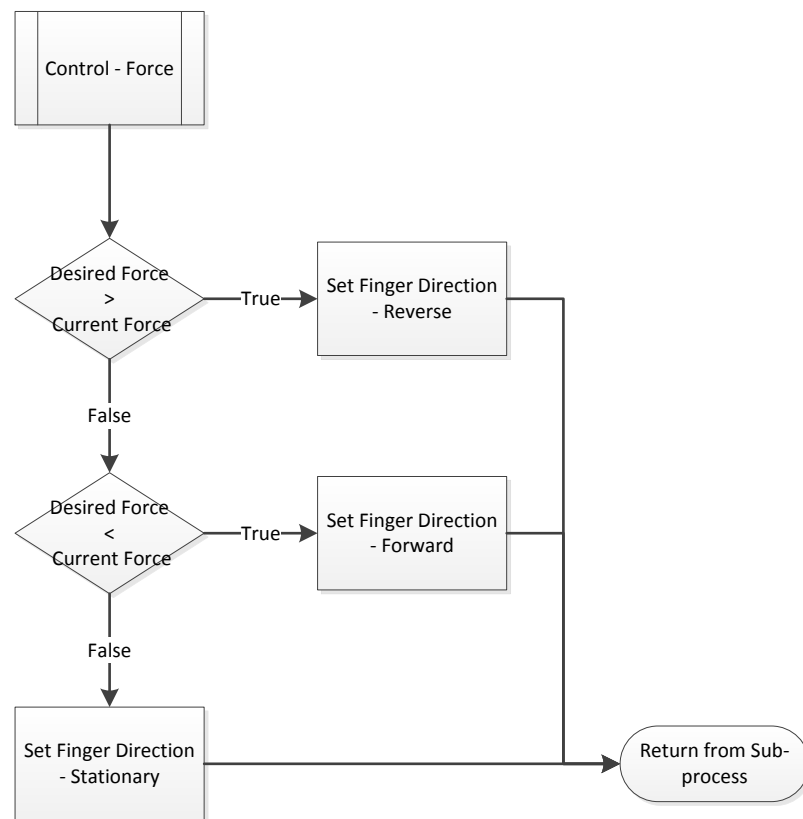


FIGURE 8.5: Flow diagram of the slave controller force control routine

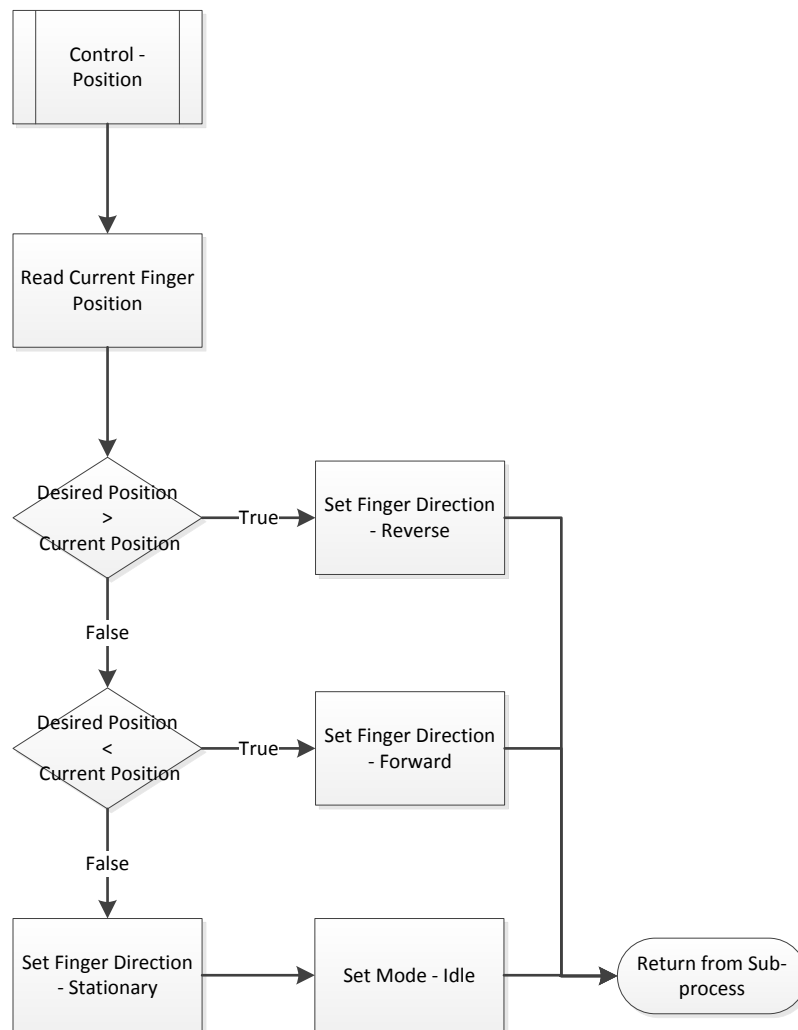


FIGURE 8.6: Flow diagram of the slave controller position control routine

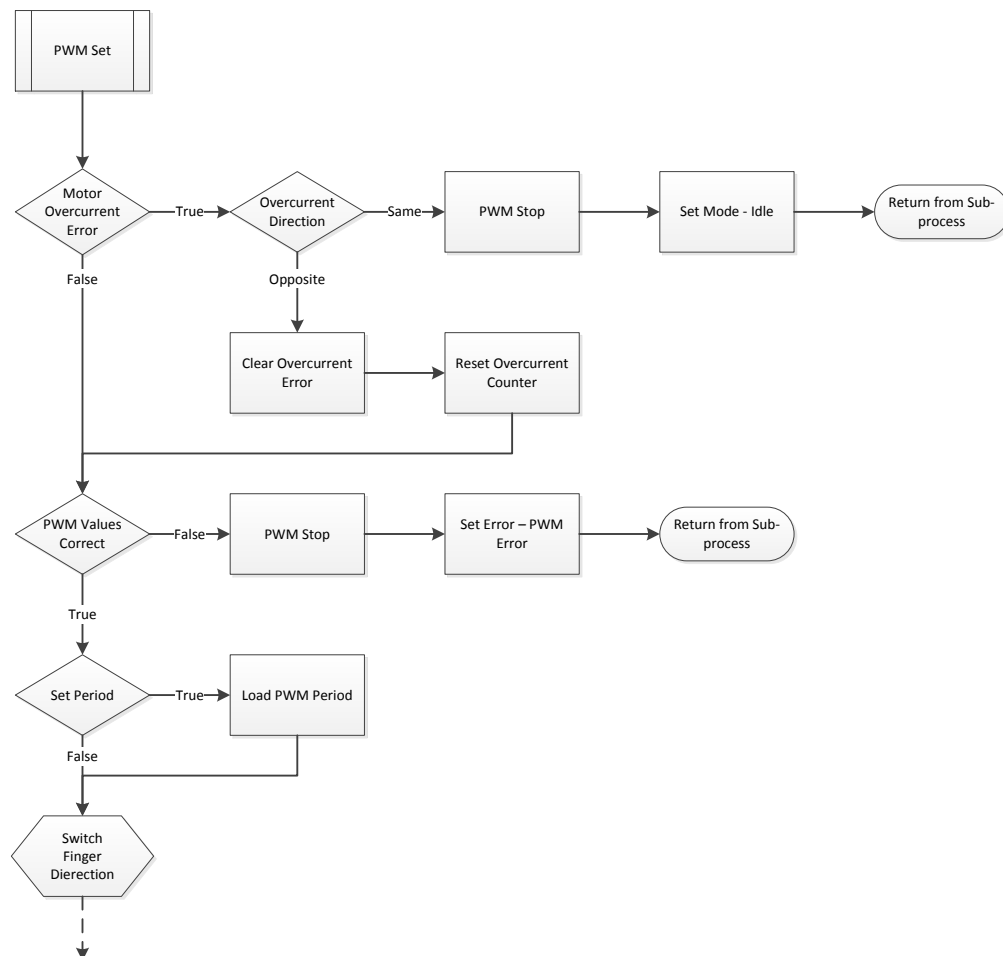


FIGURE 8.7: Flow diagram of the slave controller PWM setup algorithm - Part 1

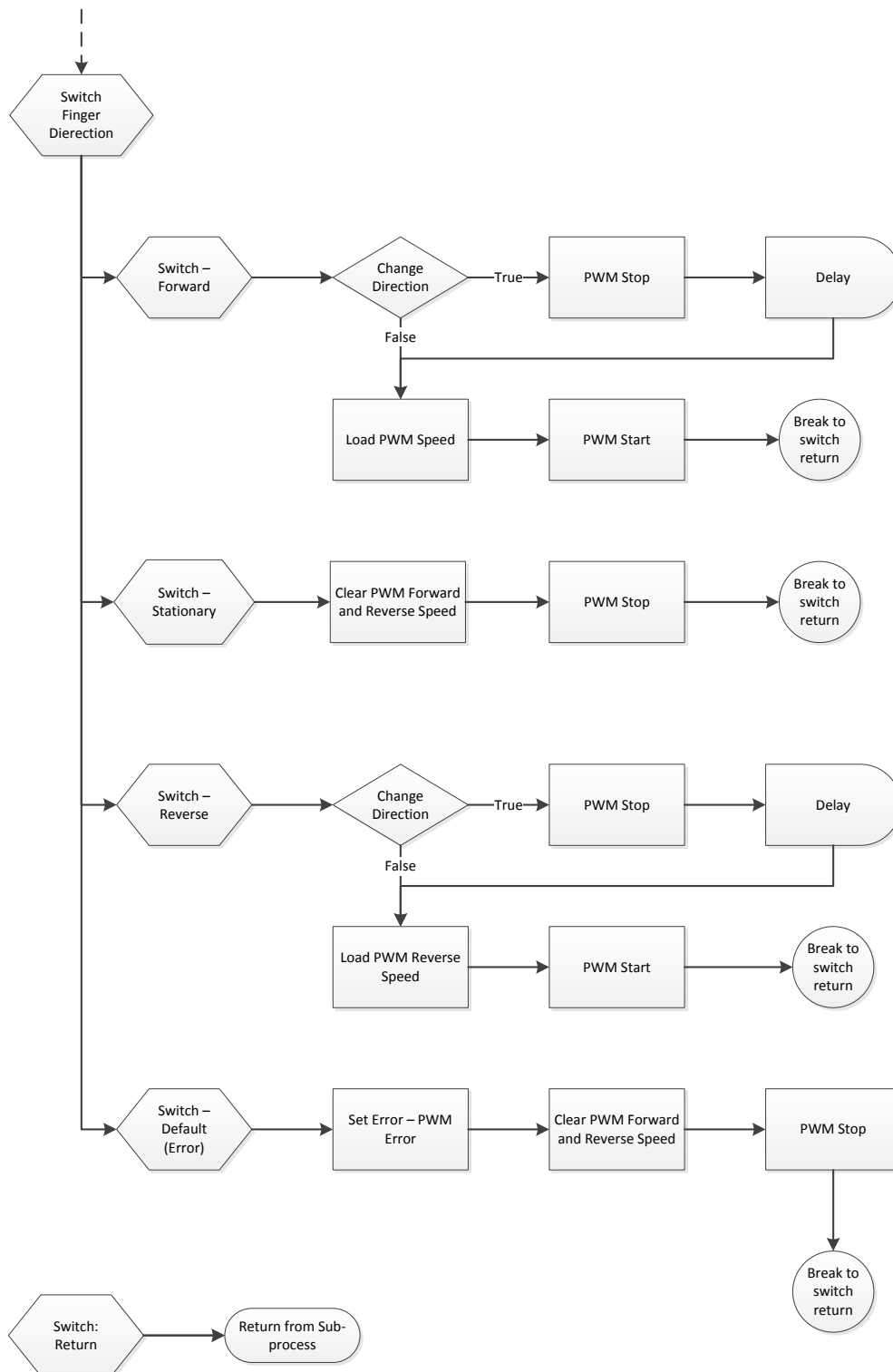


FIGURE 8.8: Flow diagram of the slave controller PWM setup algorithm - Part 2

Chapter 9

Conclusions

This thesis presents the design of a small prosthetic hand that has multiple actuators for five year old children. The device presented in this research has been aimed at five year old children, however, consideration has been made throughout the design to allow it to be scaled with minimal alterations. The research has shown that further reductions in size are limited by the lack of suitable actuators, as they have limited torque and power delivery. Thus the device presented in the thesis, having individually actuated fingers and a two degree of freedom thumb, is the smallest design that can be achieved with current technology. This outcome corresponds to the size constraints that were applied to the research; for a child the average size of a hand is 125 mm long and 57 mm wide (Table 3.3).

The Literature Review (Chapter 2) confirms the need for development of more functional prosthetic devices for children. There has been an assessment into the number of prosthetic wearers aged between five and six. This includes an estimation for the number of prostheses that would be required for fitment each year to this age group. Assuming children require the fitment of a new prosthesis twice per year as stated by Doshi and LeBlanc (1998), this analysis found that 2,260 prostheses would be needed in the G8 and EU countries for fitment to five year old children each year.

There are currently only two commercially available advanced hands designed for children in this age range. Of the users fitted with these, it has been shown that approximately 50% of children reject the devices due to a variety of reasons that are attributed to dissatisfaction with the device. This leads to the conclusion that there is insufficient choice available to young prosthetic hand users to allow for best fitment. Therefore, more commercially available devices are needed. To reduce rejection it is theorised that children require greater choice during fitment, as well as greater functionality than the existing designs offer. It was discussed that children place a greater emphasis than adults on the anthropomorphic look of the prostheses; typically driven by peer acceptance. There are advancements to pediatric upper body prosthetics discussed in the

literature, none have suggested to offer a solution that is capable of fitment. These findings drove the decision to develop an anthropomorphic prosthesis which was highly functional, whilst championing adaptivity.

The device presented in this thesis overcomes the constraints as discussed in Chapter 2.4. It is a fully functioning hand with six individually actuated degrees of freedom. Four actuators drive each of the fingers, which have a curling fingertip trajectory that is akin to that of a humanoid hand. The final two actuators provide closure and opposition of the thumb. This is the smallest prosthetic hand that has been developed for children fitted with multiple actuators. It is the smallest prosthetic hand that has been developed with individually driven actuation of the closure and opposition thumb. In addition it is, the smallest prosthetic hand that has been developed with fingers that have a curling action during closure. This means that the prosthetic hand presented in this thesis has similar functionality as the most advanced adult hand prostheses, such as the iLimb Ultra by Touch Bionics (2011) and the BeBionic v2 from RSL Steeper (2011). Thus, it provides the basis for next generation rehabilitation devices.

The hybrid finger is a novel design. Based around a four-bar linkage connected to an interchangeable fingertip, a rotational input produces a smooth curling motion not dissimilar to that of the human finger. The trajectory of the finger tip of the hybrid finger during closure has been modelled. This has allowed a comparison of the closure trajectory to be made with that of a human finger. This, leads to the conclusion that the hybrid follows a humanoid profile; as seen in Figures 5.7 & 5.9.

The transmission ration of the hybrid design has been mathematically evaluated. This shows that the design has a variable transmission ratio which is dependent on the input angle. The transmission ratio ranges from 2.5% at the edge of the operational envelope, and rises steeply to above 40% in the region where pinching is expected to occur. When fitted with the Maxon Motors RE10, it has been calculated that each of the fingers will apply between 2-8N force across the closure range. Therefore four fingers would apply a comparable force to that documented by the Otto Bock Electrohand 2000 (8-35N), a commonly fitted commercially available paediatric prosthesis.

An issue of motor cogging (stepping between coils of the motor) of the Maxon Motors had been observed in previous hand developments at University of Southampton. This was not detected in this implementation. This is likely due to the gear ratio of 1280 to 1 between the motor and the driven link of the finger.

As well as the operational advancements, this design minimises cost. The finger design is split into a curling mechanism and a fingertip section. Identical curling mechanisms are used for each of the fingers, whilst the fingertip is adjusted to define the finger length. There is a two-fold advantage of this design; the user is able to define the fingertip lengths of their hand to fulfil their needs, allowing fitment of a customised device, thus improving acceptance. Secondly, the modularity means that all of the fingers will have

the same transfer characteristics and closure profiles. This minimises the complexity of the control system, thus reducing the complexity of use and improving acceptance.

The MCP functions as the gearbox for each of the fingers and provides suitable support for all of the other components of the fingers. The split case design has made it possible to include axle bearings that reduce frictional losses within the design. It has made it easier to assemble the MCP and removed issues found in the design of the feasibility study MCP caused by misalignment of the motor-worm coupling. The mass of the MCP design including the motor and gears, has been reduced from 24.1g to 22.3g. This represents a reduction of 1.8g. However this is inclusive of a larger motor, additional bearings and a strengthened design. It can be seen in Figure 9.1 that the total mass of the MCP and finger is 29.7g. This is the minimum mass that this module can achieved; 55.9% of which is the motor and worm that cannot be reduced in mass.

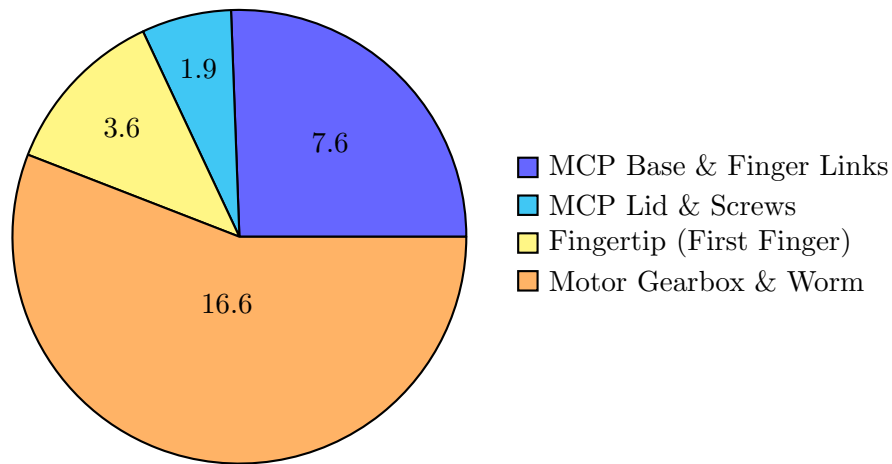


FIGURE 9.1: Mass breakdown of the Finger and MCP

The larger motor (Maxon Motor RE10) provides a higher torque output than the previous motor. The predicted value for rigid finger normal contact force has been increased from 3.5N to 19.6N per finger, when using recommended motor operation conditions. The equivalent 5.5 increase is seen in the contact force of the hybrid finger. As discussed this will provide similar gripping forces to existing commercially available prostheses and therefore the hand would be able to handle similar objects. The closing time of the finger was found to be between 1.5 and 2 seconds.

The stress distribution in the base section of the finger MCPs has been modelled using Autodesk Inventor Professional 2013. This was used to gauge the ability to withstand the force of impacts applied during use. Figures 6.8 and 6.9 show that when force is applied to the main finger axle in upwards and downwards directions respectively the forces are dissipated around the mounting and there are no significant areas of stress. In these scenarios the lowest safety factor produced is 2.14, which is focussed around the finger axle mounting holes. In Figure 6.10 the force is applied to the front of the MCP, and it shows similar results. The stress is dissipated through the design and there

is little localized stress build-ups. In this case the safety factor is 1.69, which is focused in the sides of the module. In these scenarios there are no instances where the stress on the MCP would become destructive.

The base section form MCP version 2.4 has been modelled, and baselines minimum safety factors. These are higher for version 4.2 due to the thicker side walls and the addition of bearings. This evaluation only considers the bottom half of the MCP joint without the lid or screws, which would also provide additional strength to the module. The results of this analysis show that an individual finger MCPs should withstand the expected force of 186N, the force applied when the weight of an average 5 year old is applied to the device. They will distribute pressure throughout the design effectively with few areas of high stress.

This research demonstrates the design of a thumb for pediatric prosthetic devices, that has individually driven closure and opposition. The solution and the corresponding palm sections of this device are novel in pediatric prosthetic design. The research offers a functionality that has only become available in adult prosthetics with the OttoBock Michelangelo Hand since 2013. The research has as lower mass as is achievable with current technology and fits into the modular strategy of the device.

The thumb has two axes of powered rotation, closure and opposition. In both of these axes the thumb can be driven through 90° . This allows for closure of the thumb in a pinching action with the fingers, as well as a key grip formed the against the palm. The research splits the actuation areas of the thumb. The actuator for opposition is located within the palm, whilst the closure actuator is built into the MCP of the thumb which is rotated during opposition. The closure actuator is the first to be mounted in line with the MCP and therefore lying within the thumb.

Figures 9.2 and 9.3 show the mass breakdown of the thumb and palm respectively. The mass of the thumb has once again been limited by the drive system. 55.6% of the total 25.2g mass of this module is the motor-gearbox and the worm. Meanwhile, the axles and screws account for another 8.3%. Therefore, it can be concluded that with a mass of 9.1g, the casework and thumb are as small as possible whilst ensuring functionality. Unlike the other modules, the mass of the palm (63.0g) is distributed throughout its volume and 37.3g of the palm is casework and associated screws.

The control system is not fully mature. It is a modular design in which each of the fingers is driven and controlled by a stand alone microcontroller. Designed to operate independently, the control of each finger is dependent on the finger mounted sensors (encoder and force) as well as implementing inputs from a master microcontroller. The controllers are based around a linked communication system that provides further modularity to the device. The controller for the thumb consists of two microcontrollers one for closure the other for opposition. These operate in the same manner as the finger

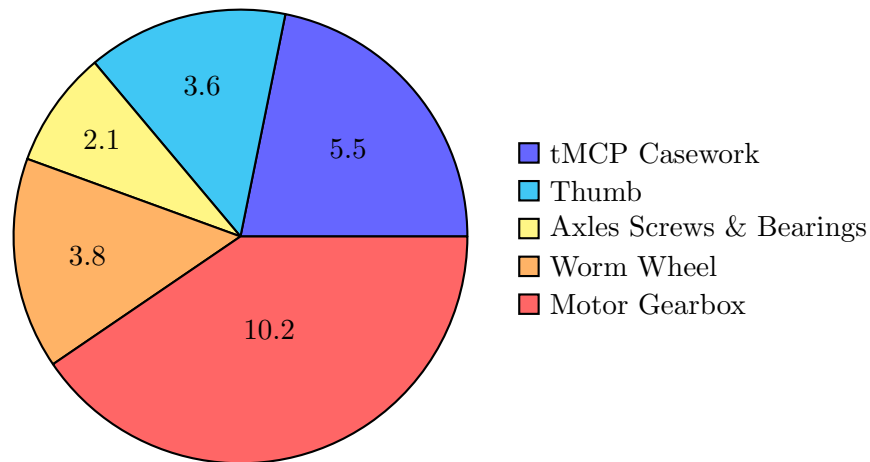


FIGURE 9.2: Mass breakdown of the Thumb

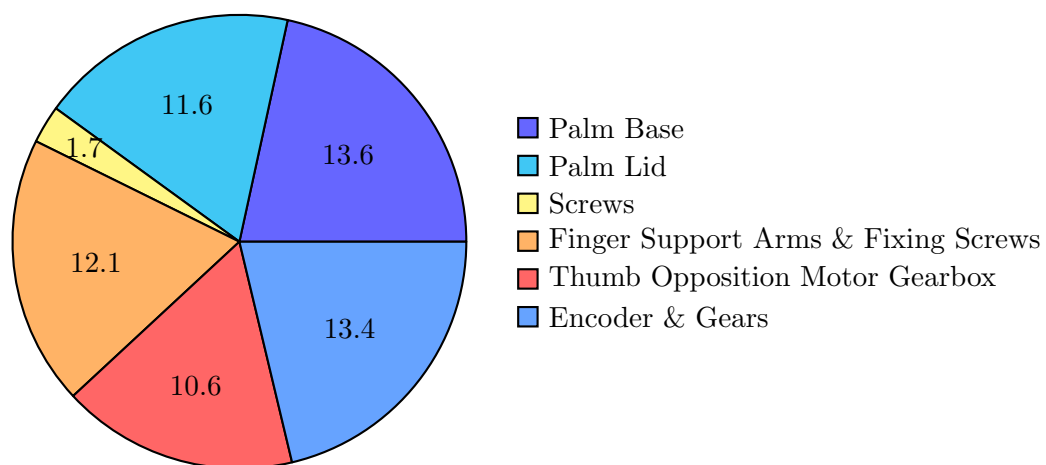


FIGURE 9.3: Mass breakdown of the Palm

controllers however they work in tandem with information of the position of the first and second fingers in order to prevent collisions of the thumb, fingers and palm.

As discussed, modularity has been a fundamental consideration in the design of the hand. This has a positive effect on both the cost and acceptance of the device during fitment. By allowing individual faulty or worn parts to be replaced, the impact on cost presents throughout its lifetime, by reducing the cost of servicing and lower replacement cost. This design has achieved a high level of modularity and component reuse throughout. The four MCP and finger modules have a total of 114 components between them, of which there are only 19 different components.

The modular design of this prosthesis spawned the novel concept of “prosthesis growth”. The hand presented in this thesis is designed to be scalable as well as modular, which has a secondary impact. It means that parts of the hand are able to be substituted and replaced with bigger components, meaning that the device can be “grown” with the

user, as they grow. Adapting the prosthesis with the user is a novel concept. There is a two-fold benefit of this. Due to the low cost of the parts, replacement can occur more regularly ensuring that the devices continuously fit the user properly. Also, as less parts would need to be replaced during a service, the cost of replacement is lowered.

These advancement will help to reduce rejection, a major issue in pediatric prosthetics whilst, a lower cost means that this advanced device would be available to a greater number of users.

Rapid prototyping was selected as the most suitable method for manufacturing a small prosthetic hand. It is untested relative to traditional engineering materials however the method is adaptable, has a low cost and, provides the ability for customisation of hands. With further evaluation, components could be made for both prototyping and use in the production of hands. A study into these materials has shown that rapid prototyped plastics are suitable for the manufacture of the MCP joint and the rest of the design. During this investigation it was highlighted that the clearances for the rapid prototyped product need to be bigger than they would if the design was machined using traditional techniques. This is due to the incomplete removal of the support material.

Producing the device from rapid prototyped materials minimises cost and enables ease of manufacture. It has been shown that this method of manufacture facilitates the commercial model that has been discussed in which a highly customisable device can be fitted to users. This concept would allow major cosmetic alterations to be made. This would be entirely aimed at improving acceptance of the device by encouraging ownership of the device during the fitment process. It was found that devices manufactured from this material process would be of sufficient strength for pediatric prostheses.

The final device that is presented is 63.0mm wide, 112.0mm long and 27.7mm thick. This corresponds to the size of a five year old child's hand, as presented in Table 3.3 and defined in the Requirements Specification (Section 4.1). The hand is 10% wider than specified however, it is 13mm shorter which would allow for the inclusion of a socket within the specified size. The size of the prosthesis would allow for fitment to children with amputations as high as Wrist Disarticulation. The final mass of the hand is 207g without the circuit boards mounted. The six circuit boards have a mass of approximately 14g in total; 2g each. This gives a total mass of 221.2g which is equivalent to the mass of the RSL Steeper Scamp prosthetic hand for five year old children.

Figure 9.4 shows the mass breakdown of the whole device. The four fingers have a mass of 118.7g which represents 53.7% of the total mass of the research device. The Palm has a total mass of 63.0g which represents 28.5% of the total mass. The mass of the actuators and gears is 106.5g which represents 48.1% of the mass of the whole device. To achieve the desired closure speed and force these actuators are required. Therefore further reductions in mass would need to be taken from the casework.

TABLE 9.1: Cost of device components in low volumes

Motor-Gearboxes	£700
Gears	£150
Rapid Prototyped Parts	£200
PCBs	£100
Additional components	£100
Total Cost	£1,250

As discussed above, the predicted fingertip force is equivalent to the commercially available hands for children. However, these devices are able to be produced for lower cost, even in small quantities. The cost breakdown of manufacturing these devices in low volumes (1-2 devices) is shown in Table 9.1; it can be seen that the Motor-Gearboxes constitute over half of the cost of the devices. The final cost of manufacturing a device would also include assembly, suggesting a low volume cost of less than £1,500. If mass produced this cost would be lower, representing a reduction in the cost of providing a prosthesis to a child, when compared with current commercially available devices.

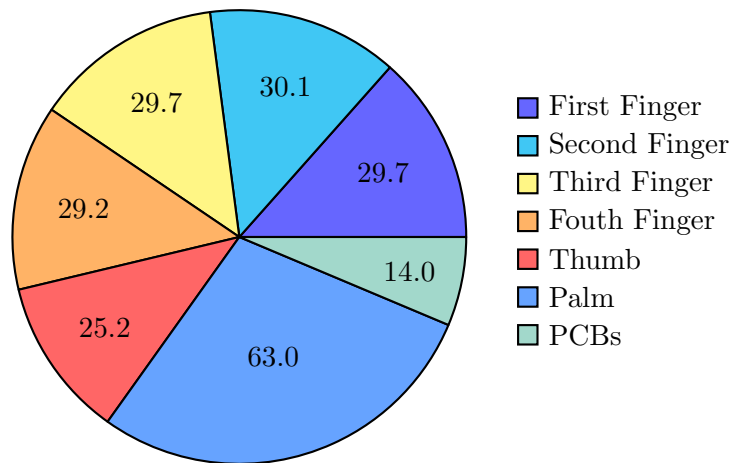


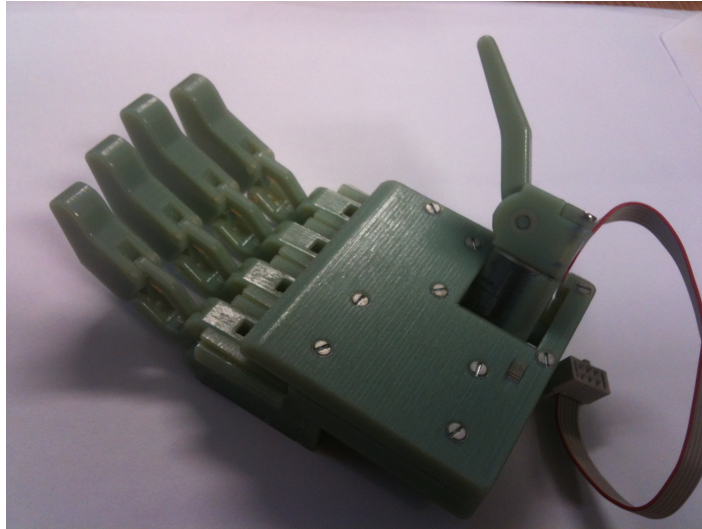
FIGURE 9.4: Mass breakdown of the Hand

It has been discussed that the device presented in this thesis is equivalent to the size, mass and, cost of the commercially available prosthetic hands for children aged five years old. However this device has six DOF compared to the commercial devices one DOF. This means that it is significantly more functional than the existing devices. It is able to form greater than fourteen grip patterns, as opposed to one pinch-style grip offered currently in hands for children. Functionality that is only matched by the most advanced adult prosthetic devices.

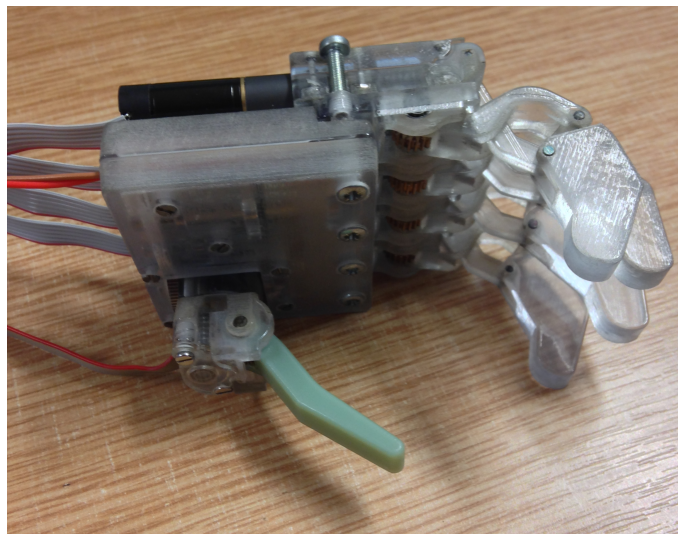
This design represents a significant step in improving the functionality of prosthetic hands for children. Multiple independent actuators, curling fingers and a driven opposable thumb are all novel to pediatric prosthesis. As well as this, the design starts to

address the issue of out-growing the device with the inclusion of interchangeable modular parts that allow the hand to be “grown” with the child.

These features combine to deliver a device for children with a high level of dexterity that has only previously been seen on advanced adult devices.



(a) Device Version 4.0



(b) Device Version 6.1



(c) Device Version 6.1 - Holding Ball

FIGURE 9.5: Images of Final Prosthetic Device.

Chapter 10

Future Work

Multiple routes to expand and exploit this research are possible as described next.

10.1 Force & Slip Sensors

Previous studies at Southampton (Cotton et al. (2005); Lowe et al. (2010); Muridan et al. (2010)) have demonstrated the concept of putting sensors on the fingers to improve the effectiveness of grips. It was decided that this could be scaled and implemented in the child's hand. This would give the ability to have multiple grip strengths that are automatically adjusted by the controller to prevent an unstable grip. Recent work at the university has showed the potential of placing sensors further down the finger instead of directly on the fingertip. Since the size of the finger body is similar or larger than the links on the Southampton Hand, little to no scaling would be required.

Advanced prostheses requires sensors to detect contact forces, slip and temperature. Therefore a study into implementing these sensors into the design will be undertaken. This process has been started with the design of a small wearable vibration unit. It will initially use a force sensitive resistor (FSR) to detect a force at the finger. However, the design of this unit will allow it to accept multiple types of sensors.

10.2 Testing

The results that have been calculated mathematically need to be compared to the values found practically. To do this the force transmitted by the finger, the accuracy of the encoder and the trajectory all need to be investigated. As well as this an area of testing that needs to be considered is the ability to withstand the forces applied to a prosthetic device during normal operation. These verification tests would act as the precursor to clinical trials.

10.3 Children's Measurement Workshop

New data on a child's hand is needed since significant amounts of the existing data are out of date or have not been collected. An example of this is the "Handbook of normal physical measurements", Hall (1989) that was published in 1989. This data could be out of date which may cause the hand to be designed with proportions that were incorrect in the modern situation. During this project another serious consideration was the force that a child's hand could exert. The final prototype needed to be able to exert a similar force to a child of that age. If the prosthetic was significantly stronger than required the child could cause inadvertent injury to themselves or others through misunderstanding the effects of their strength.

This workshop would be designed to gather information on the exact dimensions of children's hands, the grips and postures that they can achieve and the forces that a child can exert. Moulds of the hand would be taken that will be measured using callipers later. This will help reduce the time taken to complete the workshop; a necessity when working with young children. The moulds will also allow for additional measurement to be taken after the workshop is completed.

The forces that the child's hand can exert will be measured using bespoke measurement tools. These tools are likely to be designed around standard measurement devices to give clear, accurate and repeatable readings.

10.4 Additional Refinements

Since the human hand is flexible it can conform to many shapes that it is infeasible for a prosthetic device to adapt too. Because of this there are situations when a conventional prosthetic device can not be expected to function effectively. Some alterations that could be investigated to help ease this problem are as follows:

Rotatable MCP - If the MCP to palm connection was circular then the MCP could be rotated by a few degrees in either direction. This would allow the user to set the exact trajectory of the fingers to best fit around an object.

Task specific - Palms for specific tasks could be produced for use when the anatomical prosthesis does not provide a fully capable solution. Due to the modular nature of the design, palms that could quickly accept the fMCPs could be produced at low cost. These would greatly increase the usability of the hands.

Quick release fMCPs - an alteration to the method in which the fMCPs are held into place could increase the speed in which they could be removed, which could be of benefit when both mending or adapting the devices.

Split cosmesis - This would be a system where the entire hand is not covered in a silicone cosmesis. One of the most common complaints from prosthetic users is that the cosmesis becomes ripped, dirty or worn (Donovan-Hall et al. (2002)). Areas where a cosmesis is not essential such as the back of the hand could simply have a plastic shield as a covering. This would make it more robust to knocks, wear and staining. The opposite approach would be used in areas that suffer high levels of wear where a cosmesis is essential, such as the finger tip. If smaller standardised parts were used they could be replaced with a high regularity, at low cost to avoid these issues. This system would also support the aim to have reconfigurable fMCPs as each one could have its own individual cosmesis which would increase the simplicity of removal and rearrangement.

Individual Customisation - with the use of a specially designed CAD package. Trained prosthetists would be able to customise the size and shape of a device to a user, without altering the mating surfaces or mechanical interfaces.

Glossary

ADQ	Abductordigiti quinti
AP	Adductor pollicis
APB	Abductor pollicis brevis
APL	Abductor pollicis longus
APO	Adductor pollicis obliquus
APT	Adductor pollicis transversus
CAD	Computer Aided Design
dB	Decibel
DC	Direct Current
DI	Dorsal interosseus
DOF	Degrees of Freedom
ECRB	Extensor carpi radialis brevis
ECRL	Extensor carpi radialis longus
ECU	Extensor carpi ulnaris
EDC	Extensor digitorum communis
EDQP	Extensor digiti quinti proprius
EIP	Extensor indicis proprius
EMG	Electromyography
EPB	Extensor pollicis brevis
EPL	Extensor pollicis longus
FCR	Flexor carpi radialis
FCU	Flexor carpi ulnaris
FDP	Flexor digitorum profundus
FDQB	Flexor digiti quinti brevis
FDS	Flexor digitorum sublimis
fMCP	Finger Metacarpophalangeal
FPB	Flexor pollicis brevis
FPL	Flexor pollicis longus
Hz	Hertz
I	interosseus
I2C	Inter-Integrated Circuit
L	Lumbricalis

MCP	Metacarpophalangeal
ODQ	Opponens digiti quinti
OP	Opponens pollicis
PL	Palmaris longus
PWM	Pulse Width Modulation
RMS	Root Mean Squared
SAMS	Southampton Adaptive Manipulation Scheme
SMA	Shape Memory Alloy
tMCP	Thumb Metacarpophalangeal
UV	Ultraviolet
V	Volt
VI	Volar interosseus
3D	Three Dimension

Appendix A

Fingertip positions with relation to normalised input angle

TABLE A.1: Table showing fingertip positions of the hybrid finger with relation to normalised input angle. Reference angle 0 represents fully open and 55 fully closed. Dimensions in mm

Reference Angle	First Finger		Second Finger		Third Finger		Fourth Finger	
	Xot	Yot	Xot	Yot	Xot	Yot	Xot	Yot
0.0	-20.2	49.2	-21.9	51.7	-20.2	49.2	-17.9	46.2
1.0	-21.7	47.9	-23.5	50.4	-21.7	47.9	-19.2	45.1
2.0	-23.2	46.7	-25.0	49.0	-23.2	46.7	-20.5	43.9
3.0	-24.5	45.3	-26.5	47.6	-24.5	45.3	-21.7	42.7
4.0	-25.8	44.0	-27.8	46.1	-25.8	44.0	-22.8	41.5
5.0	-26.9	42.6	-29.1	44.6	-26.9	42.6	-23.9	40.3
6.0	-28.1	41.2	-30.3	43.1	-28.1	41.2	-24.9	39.0
7.0	-29.1	39.7	-31.5	41.6	-29.1	39.7	-25.8	37.7
8.0	-30.1	38.3	-32.5	40.0	-30.1	38.3	-26.7	36.4
9.0	-30.9	36.8	-33.5	38.4	-30.9	36.8	-27.5	35.1
10.0	-31.8	35.3	-34.4	36.8	-31.8	35.3	-28.3	33.8
11.0	-32.5	33.9	-35.2	35.2	-32.5	33.9	-28.9	32.5
12.0	-33.2	32.4	-35.9	33.6	-33.2	32.4	-29.6	31.2
13.0	-33.8	30.9	-36.6	32.0	-33.8	30.9	-30.1	29.9
14.0	-34.3	29.4	-37.2	30.4	-34.3	29.4	-30.6	28.5
15.0	-34.8	27.9	-37.7	28.8	-34.8	27.9	-31.0	27.2
16.0	-35.2	26.4	-38.1	27.1	-35.2	26.4	-31.4	25.9
17.0	-35.6	24.9	-38.5	25.5	-35.6	24.9	-31.8	24.6
18.0	-35.8	23.5	-38.8	23.9	-35.8	23.5	-32.0	23.3

Continued on next page

Table A.1 – Continued

Reference Angle °C	First Finger		Second Finger		Third Finger		Fourth Finger	
	Xot	Yot	Xot	Yot	Xot	Yot	Xot	Yot
19.0	-36.1	22.0	-39.0	22.4	-36.1	22.0	-32.2	22.0
20.0	-36.2	20.6	-39.2	20.8	-36.2	20.6	-32.4	20.7
21.0	-36.3	19.2	-39.3	19.2	-36.3	19.2	-32.5	19.5
22.0	-36.4	17.8	-39.4	17.7	-36.4	17.8	-32.6	18.2
23.0	-36.4	16.4	-39.4	16.2	-36.4	16.4	-32.6	17.0
24.0	-36.3	15.0	-39.3	14.7	-36.3	15.0	-32.6	15.8
25.0	-36.2	13.7	-39.2	13.2	-36.2	13.7	-32.5	14.6
26.0	-36.1	12.3	-39.0	11.8	-36.1	12.3	-32.4	13.4
27.0	-35.9	11.0	-38.8	10.4	-35.9	11.0	-32.3	12.3
28.0	-35.6	9.8	-38.5	9.0	-35.6	9.8	-32.1	11.2
29.0	-35.3	8.5	-38.2	7.6	-35.3	8.5	-31.8	10.1
30.0	-35.0	7.3	-37.8	6.3	-35.0	7.3	-31.6	9.0
31.0	-34.6	6.1	-37.4	5.0	-34.6	6.1	-31.2	8.0
32.0	-34.2	5.0	-36.9	3.7	-34.2	5.0	-30.9	6.9
33.0	-33.7	3.8	-36.4	2.5	-33.7	3.8	-30.5	5.9
34.0	-33.2	2.8	-35.8	1.3	-33.2	2.8	-30.1	5.0
35.0	-32.7	1.7	-35.2	0.1	-32.7	1.7	-29.6	4.0
36.0	-32.1	0.7	-34.6	-1.0	-32.1	0.7	-29.2	3.1
37.0	-31.5	-0.3	-33.9	-2.1	-31.5	-0.3	-28.6	2.3
38.0	-30.8	-1.3	-33.1	-3.2	-30.8	-1.3	-28.1	1.4
39.0	-30.1	-2.2	-32.4	-4.2	-30.1	-2.2	-27.5	0.6
40.0	-29.4	-3.1	-31.6	-5.2	-29.4	-3.1	-26.9	-0.2
41.0	-28.6	-3.9	-30.7	-6.1	-28.6	-3.9	-26.3	-0.9
42.0	-27.8	-4.7	-29.8	-7.0	-27.8	-4.7	-25.6	-1.6
43.0	-27.0	-5.5	-28.9	-7.8	-27.0	-5.5	-24.9	-2.3
44.0	-26.1	-6.2	-27.9	-8.6	-26.1	-6.2	-24.2	-2.9
45.0	-25.2	-6.9	-26.9	-9.4	-25.2	-6.9	-23.4	-3.5
46.0	-24.3	-7.5	-25.9	-10.1	-24.3	-7.5	-22.6	-4.1
47.0	-23.3	-8.1	-24.8	-10.7	-23.3	-8.1	-21.8	-4.6
48.0	-22.3	-8.6	-23.7	-11.3	-22.3	-8.6	-21.0	-5.0
49.0	-21.3	-9.1	-22.5	-11.8	-21.3	-9.1	-20.1	-5.5
50.0	-20.2	-9.5	-21.3	-12.3	-20.2	-9.5	-19.2	-5.8
51.0	-19.1	-9.9	-20.1	-12.7	-19.1	-9.9	-18.2	-6.1
52.0	-17.9	-10.2	-18.8	-13.0	-17.9	-10.2	-17.3	-6.4
53.0	-16.7	-10.4	-17.4	-13.3	-16.7	-10.4	-16.2	-6.6
54.0	-15.4	-10.5	-16.0	-13.5	-15.4	-10.5	-15.1	-6.7

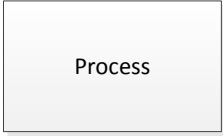


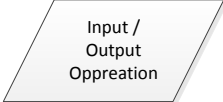
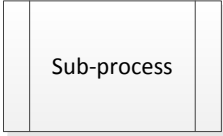



Continued on next page

Table A.1 – Continued								
Reference Angle	First Finger		Second Finger		Third Finger		Fourth Finger	
$^{\circ}C$	Xot	Yot	Xot	Yot	Xot	Yot	Xot	Yot
55.0	-14.1	-10.5	-14.5	-13.5	-14.1	-10.5	-14.0	-6.7

Appendix B

Flowchart Symbols

TABLE B.1: Flowchart Symbols

	Symbol	Use In Flowchart
Process		Denotes a process to be completed.
Arrow		Denotes direction of logic flow through program.
Decision		Denotes a decision or conditional branch to be taken. Usually due to the outcome of a previous process or an input.
Input/Output		Denotes either an INPUT or an OUTPUT operation.
SubProcess		Denotes the transition to a sub-process and the start of a sub-process.
Start, End		Denotes the start and end of a process as well the return from a sub-process.
Switch Statement		Denotes a switch statement. This is similar to the decision statement however it allows for a larger number of possible branches. These branches are self contained and have several operations before breaking and returning.
Break		Denotes a break from a switch statement which, moves the program to the switch return protocol.

Appendix C

Electromyography Tomographic Array Reconstruction (EMG TAR)

The time taken for an EMG signal to reach different parts of the surface of the arm differs depending on the distance from the source; The greater the distance the greater the time to reach the skin. This is due to the fact that EMGs are conducted across tissue therefore with an assumed constant conduction velocity an increased conduction path causes an increase in the time before the detection of the signal. The propagation velocity of EMG signals in muscle fibre is approximately $4ms^{-1}$ (Zwarts and Stegeman (2003)).

If this is true then it would be possible to detect the relative locations of the origin each signal using basic tomographic reconstruction methods. The basic principal of this idea would be to detect the signals emitted at regular intervals around the forearm using sensors placed in known locations. With this level of signal detection each individual muscle could be detected and therefore could provide multiple input signals.

This would allow the controller more inputs and could provide a human like control of a prosthetic hand. The method would rely on multiple EMG sensors placed around the forearm. Designed to detect the signals from the muscles at different points. The time of detection would be then identified and the differences could be used to locate the origin. This process would use a characteristic defined in some reports as “cross talk”[Luca (1997)]; the detection of the EMG emitted by an adjacent muscle with the sensor on another muscle. This technique could also be used to identify and remove external artefacts that are detected by conventional EMG systems by causing ghost signals. This would be because these external signals would have inconsistent arrival sequences. Therefore, they could be filtered out without significant computing through the use of sequence analysis.

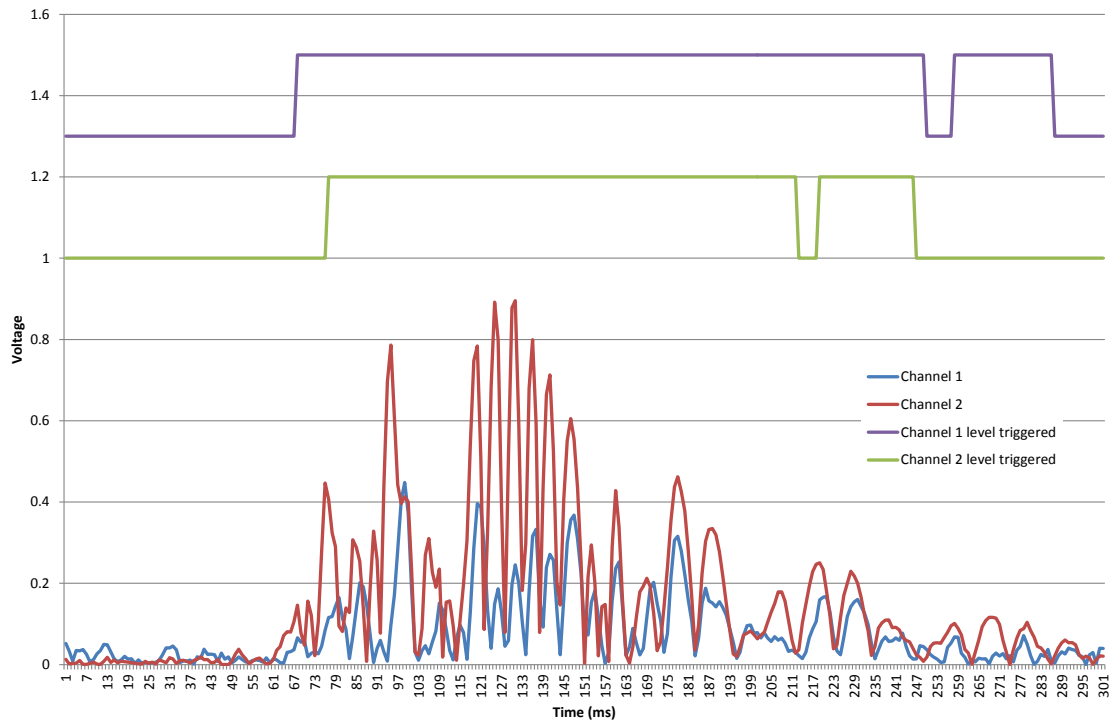


FIGURE C.1: Plot of two EMG signals taken from an adult male's forearm against time

The first stage of this research was to gather basic data to analyse the basic theory. Fifty six seconds of data were captured from two differential pairs of contact electrodes placed on the anterior of the left forearm of a healthy person. The electrodes were spaced approximately 50mm apart. This data contained about 30 flexions of the middle and ring fingers and the same number of flexions of the first finger. The equipment used to capture this data was a dual differential pair EMG electrode amplifier with a common ground as presented in Spinelli et al. (2003). This then uses a National Instruments USB-6008, 12-bit digital to analogue (DAC) data capture device, with a data capture rate set at 1K bits per channel per second. A 50Hz notch filter is used to remove any mains signals that are detected by the system.

It can be seen in Figure C.1 that the time between the detection of the EMG signals differs between the two figures. As well as this the ratio between the amplitudes of signals 1 and 2 differ between the plots, this suggests that more than one processing method could be used for each device.

The analysis of this data shows that when the data was compared on a X-Y plot (Figure C.2) there were different characteristics between the three sets of data and therefore the different fingers could be identified. This suggests that the conduction velocity and or attenuation are causing this difference in the received signals. With these preliminary results it was decided to try and repeat the results with more sets of differential sensors spaced at 25mm.

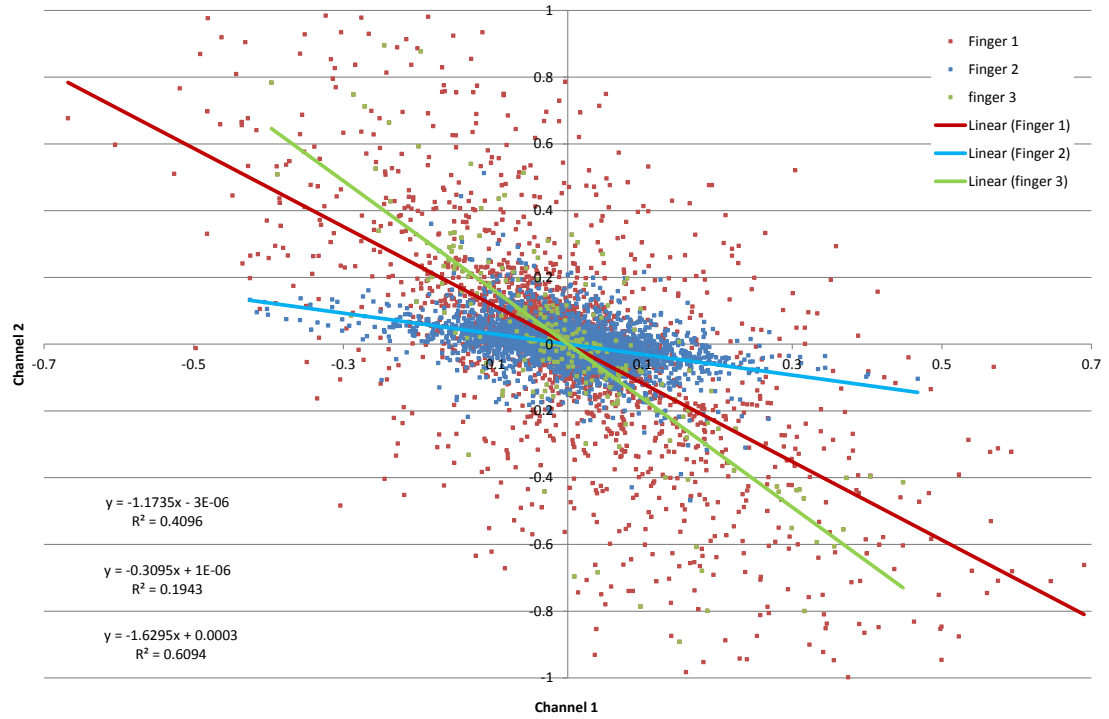


FIGURE C.2: X-Y plot of three sets of finger data from two EMG channels on the forearm of an adult male.

With the preliminary results showing that this approach could be a viable solution for the control of upper body prosthetic.

A set-up with 15 pairs of contact sensors will be designed using the backs of riveted button poppers as the contacts, mounted on a fabric arm band. The buttons will be used as the head of the electrode lead, to allow quick addition and rearrangement of electrode pairs. This set up will use the same EMG amplifier circuit design as the initial study and will allow for the investigation of both series and parallel differential pairs as well as individual electrodes with a common ground. This set-up will also require the use of a DAC however a National Instruments NI DAQPad-6016 device will be used as it has a higher resolution and data capture rate than the previous device.

References

- Allen-Prince, M. Walton, D. J. Finger motion modeling for bionic fingers. In *Tenth Annual NC OPT-ED Alliance Day*, 2011.
- Asyali, M. H., Yilmaz, M., Tokmakc, M., Sedef, K., Aksebzec, B. H., Mittal, R. Design and implementation of a voice-controlled prosthetic hand. *Elektrik-Turkish Journal of Electrical Engineering and Computer Sciences*, 19(1):33, 2011.
- Autodesk, inc. Autodesk inventor 3d cad software. <http://usa.autodesk.com/autodesk-inventor/>, 2011. accessed on 09/2011.
- Baggott, K. Upgrading the prosthetic hand. *Technology Review (MIT)*, may 19 2008. <http://www.technologyreview.com/computing/20791>.
- Bahari, M., Jaffar, A., Low, C., Jaafar, R., Roese, K., Yussof, H. Design and development of a multifingered prosthetic hand. *International Journal of Social Robotics*, 4:1–8, 2011. ISSN 1875-4791. 10.1007/s12369-011-0133-8.
- Barata, S. D. O. The alternative limb project. <http://www.thealternativelimbproject.com/> accessed on 02/2015, 2015.
- Barlow, O. An investigation into the properties of composites within upper limb prosthetics. Master’s thesis, School of Marine Science and Engineering, Faculty of Science and Technology, University of Plymouth, April 2012.
- Bell, C. *The Hand: Its Mechanism and Vital Endowments as Evincing Design*. William Pickering, London, third edition, 1833.
- Belter, J. T., Segil, J. L., Dollar, . A. M., Weir, R. F. Mechanical design and performance specifications of anthropomorphic prosthetic hands: A review. *Journal of Rehabilitation Research & Development*, 50(5):599–618, 2013.
- Biddiss, E., Beaton, D., Chau, T. Consumer design priorities for upper limb prosthetics. *Disability & Rehabilitation: Assistive Technology*, 2(6):346–357, 2007.
- Biddiss, E. A. Chau, T. T. Upper limb prosthesis use and abandonment: A survey of the last 25 years. *Prosthetics and Orthotics International*, 31(3):236–257, 2007.

- Bracht, C. G8 and g20 demographics. http://www.g8.utoronto.ca/evaluations/factsheet/factsheet_demography.html accessed on 02/2014, May 2010.
- Bundhoo, V., Park, E. Design of an artificial muscle actuated finger towards biomimetic prosthetic hands. In *Advanced Robotics, 2005. ICAR '05. Proceedings., 12th International Conference*, pages 368–375, jul. 2005.
- C Enterprise UK LTD. Robox, 2015. www.cel-robox.com (Accessed on 27/04/2015).
- Carey, S. L., Dubey, R. V., Bauer, G. S., Highsmith, M. J. Kinematic comparison of myoelectric and body powered prostheses while performing common activities. *Prosthetics and Orthotics International*, 33(2):179–186, 2009.
- Childress, D. Historical aspects of powered limb prostheses. *Clinical Prosthetics & Orthotics*, 9:2–13, 1985.
- Colditz, J. C. Anatomic considerations for splinting the thumb. *Rehabilitation of the hand. 4th ed. St. Louis: Mosby*, pages 1161–1172, 1995.
- Cotton, D. P. J., Cranny, A., Chappell, P. H., White, N. M., Beeby, S. P. Fingertip force, slip and temperature sensors for prosthetic hands. In *International Society of Prosthetics and Orthotics (ISPO) Trent Prosthetic Symposium*, 2005.
- Datta, D., Ibbotson, V. Powered prosthetic hands in very young children. *Prosthetics and Orthotics International*, 22(2):150–154, 1998.
- Dechev, N., Cleghorn, W. L., Naumann, S. Multiple finger, passive adaptive grasp prosthetic hand. *Mechanism and Machine Theory*, 36(10):1157 – 1173, 2001. ISSN 0094-114X.
- Disabled World. Average height to weight chart - babies to teenagers. <http://www.disabled-world.com/artman/publish/height-weight-teens.shtml>, March 2008.
- Donovan-Hall, M., Yardley, L., Watts, R. Engagement in activities revealing the body and psychosocial adjustment in adults with a transtibial prosthesis. *Prosthetics and Orthotics International*, 26(1):15–22, 2002.
- Donovan-Hall, M. Our bodies our views.
- Doshi, R., LeBlanc, M. The design and development of a gloveless endoskeletal prosthetic hand. *Journal of Rehabilitation Research and Development*, 35(4):388–395, October 1998.
- e-NABLE. E-nabling the future. <http://enablingthefuture.org/> accessed on 02/2015, 2014.
- Electro Mechanical Systems Limited. www.ems-limited.co.uk/ (Accessed 05/03/2015).

- Fishman, S.Kay, H. Acceptability of a functional-cosmetic artificial hand for young children, part i. *Artificial Limbs*, 8:15–27, 1964.
- Frigo, C., Ferrarin, M., Frasson, W., Pavan, E.,Thorsen, R. EMG signals detection and processing for on-line control of functional electrical stimulation. *Journal of Electromyography and Kinesiology*, 10(5):351 – 360, 2000. ISSN 1050-6411.
- Fukaya, N., Toyama, S., Asfour, T.,Dillmann, R. Design of the tuat/karlsruhe humanoid hand. In *Intelligent Robots and Systems, 2000. (IROS 2000). Proceedings. 2000 IEEE/RSJ International Conference on*, volume 3, pages 1754 –1759 vol.3, 2000.
- Gaiser, I. N., Pylatiuk, C., Schulz, S., Kargov, A., Oberle, R.,Werner, T. The FLU-IDHAND III: A Multifunctional Prosthetic Hand : JPO: Journal of Prosthetics and Orthotics. *JPO: Journal of Prosthetics and Orthotics*, 21(2):91–96, 2009.
- Galiano, L., Montaner, E.,Flecha, A. Research, design and development project myoelectric prosthesis of upper limb. *Journal of Physics: Conference Series*, 90(1):012089, 2007.
- Guo, G., Zhang, J.,Gruver, W. A. Optimal design of a six-bar linkage with one degree of freedom for an anthropomorphic three-jointed finger mechanism. *Proceedings of the Institution of Mechanical Engineers, Part H: Journal of Engineering in Medicine*, 207(3):185–190, 1993.
- Hall, J. *Handbook of normal physical measurements*. Oxford University Press, 1989.
- Han, L.Huang, H. Development of a modular prosthetic hand. Master's thesis, Nation Taiwan University, 1998.
- Hosmer Dorrance Corp. Improving lives for 100 years. <http://hosmer.com/hosmer-100th.html> accessed on 10/2011, 2012.
- HPC Gears Ltd. Hpc gears catalogue. http://www.hpcgears.com/newpdf/hpc_cataloguesinside.pdf accessed on 09/2011, 2011.
- Hu, P. X. B. *Deveiopment of A Paediatric Prosthetic Hand with A Two-Degree-of-Freedom Thumb*. PhD thesis, University of Toronto, 1997.
- Internationa Organization for Standardization. Iso/iec7810:2003 - identification cards – physical characteristics - bank cards. http://www.iso.org/iso/catalogue_detail?csnumber=31432; http://en.wikipedia.org/wiki/ISO/IEC_7810 accessed on 09/2011, 2003.
- Kargov, A., Pylatiuk, C., Oberle, R., Klosek, H., Werner, T., Roessler, W.,Schulz, S. Development of a multifunctional cosmetic prosthetic hand. In *Rehabilitation Robotics, 2007. ICORR 2007. IEEE 10th International Conference on*, pages 550 – 553, june 2007.

- Krebs, D. E., Edelstein, J. E., Thornby, M. A. Prosthetic management of children with limb deficiencies. *PHYS THER*, 71(12):920–934, December 1991.
- Kuniholm, J. Open arms. *IEEE Spectrum*, 46(3):36–41, March 2009.
- Kyberd, P. J., Chappell, P. H. The southampton hand: An intelligent myoelectric prosthesis. *Journal of Rehabilitation Research and Development*, 31(4):326–334, 1994.
- Kyberd, P. J., Light, C., Chappell, P. H., Nightingale, J. M., Whatley, D., Evans, M. The design of anthropomorphic prosthetic hands: A study of the southampton hand. *Robotica*, 19(06):593–600, 2001.
- LeBlanc, M., Setoguchi, Y., Bowen, W. D., Miner, C., Burkholder, F., Chen, S. Design concepts for an endoskeletal child-size hand. *American Academy of Orthotists & Prosthetists*, 9(3):123–126, 1997.
- Light, C. M., Chappell, P. H. Development of a lightweight and adaptable multiple-axis hand prosthesis. *Medical Engineering & Physics*, 22(10):679 – 684, 2000. ISSN 1350-4533.
- Light, C., Chappell, P., Hudgins, B., Engelhart, K. Intelligent multifunction myoelectric control of hand prostheses. *Journal of Medical Engineering & Technology*, 26:139–146(8), July 2002.
- Lowe, R., Chappell, P., Ahmad, S. Using accelerometers to analyse slip for prosthetic application. *Measurement Science and Technology*, 21, January 2010.
- Luca, C. J. D. The use of surface electromyography in biomechanics. *Journal of Applied Biomechanics*, 13(2):135–163, 1997.
- Marquardt, E. The heidelberg pneumatic arm prosthesis. *The Journal Of Bone And Joint Surgery*, 47 B(6):425–434, 1965.
- Massa, B., Roccella, S., Carrozza, M., Dario, P. Design and development of an underactuated prosthetic hand. In *Robotics and Automation, 2002. Proceedings. ICRA '02. IEEE International Conference on*, volume 4, pages 3374 – 3379 vol.4, 2002.
- Maxon - Encoder MR Type S, 16 Counts per turn, 2 Channel - Datasheet. Maxon - Sensors, May 2013. Catalogue Page 295.
- Micera, S., Sabatini, A. M., Dario, P., Rossi, B. A hybrid approach to emg pattern analysis for classification of arm movements using statistical and fuzzy techniques. *Medical Engineering & Physics*, 21(5):303 – 311, 1999. ISSN 1350-4533.
- Muridan, N., Chappell, P. H., Cranny, A., White, N. M. Texture sensor for a prosthetic hand. In *Euroensors XXIV*, pages 1–4. Elsevier, September 2010.

- Nazarpour, K., Steenson, D., Sepulveda, F., O'Connor, R., Chadwick, E., Jiang, L., Constandinou, T. Enabling technologies for sensory feedback in next-generation assistive devices. EPSRC Grant Reference: EP/M025977/1, March 2015.
- Objet Geometries Ltd. Objet materials data sheet. http://objet.com/sites/default/files/pdfs/Objet_Materials_Data_Sheets.pdf, 2010.
- Objet Geometries Ltd. Polyjet technology 3d printer. http://www.objet.com/PRODUCTS/PolyJet_Technology/, 2011.
- Otto Bock. Otto bock system electric greifer dmc variplus. http://www.ottobock.com/cps/rde/xbcr/ob_com_en/ifu_647g278_8e33_8e34.pdf accessed on 09/2011, a.
- Otto Bock. Otto bock system electric hand. http://corporate.ottobock.co.uk/cps/rde/xchg/ob_uk_en/hs.xsl/5734.html accessed on 01/2015, b.
- Otto Bock. 2000 electric hand for children. http://www.ottobock.co.uk/cps/rde/xchg/ob_uk_en/hs.xsl/3685.html?id=teaser2 accessed on 06/2011, 2011.
- Oxford Dictionaries. "modular". *Oxford Dictionaries*. Oxford University Press, April 2010. <http://oxforddictionaries.com/definition/modular> accessed on 09/2011.
- Proto Labs, Inc. Prototyping process: Choosing the best process for your project. <http://www.appliancedesign.com/ext/resources/WhitePapers/PPWP-FINAL.pdf?1355776273> accessed on 26/04/2015, 2009.
- Pylatiuk, C., Kargov, A., Schulz, S. Design and evaluation of a low-cost force feedback system for myoelectric prosthetic hands. *Journal of Prosthetics and Orthotics*, 18(2): 1–5, 2006.
- Ramirez-Garcia, A., Toledo, C., Leija, L., Muoz, R. Status of elbow myoelectric prosthesis: Cinvestav-ipn prosthesis. *Revista Mexicana de Ingeniera Biomedica*, 07:66–73, 2009.
- Redman, T., Sims, T., Chappell, P., Donovan-Hall, M., Cranny, A., Metcalf, C., White, N. The design of a myoelectrically controlled hand with multiple actuators for five-year old children. In *MEC '11 Raising the standard*, pages 83–86. UNB, August 2011. Event Dates: 14 -19 August 2011.
- RSL Steeper. "scamp" myo electric hand for children. http://rslsteeper.com/products/prosthetics/products/upper_limb/electric/scamp_myoelectric_hand_for_children accessed on 06/2011.
- RSL Steeper. Upper limb prosthetic components - catalogue 2008-9. http://rslsteeper.com/uploads/files/281/upper_limb_catalogue.pdf acceses on 06/2013, 2008.

- RSL Steeper. Bebionic v2 product brochure. www.bebionic.com accessed on 05/2013, 2011.
- Shadow Robot Company Ltd. Technical specification - kinematics. <http://www.shadowrobot.com/hand/techspec.shtml> accessed on 06/2011, 08 2011.
- SHAP Business Enterprise. *Southampton Hand Assessment Procedure - Assessor's SHAP Protocol*. University of Southampton. <http://www.shap.ecs.soton.ac.uk/files/protocol.pdf> Accessed 21/11/2013.
- Shida-Tokeshi, MA, J., Bagley, A., Molitor, F., Tomhave, W., Liberatore, J., Brasington, K., Montpetit, K. Predictors of continued prosthetic wear in children with upper extremity prostheses. *JPO Journal of Prosthetics & Orthotics*, 17(4):119–124, October 2005.
- Sinha, A. The design and fabrication of a myoelectric prosthetic hand. In *Bioengineering Conference (NEBEC), 2011 IEEE 37th Annual Northeast*, pages 1–3, april 2011.
- Sorbye, R. Myoelectric controlled hand prostheses in children. *International Journal of Rehabilitation Research*, 1:15–25, 1977.
- Sorbye, R. Myoelectric prosthetic fitting in young children. *Clinical Orthopaedics and Related Research*, 148:34–40, 1980.
- Spinelli, E., Pallas-Areny, R., Mayosky, M. Ac-coupled front-end for biopotential measurements. *Biomedical Engineering, IEEE Transactions on*, 50(3):391–395, march 2003. ISSN 0018-9294.
- Tang, L., Hayton, A., Brunette, E., Roldan, J., Quazi, T., Zhou, J. Prosthetic hand with a simple driving system. In *Robotics, Automation and Mechatronics (RAM), 2011 IEEE Conference on*, pages 208–213, sept. 2011.
- Taylor, C.Schwarz, R. The anatomy and mechanics of the human hand. *The Journal of Orthotics and Prosthetics*, 2(2):22–35, 1955.
- Thayer, N.Priya, S. Design and implementation of a dexterous anthropomorphic robotic typing (dart) hand. *Smart Materials and Structures*, 20(3):035010, 2011.
- Touch Bionics. The i-limb hand. <http://www.touchbionics.com/i-LIMB> accessed on 09/2011, 2011.
- Ulrich, N., Paul, R., Bajcsy, R. A medium-complexity compliant end effector. In *IEEE Int. Conf. Robotics and Automation*,, pages 434–436, 1989.
- United States Census Bureau. Resident population estimates of the united states. <http://www.census.gov/popest/data/national/totals/1990s/tables/nat-agesex.txt> accessed on 02/2014, 2001.

- United States Census Bureau. U.s. and world population clock. <http://www.census.gov/popclock> accessed on 02/2014, 2013.
- Walker, J. L., Coburn, T. R., Cottle, W., Burke, C., Talwalkar, V. R. Recreational terminal devices for children with upper extremity amputations. *Journal of Pediatric Orthopaedics*, 28(2):271–273, March 2008.
- Whitney, D. E. Nippondenso co. ltd: A case study of strategic product design. *Research in Engineering Design*, 5(1):1–20, 1993.
- Yamano, I. Maeno, T. Five-fingered robot hand using ultrasonic motors and elastic elements. In *Robotics and Automation, 2005. ICRA 2005. Proceedings of the 2005 IEEE International Conference on*, pages 2673 – 2678, april 2005.
- Yang, J., Pitarch, E. P., Abdel-Malek, K., Patrick, A., Lindkvist, L. A multi-fingered hand prosthesis. *Mechanism and Machine Theory*, 39(6):555 – 581, 2004. ISSN 0094-114X.
- Zaini, M., Ahmad, S., Marhaban, M., Hasan, W. Upm prosthetic hand system design - preliminary results. In *Research and Development (SCOReD), 2011 IEEE Student Conference on*, pages 174 –177, dec. 2011.
- Zecca, M., Micera, S., PhD, Carrozza, M. C., Dario, P. Control of multifunctional prosthetic hands by processing the electromyographic signal. *Critical Reviews in Biomedical Engineering*, 30(4-6):27, 2002.
- Ziegler-Graham, K., MacKenzie, E. J., Ephraim, P. L., Travison, T. G., Brookmeyer, R. Estimating the prevalence of limb loss in the united states: 2005 to 2050. *Archives of Physical Medicine and Rehabilitation*, 89(3):422 – 429, 2008. ISSN 0003-9993.
- Zwarts, M. J. Stegeman, D. F. Multichannel surface emg: Basic aspects and clinical utility. *Muscle Nerve*, 28(1):1–17, 2003. ISSN 1097-4598.